



Research paper

Hit-to-lead optimization of a 2-aminobenzimidazole series as new candidates for chagas disease

Celso de Oliveira Rezende Júnior^{a,1}, Pablo David Grigol Martinez^{a,1},
 Rafael Augusto Alves Ferreira^{a,1}, Paul John Koovits^a, Bruna Miranda Soares^a,
 Leonardo L.G. Ferreira^b, Simone Michelin-Duarte^b, Rafael Consolin Chelucci^b,
 Adriano D. Andricopulo^b, An Matheeussen^c, Natascha Van Pelt^c, Guy Caljon^c, Louis Maes^c,
 Simon Campbell^d, Jadel M. Kratz^d, Charles E. Mowbray^d, Luiz Carlos Dias^{a,*}

^a Institute of Chemistry, University of Campinas (UNICAMP), Campinas, SP, 13083-861, Brazil

^b Laboratory of Medicinal and Computational Chemistry, Physics Institute of São Carlos, University of São Paulo (USP), São Carlos, SP, 13563-120, Brazil

^c Laboratory of Microbiology, Parasitology and Hygiene (LMPH), Universiteitsplein 1, 2610, Antwerpen, Belgium

^d Drugs for Neglected Diseases Initiative (DNDi), 15 Chemin Camille-Vidart, 1202, Geneva, Switzerland

ARTICLE INFO

Keywords:

2-Aminobenzimidazole derivatives

Chagas disease

Hit-to-lead

Multiparametric optimization

Trypanosoma cruzi

ABSTRACT

Chagas disease is a neglected tropical disease caused by *Trypanosoma cruzi*. Because current treatments present several limitations, including long duration, variable efficacy and serious side effects, there is an urgent need to explore new antitrypanosomal drugs. The present study describes the hit-to-lead optimization of a 2-aminobenzimidazole hit 1 identified through *in vitro* phenotypic screening of a chemical library against intracellular *Trypanosoma cruzi* amastigotes, which focused on optimizing potency, selectivity, microsomal stability and lipophilicity. Multiparametric Structure–Activity Relationships were investigated using a set of 277 derivatives. Although the physicochemical and biological properties of the initial hits were improved, a combination of low kinetic solubility and *in vitro* cytotoxicity against mammalian cells prevented progression of the best compounds to an efficacy study using a mouse model of Chagas disease.

1. Introduction

Chagas disease, endemic in Latin America [1], is caused by the protozoan parasite *Trypanosoma cruzi* (*T. cruzi*), which is transmitted either by the faeces of infected triatomine bugs (vector transmission), orally through contaminated food or drink, or from human-to-human through congenital transmission or uncontrolled blood transfusion and organ/tissue transplantation [2,3]. During the usually asymptomatic and undiagnosed acute phase of the disease, trypomastigotes can be observed in high numbers in the bloodstream [4]. The host immune response usually controls this parasitemia, drastically reducing the number of circulating trypomastigotes. Subsequently, intracellular amastigotes lodge in deep organ tissues, particularly the heart and digestive tract, and the infection enters a lifelong chronic phase [5,6]. While most remain in an asymptomatic or indeterminate phase, the infection and associated inflammatory responses result in symptomatic

cardiac and digestive manifestations, with significant morbidity and mortality in 30–40% of patients [7,8]. More than 6 million people are infected worldwide, with an estimated 14,000 deaths per year [9].

Treatment is based on eliminating the parasite from infected individuals. The nitroheterocycles nifurtimox and benznidazole are currently the only drugs available [10,11]. These are prodrugs that exert trypanocidal activity upon activation to produce reactive metabolites and are effective against the trypomastigote and amastigote forms [12,13]. Both can cure or significantly reduce the parasite burden in acute cases, preventing tissue damage. However, they remain relatively ineffective in the chronic stage [14]. Long treatment courses (60–90 days), variable efficacy and serious side effects, including allergic dermatitis, pruritus, fever and gastrointestinal intolerance, result in discontinuation of treatment in approximately 20–25% of patients [5,15]. Few new chemical entities have progressed to clinical trials. In the past decade, clinical trials evaluating posaconazole and ravuconazole, two CYP51

* Corresponding author.

E-mail address: ldias@unicamp.br (L.C. Dias).

¹ These authors contributed equally.

inhibitors, were unsuccessful. Despite an initial rapid and significant reduction of parasitemia, follow-up revealed high relapse rates within six months after treatment in both studies [16–19]. Thus, the need remains for continued drug discovery efforts to find new chemotypes, especially compounds with novel mechanisms of action [20,21].

The main goal of hit-to-lead optimization is to find an *in vivo* active compound with a suitable drug-like profile and good absorption, distribution, metabolism, excretion and toxicity (ADME-Tox) properties [21–24]. Acceptable and ideal criteria have been compiled to define profiles of hits, leads, optimized leads, and preclinical candidates [21, 25].

The quality of initial hits is a key factor which increases the likelihood of success in the lead optimization process and thus the identification of clinical candidates [22,26,27]. Compound **1** was selected as the initial hit from a high-throughput screening campaign performed by GlaxoSmithKline (GSK), based on its potency (IC₅₀ 0.63 μ M), high selectivity over mammalian cells lines (SI of 159 relative to HepG2 cells), and chemical tractability (Fig. 1) [28]. Whilst the mechanism of action of this compound is unknown, it was confirmed not to act via CYP51 inhibition (IC₅₀ > 100 μ M).

We previously reported the hit-to-lead study of a 2-aminobenzimidazole series against leishmaniasis [29]. In this paper, we report the structure-activity relationship (SAR) study and hit-to-lead campaign of this same 2-aminobenzimidazole series against *T. cruzi* through multi-parameter optimization. Recently, a SAR study against *T. cruzi* and *Trypanosoma brucei* was performed and published using **1** as a reference compound [30]. Here we report an alternative strategy to optimize potency against *T. cruzi* and ADME properties, using a different set of chemical modifications.

2. Results and discussion

2.1. Hit confirmation and initial profiling

Hit confirmation was performed after re-synthesis and *in vitro* reassessment of potency against intracellular *T. cruzi* amastigotes and evaluation of preliminary ADME and physicochemical properties, such as lipophilicity, permeability, and metabolic stability in mouse liver microsomes (MLM) (Fig. 1). Potency and selectivity were confirmed, and **1** showed good permeability, but revealed rapid *in vitro* intrinsic microsomal clearance and a high LogD [29].

2.2. Synthesis

Most final compounds were synthesized by the strategies reported in Schemes 1 and 2. As few 2-aminobenzimidazoles were commercially available, the simpler candidates were prepared via alkylation of the 1-nitrogen atom yielding the representative 2-aminobenzimidazole intermediates **iii** (route 1, Scheme 1). **iii** was also prepared from *ortho*-fluoronitrobenzene derivatives **i** via aromatic nucleophilic substitution

(S_NAr) with primary amines or ammonium chloride, followed by nitro reduction and cyclization with cyanogen bromide (route 2, Scheme 1). Alternatively, **iii** was prepared by S_NAr reaction of *ortho*-fluoronitrobenzene with ammonia, followed by reductive amination with aldehydes, nitro reduction and cyclization (route 3, Scheme 1). The aminopurine intermediates **vii** were prepared from nitropyrimidine derivative **iv** by regioselective aromatic nucleophilic substitution with primary amines, followed by reduction of the nitro group, cyclization with 1,1'-thiocarbonyldiimidazole and reaction with bromine under acidic conditions. The resulting bromide **vi** was then transformed into the aminopurine **vii** by reaction with ammonia under microwave conditions (route 4, Scheme 1). Subsequently, the intermediates **iii** and **vii** were transformed into the final compounds by amide coupling with commercial or previously prepared carboxylic acid derivatives (Scheme 2). Further details can be found in the Supporting Information.

2.3. Structure-activity and structure-properties relationships

Identification of the minimal pharmacophoric group necessary for biological activity is an important step in the design of chemical modifications in the hit-to-lead phase. In addition, the generation of structure-properties relationship (SPR) information offers a rational path to early-stage optimization of compounds.

We started this investigation by synthesizing several truncated analogues to identify the minimal pharmacophore associated with acceptable levels of *in vitro* potency (IC₅₀ < 5 μ M) and by conducting a small hit expansion campaign to identify regions in the scaffold that were amenable to structural modifications (Table 1). The chlorine at the right-hand side of **1** can be replaced by fluorine (compounds **2** and **3**). Removal of the hydrophobic moieties such as the benzene ring of the benzimidazole fragment and *N*-propyl chain (compounds **4** and **5**) drastically reduced activity, as also observed by McNamara and co-workers [30]. Loss of potency was also observed for the benzothiazole analogue **6**. Replacement of the amide functionality by sulfonamide and urea, and addition of an ethyl linker between the benzimidazole ring and amide functionality (compounds **7–9**) also resulted in inactive compounds or drops in potency. Removal of methylene or carbonyl groups in the right-hand side (compounds **10** and **11**) also reduced potency. The *N*-alkyl-*N'*-acylaminobenzimidazole fragment seems to be the minimal pharmacophore for this series so we then designed modifications in the benzimidazole ring, *N*-alkyl chain and acyl fragment (Fig. 1).

Given the promising activity of **1** and the preliminary SAR data described in Table 1, we started a hit-to-lead campaign with the initial goal of improving potency and selectivity while reducing overall lipophilicity. High lipophilicity (LogD > 4) plays a crucial role in drug discovery campaigns since it can impact the quality of *in vitro* data generated in biological assays (poor specificity and promiscuity) and likely decreases overall aqueous solubility and metabolic stability [31–34]. The acceptable parameters of ADME-Tox properties we sought at this stage were IC₅₀ < 5 μ M, selectivity index (SI) > 30, MLM clearance < 30 μ L/min/mg and LogD close to 3.

McNamara and co-workers highlighted in their work with this chemical class that aspects of the SAR were relatively shallow, and there was a general lipophilic observed effect, suggesting that further optimization could be relatively challenging [30]. However, our previous work with this 2-aminobenzimidazole series indicated that multiple strategies were suitable to reduce lipophilicity and consequently improve *in vitro* metabolic stability, including the addition of electron withdrawing groups (EWG) in the benzimidazole ring, bulky and/or polar groups on the *N*-alkyl chain and heteroaromatic groups at the acyl fragment [29]. Therefore, we initially explored the attachment of EWGs to the aromatic ring of the benzimidazole fragment (Table 2). Positions 5 and/or 6 appeared to be the ideal sites for substitution since fluorine and trifluoromethyl derivatives (**12–16**) showed equivalent potency to the original hit with a slight reduction of LogD, while introduction of fluorine at position 4 was inactive (compound **17**). This same trend was

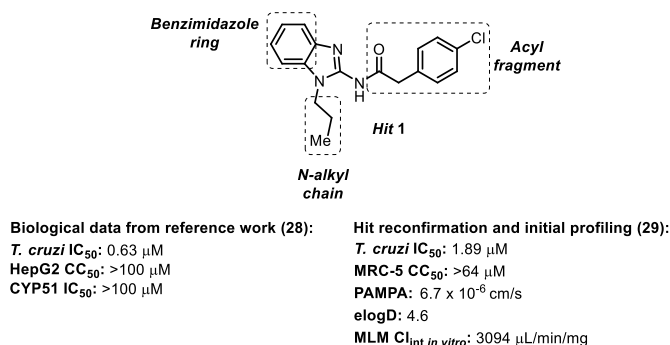
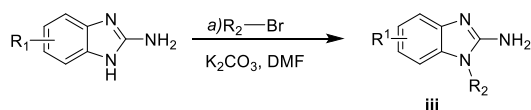
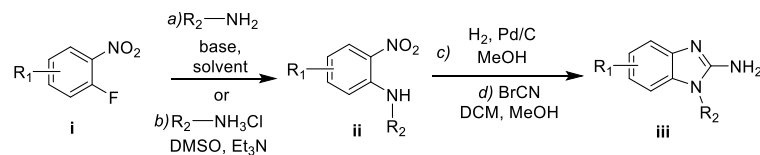


Fig. 1. Chemical structure, biological data and early ADME-Tox properties of hit **1** [28,29].

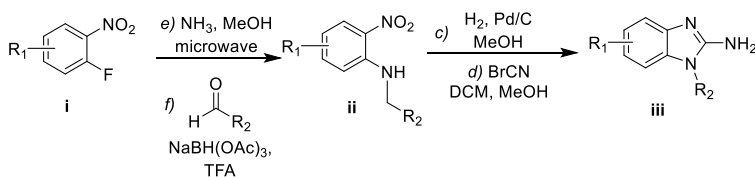
1) ABZ commercially available



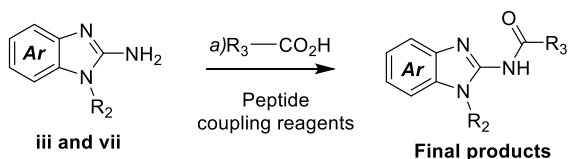
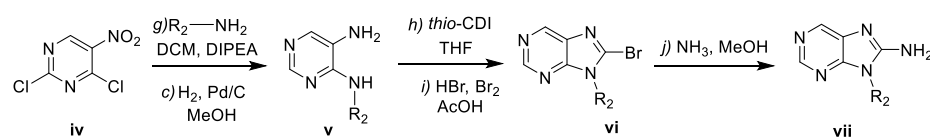
2) S_NAr / BrCN cyclization route:



3) Reductive amination / BrCN cyclization route:



4) S_NAr / thio-CDI cyclization route:



Scheme 2. Synthesis of final products. Reagents and conditions: a) peptide coupling reagents (EDC, HOBt, DMF, r.t. or HATU, DIPEA, DCM, r.t.).

previously observed against *L. infantum* [29].

Whilst a methyl ester in position 6 showed good potency (compound **18**), the carboxylic acid analogue was inactive (compound **19**). Given that esters are readily hydrolysed both chemically and biologically, this group was not pursued. Although greatly reducing lipophilicity and MLM clearance, the amides, hydroxamic acids and nitrile (**20–24**), showed reduced potency (IC_{50} 8–35 μM). The better MLM clearance values (< 70 $\mu L/min/mg$) observed for **20** and **22** can be attributed to their lower lipophilicity (LogD 3.2 and 3.1, respectively) when compared to the initial hit. Via the introduction of nitrogen in the benzimidazole ring (compound **25**), it was possible to maintain potency with reduced lipophilicity, but MLM clearance increased, probably due to the introduction of an additional metabolic soft spot.

Further reduction of overall lipophilicity could be achieved by replacing the hydrophobic phenylacetic fragment on the right-hand side of the scaffold (Table 3). Picolinic (**26–29**) and nicotinic acid derivatives (**30–34**) showed acceptable potency (IC_{50} < 10 μM) and reduced lipophilicity, especially compounds **26**, **27**, **31** and **32**. The only exception was the nitrile derivative **31** (IC_{50} 18 μM).

Metabolite identification (MetID) studies were conducted with

Scheme 1. Synthesis of 2-aminobenzimidazole intermediates **iii** and **vii**. Reagents and conditions: a) alkylamine, K_2CO_3 , KF, DMF, 0 °C-r.t.; b) ammonium chloride, DIPEA, DMSO, 80 °C; c) H_2 (1 bar), Pd/C, EtOAc/MeOH, r.t.; d) BrCN (1 M in DCM), MeOH, 60 °C; e) NH_3 (7.0 mol L^{-1} in MeOH), 80 °C, 1h, microwave; f) aldehyde, $NaBH(OAc)_3$, TFA, 0 °C-r.t.; g) alkylamine, DIPEA, DCM, –78 °C-r.t.; h) thio-CDI, THF, 70 °C; i) HBr (48%), bromine, AcOH, 0 °C-r.t.; j) NH_3 (7 mol L^{-1} in MeOH), 120 °C, microwave.

isomers **26** and **33** to identify the influence of nitrogen position of the pyridine fragment on metabolism (Fig. 2). These compounds showed minor oxidation on the aromatic carbons and *N*-alkyl chain. Compound **26** suffered significant hydrolysis of the amide, suggesting that the position of the nitrogen atom in the pyridyl fragment has a strong effect on metabolism via hydrolysis.

To minimize metabolism on the propyl chain, this region was explored via the addition of different groups, varying the size, shape and polarities of the alkyl chain (Table 3, compounds **35–45**). Decreasing the hydrophobicity of this fragment using polar groups and/or ionizable centers, such as tetrahydropyran and piperidine (compounds **35–37**) resulted in much lower MLM clearance and lipophilicity but was accompanied by a significant drop in potency. Cyclopropyl derivatives (**38–39**) were less active while trifluoroethyl and neopentyl analogues (**40–45**) presented a large variability with IC_{50} values ranging from 0.8 μM to > 64 μM . The substitution of fluorine for nitrile in the benzimidazole ring (**44** vs **45**) considerably improved potency, microsomal stability, and reduced lipophilicity. Combining good potency and selectivity (IC_{50} 2.6 μM ; SI > 25), microsomal stability (MLM clearance 18 $\mu L/min/mg$) and LogD (3.1), nitrile derivative **45** was the compound with the most balanced profile at this stage.

As the nitrile group and trifluoroethyl chain of **45** offered the best combination of properties, we further explored the right-hand side of the scaffold focusing on alternative heteroaromatic amides (Table 4 and Table S1). The trifluoromethylpyridine isomer **46** was almost 10 times more potent than **45** (IC_{50} 0.28 vs 2.6 μM), with good selectivity over mammalian cells, acceptable MLM clearance and lipophilicity. Despite retaining good potency, substituted pyridine, pyrimidine, thiazole, and pyrazole derivatives (**47–52**) generally did not display suitable microsomal metabolic stability and/or selectivity. However, compounds **53**

Table 1

Antitrypanosomal activities of analogues with modifications to determine the minimal pharmacophore group.

Compound	Structure	<i>T. cruzi</i> IC ₅₀ ^a (SD)	Compound	Structure	<i>T. cruzi</i> IC ₅₀ ^a (SD)
2 ^b		2.1 (0.08)	7		>64
3		2.2 (0.15)	8		>64
4		35 (0.22)	9		33 (2.76)
5		>64	10		>64
6		>64	11		25 (1.54)

^a IC₅₀ represented in μM . IC₅₀ of benznidazole (reference) was 2.1 μM .^b The antitrypanosomal activity of **2** has already been reported [30]. SD represents the standard deviation of the analyses.**Table 2**

Antitrypanosomal activity, selectivity and initial ADME properties for analogues with modifications at the benzimidazole ring.

Compound	R ¹	R ²	X	<i>T. cruzi</i> IC ₅₀ ^a (SD)	SI	MLM Cl _{int} ^b in vitro	eLogD
12 ^c	6-F	4'-Cl	CH	0.56 (0.08)	102	1590	4.3
13	5-F	4'-Cl	CH	0.92 (0.92)	>70	1510	4.3
14	5,6-di-F	4'-F	CH	0.53 (0.01)	>121	399	4.0
15	5,6-di-F	2',5'-di-F	CH	0.58 (0.06)	52	389	4.2
16	5-CF ₃	4'-Cl	CH	0.74 (0.28)	15	283	4.7
17	4-F	4'-F	CH	>64	1	715	3.6
18	6-CO ₂ Me	4'-F	CH	0.53 (0.01)	35	1253	4.0
19	6-CO ₂ H	4'-F	CH	>64	1	ND	2.4
20	6-	4'-F	CH	34 (0.31)	1	66	3.2
21	6-	4'-F	CH	8.5 (0.06)	>8	ND	4.0
22	6-	4'-F	CH	35 (1.16)	>2	23	3.1
23	6-	4'-F	CH	8.3 (0.54)	7	128	3.3
24	6-CN	4'-Cl	CH	24 (38.8)	>3	226	3.6
25	H	4'-F	N	1.3 (1.36)	>49	1500	3.3

ND: not determined; SD represents the standard deviation of the analyses; SI: Selectivity index relative to MRC-5 cells (CC₅₀/IC₅₀); MLM: Mouse Liver Microsome; ^a IC₅₀ represented in μM , ^b Intrinsic clearance represented in $\mu\text{L}/\text{min}/\text{mg}$. ^c The antitrypanosomal activity of **12** has already been reported [30]. IC₅₀ of benznidazole (reference) was 2.1 μM .

Table 3

Evaluation of antitrypanosomal activity, selectivity and initial ADME properties for compounds with pyridine groups at the acyl fragment.

Compound	Structure	<i>T. cruzi</i> IC ₅₀ ^a (SD)	SI	MLM Cl _{int} ^b in vitro	eLogD
26		1.1 (1.03)	7	413	3.3
27		8.4 (0.29)	>8	265	2.5
28		2.4 (0.20)	>27	285	3.5
29		2.3 (0.02)	>28	467	4.0
30		2.1 (0.01)	>30	446	3.9
31		18 (18.2)	>4	200	3.3
32		4.4 (4.67)	>15	275	3.0
33		8.2 (5.60)	>8	164	3.8
34		3.2 (3.34)	15	ND	4.2
35		9.2 (3.46)	3	ND	1.1
36		8.5 (0.15)	5	26	3.1
37		35 (0.16)	>2	23	4.0
38		34 (0.08)	>2	160	3.2

(continued on next page)

Table 3 (continued)

Compound	Structure	<i>T. cruzi</i> IC ₅₀ ^a (SD)	SI	MLM Cl _{int} ^b in vitro	eLogD
39		>64		1350	3.6 ^c
40		0.80 (0.23)	>80	131	4.5
41		8.7 (0.16)	>7	87	3.9
42		52 (15.4)	>1	ND	4.8
43		4.2 (3.56)	13	98	3.6
44		42 (1.59)	>2	86	4.6
45		2.6 (0.66)	>25	18	3.1

ND: not determined; SD: standard deviation of the analyses; SI: Selectivity index relative to MRC-5 cells (CC₅₀/IC₅₀); MLM: Mouse Liver Microsome; ^a IC₅₀ represented in μ M, ^b Intrinsic clearance represented in μ L/min/mg. ^c Calculated LogD. IC₅₀ of benznidazole (reference) was 2.1 μ M.

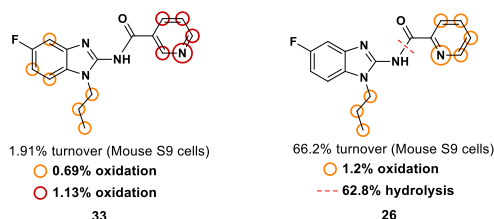


Fig. 2. MetID of 26 and 33.

and **54**, with trifluoromethyl attached to a pyrazole ring, showed good potency (IC₅₀ 0.23 and 1.5 μ M, respectively) with SI > 30 and MLM clearance < 30 μ L/min/mg.

Secondary mechanistic *in vitro* studies using high-content screening methods were performed to investigate additional aspects of the anti-*T. cruzi* activity of selected compounds, such as the maximum activity considering both reduction in the numbers of amastigotes per cell and decrease of total infected cells, and the ability to prevent *in vitro* parasite relapse in wash-out assays [18]. These secondary assays are critical for Chagas disease drug discovery, which requires compounds that can eliminate the parasites from infected cells and prevent disease re-emergence. Upon treatment, low numbers of residual viable parasites can recrudescence and potentially cause failure of clinical candidates. At 10 μ M, **45**, **46**, **53** and **54** had maximal activities comparable to benznidazole (> 95%) for reduction of intracellular amastigote populations and infection rates in primary mouse macrophages (PMM) after 96 h incubation (Table 5). When compounds were tested using an assay that employs 3T3 cells and a shorter treatment duration (48 h), only analogues **53** and **46** showed measurable IC₅₀ values (0.99 and 1.32 μ M, respectively) (Benznidazole IC₅₀ in this assay was around 4 μ M). The

maximum activity values at 36.6 μ M and 48 h of incubation were 60% and 56% for **45** and **54**, respectively. These data indicate that the antiparasitic activity for this series is both concentration- and time-dependent. The compounds might be slow killers that require more cycles of parasite replication to exert antiparasitic activity (in comparison with standard reactive drugs that are fast killers). However, an effect related to the different cell lines used in these assays cannot be discarded.

We also tested compounds in a wash-out assay to assess their ability to clear all parasites *in vitro*. Wash-out assays were performed using PMM cells infected with *T. cruzi* and treated at different concentrations for 4 days followed by a recovery period of 7 days. Under these conditions, the tested compounds were unable to sterilize the cultures, indicating a suppressive, rather than a curative, effect *in vitro*. Under the same conditions, neither Benznidazole nor Posaconazole sterilized the *in vitro* cultures.

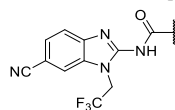
ND: not determined; ^a *in vitro* maximal activity in terms of reduction of intracellular amastigote population and infection rate in PMM cells at 96 h of incubation when tested at 10 μ M; ^b IC₅₀ and IC₉₀ against amastigote in PMM cells at 96 h of incubation; ^c IC₅₀ against amastigote in 3T3 cells at 48 h of incubation.

Further *in vitro* ADME-Tox and physicochemical properties were evaluated (Table 6). These compounds showed moderate to high permeability; however, kinetic solubilities (KS) were poor at both pH 2.0 and pH 7.4. *In vitro* cytotoxicity against various mammalian cell lines was assessed. Whilst cytotoxicity against the *T. cruzi* assay host cell line (MRC-5) used in the first-tier screening was generally low, it was significantly more pronounced against HepG2 and PMM cells, representing a major liability for this series. In contrast, screening against an off-target panel covering key human targets showed little cause for concern. The full dataset is presented in the Supporting Information.

The low solubility of this series is likely a result of a flat

Table 4

Antitrypanosomal activity, selectivity and initial ADME properties for the most active compounds with introduction of heteroaromatic groups at acyl fragment..

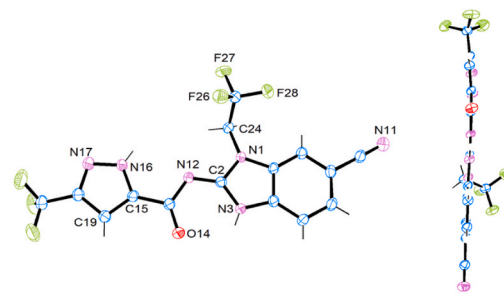


Compound	Substituent	<i>T. cruzi</i> IC ₅₀ ^a (SD)	SI	MLM Cl _{int} ^b in vitro	eLogD
46		0.28 (0.30)	>231	27	3.1
47		2.3 (2.22)	>28	170	4.9
48		0.24 (0.21)	8	ND	3.4 ^c
49		0.54 (0.01)	14	595	3.5 ^c
50		1.6 (1.58)	8	20	2.7
51		0.99 (0.93)	3	ND	2.9 ^c
52		4.3 (1.19)	>15	299	4.9
53		0.23 (0.96)	34	28	3.0
54		1.5 (3.19)	>42	25	2.9

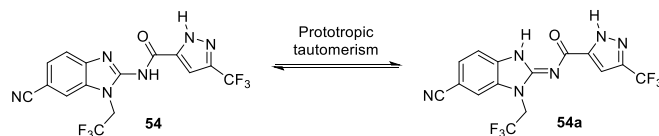
ND: not determined; SD: standard deviation of the analyses; SI: Selectivity index relative to MRC-5 cells (CC₅₀/IC₅₀); MLM: Mouse Liver Microsome; ^a IC₅₀ represented in μ M; ^b Intrinsic clearance represented in μ L/min/mg; ^c Calculated LogD. IC₅₀ of benznidazole (reference) was 2.1 μ M.

Table 5*In vitro* secondary parasitology for selected compounds.

Compound	% Efficacy (amastigote population) ^a	% Efficacy (infection rate) ^a	IC ₅₀ (μ M) 96h ^b	IC ₉₀ (μ M) 96h ^b	IC ₅₀ (μ M) 48h ^c
45	99	98	0.19	0.57	ND
54	99	97	0.57	0.88	ND
53	99	97	0.19	0.36	0.99
46	98	91	0.14	0.31	1.32
Benznidazole	99	94	2.62	12.59	2.57
Posaconazole	100	98	0.0007	0.002	0.002



conformation, as observed in the X-ray crystal structure of **54** (Fig. 3). This flat conformation is the result of a prototropic tautomerism in **54** generating the tautomer **54a**, with contribution of probable hydrogen bonds between the N–H moieties and carbonyl group. Decreasing crystal packing energy by introducing out-of-plane substitution and increasing the polarity are effective strategies to increase solubility for this series of

**Fig. 3.** Crystal structure of **54**.**Table 6***In vitro* ADME-Tox and physicochemical properties of selected compounds.

Compound	KS at pH 2.0 (μ M)	KS at pH 7.4 (μ M)	PAMPA (10^{-6} cm/s)	CC ₅₀ 3T3	CC ₅₀ MRC-5	CC ₅₀ PMM	CC ₅₀ L6	CC ₅₀ HepG2
45	<1.0	<1.0	5.4	>40	>64	8.0	18	1.1
46	<1.0	<1.0	2.3	>40	>64	4.0	50	2.4
53	<1.0	<1.0	2.4	>40	8.0	1.0	19	1.1
54	<1.0	<1.0	2.0	>40	>64	25	12	1.8

KS: kinetic solubilities; PAMPA: Parallel Artificial Membrane Permeation Assay; 3T3: mouse embryonic fibroblasts; MRC-5: human lung fibroblasts; PMM: primary peritoneal mouse macrophages; L6: rat skeletal muscle myoblast; HepG2: human hepatocyte carcinoma.

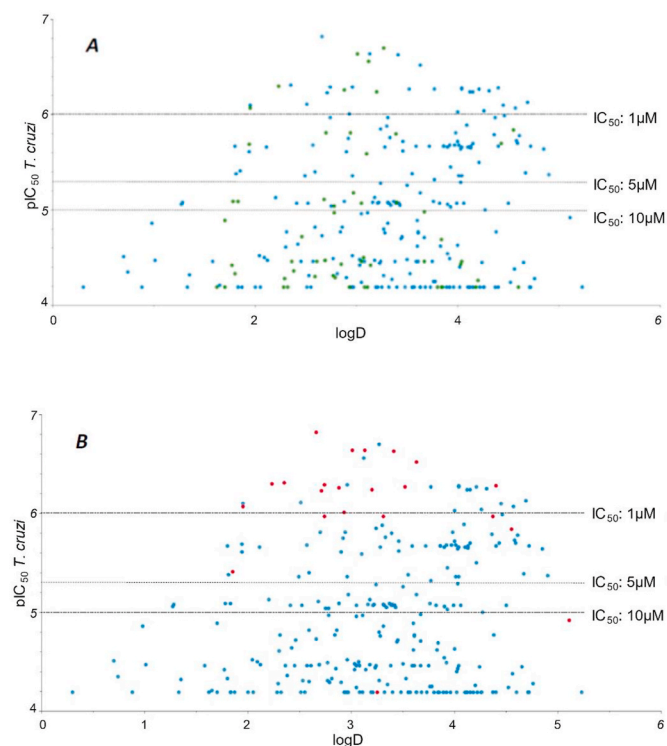


Fig. 4. Graphic of cLogD vs *T. cruzi* pIC₅₀. A) Green spots represent compounds with MLM clearance < 50 µL/min/mg; B) Red spots represent compounds with MRC-5 CC₅₀ < 10 µM.

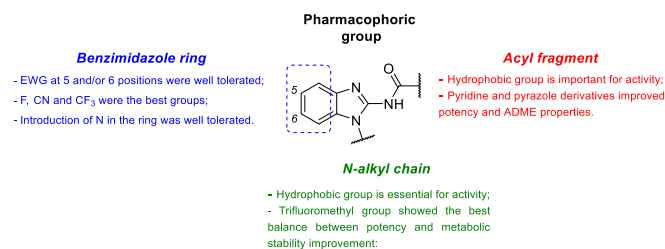


Fig. 5. Summary of SAR and SPR analysis.

molecules [35].

A few additional structural modifications were explored through inclusion of polar and/or ionizable groups or reduction of hydrophobicity in the benzimidazole ring and *N*-alkyl chain (Table S2) in an attempt to generate candidates with a better combination of potency, selectivity and *in vitro* pharmacokinetic properties. Despite significant medicinal chemistry efforts, we were unable to identify further optimized analogues. For this reason, and in combination with the toxic effects observed in another study with this series [29], we decided to terminate the hit-to-lead efforts without progressing a lead candidate into animal models of *T. cruzi* infection.

In summary, a total of 277 compounds were synthesized and evaluated. An overview of the interplay between potency, lipophilicity, cytotoxicity and microsomal metabolic stability is shown in Fig. 4. Good levels of potency (IC₅₀ < 10 µM) were observed within a wide range of lipophilicity values (LogD between 1.5 and 5), and the great majority of compounds showed submicromolar IC₅₀ values with LogDs between 1.7 and 3.5. The most metabolically stable compounds (MLM clearance < 50 µL/min/mg) had LogDs < 3.5, corroborating the assumption that reducing lipophilicity is a useful strategy to lower overall *in vitro* microsomal clearance. The hit-to-lead strategy to decrease LogD and block metabolic soft spots was successful in generating compounds with

satisfactory levels of *in vitro* potency, metabolic stability, and lipophilicity (Fig. 4A). Unfortunately, some of the most potent compounds (IC₅₀ < 1 µM) also showed high cytotoxicity (MRC-5 CC₅₀ < 10 µM), which may be related to the mechanism of action. However, not all active compounds were cytotoxic at this level (Fig. 4B).

The main SAR and SPR conclusions are reported in Fig. 5. The *N*-alkyl-*N'*-acylaminobenzimidazole moiety seems to be the minimal pharmacophore for anti-*T. cruzi* activity. Introduction of EWGs in the benzimidazole ring and addition of nitrogen within the benzimidazole ring were well tolerated in terms of potency and improved microsomal stability. A hydrophobic group at the *N*-alkyl chain is essential for potency, with a trifluoroethyl group showing the best balance between anti-*T. cruzi* activity and microsomal stability. Reduction of lipophilicity on the right-hand side with pyridine and pyrazole derivatives led to analogues with low micromolar potency and suitable ADME properties.

3. Conclusion

Starting from a highly lipophilic and metabolically unstable benzimidazole hit **1**, we identified multiple compounds with good potency against intracellular *T. cruzi* amastigotes and much improved ADME properties. Due to low kinetic solubility and *in vitro* cytotoxicity, a proof-of-concept study in a Chagas disease animal model was not considered. Ongoing research is currently trying to identify the mechanism of action of this series to support additional drug discovery campaigns and evaluate the possibility of decoupling the observed cytotoxic effects from the antitrypanosomal activity.

4. Materials and methods

4.1. Parasite and cell cultures

T. cruzi, Tulahuen CL2, beta-galactosidase strain was used for the routine antiparasitic assay. The strain was maintained on MRC-5 (human lung fibroblast) cells in MEM medium, supplemented with 200 mM L-glutamine, 16.5 mM NaHCO₃, and 5% inactivated fetal calf serum (FCS). All cultures and assays were conducted at 37 °C under an atmosphere of 5% CO₂.

4.2. Compound solutions/dilutions

Compound stock solutions were prepared in 100% DMSO at 20 mM. The compounds were serially pre-diluted (2-fold or 4-fold) in DMSO followed by a further (intermediate) dilution in demineralized water to assure a final in-test DMSO concentration of < 1%. The compounds were tested at 4-fold compound dilutions covering a range of 64 down to 0.00024 µM.

4.3. Parasitology assays

Routine *T. cruzi* assays were performed in sterile 96-well microtiter plates. Each well contained 10 µL of the compound dilutions together with 190 µL of MRC-5_{v2} cell/parasite inoculum (4 × 10³ cells/well + 4 × 10⁴ parasites/well). Parasite growth was compared to untreated-infected controls (100% growth) and non-infected controls (0% growth) after 7 days incubation at 37 °C and 5% CO₂. Parasite burdens were assessed after adding the substrate CPRG (chlorophenol red β-D-galactopyranoside): 50 µL/well of a stock solution containing 15.2 mg CPRG + 250 µL Nonidet in 100 mL PBS. Change in color was measured spectrophotometrically at 540 nm after 4 h incubation at 37 °C. The results were expressed as % reduction in parasite burdens compared to control wells, and an IC₅₀ (50% inhibitory concentration) was calculated. Benzimidazole was included as the reference drug (IC₅₀ ~2–5 µM). The wash-out assay was performed as described by Kaiser et al. [36]. The 48 h incubation assay in 3T3 cells was performed as described by Varghese et al. [36].

4.4. Cytotoxicity assays

Assays were performed in sterile 96-well microtiter plates, each well containing 10 μ L of the watery compound dilutions together with 190 μ L of MRC-5 inoculum (1.5×10^5 cells/mL). Cell growth was compared to untreated-control wells (100% cell growth) and medium-control wells (0% cell growth). After 3 days incubation, cell viability was assessed fluorometrically after addition of 50 μ L resazurin per well. After 4 h at 37 °C, fluorescence was measured (λ_{ex} 550 nm, λ_{em} 590 nm). The results were expressed as % reduction in cell growth/viability compared to control wells and a CC_{50} (50% cytotoxic concentration) was determined. Cytotoxic reference compounds included vinblastine or paclitaxel ($\text{CC}_{50} < 0.01 \mu\text{M}$). Cytotoxicity assays using other cell lines were performed using a similar colorimetric assay as previously described [36] or by measuring the cell ratio values during high-content screening assays.

4.5. Off-target panel

The compounds were evaluated across a panel of 20 liability targets (37 functional assays) which included functional cell-based GPCRs and ion channels in both agonist and antagonist readout, measuring calcium flux and biochemical functional assays for nuclear hormone receptors and phosphodiesterases using TR-FRET format, in a 6 point 1:3 dilution dose series (maximum final concentration of 10 μM).

4.6. Experimental determination of distribution coefficient (eLogD)

To determine the lipophilicity of the compounds, a methodology based on the retention time of molecules in reverse stationary phase (Supelco Ascentis express RP amide HPLC column 5 cm \times 2.1 mm, 2.7 μM) was used. The chromatogram was obtained using liquid chromatography-tandem mass spectrometry (LC-MS/MS). Test compounds were prepared at 1.0 $\mu\text{g/mL}$ by adding the stock solution at (1:1) mobile phases A:B + internal standard at 200 nM (A: 5% methanol in 10 mM ammonium acetate pH 7.4/B: 100% methanol), with a DMSO concentration lower than 2%. The lipophilicity of compounds was assessed by individually injecting the test compounds and a series of eight commercial drugs for which LogD values had already been determined, covering a LogD range of -1.86 to 6.1 . The retention time (in minutes) of each of the eight standards was plotted against their LogD values. The resulting equation for the calibration curve ($y = mx + b$) was used to calculate the LogD values for the test compounds.

4.7. Mouse liver microsomal stability assay

The metabolic stability of the compounds was evaluated in mouse liver microsomes (CD1 mouse, GIBCO). Test compounds were prepared at a concentration of 0.5 μM and incubated with 0.25 mg/mL liver microsomes at pH 7.4 and 37 °C. The reaction started by addition of NADPH at 0.5 μM . Samples were taken at 0, 5, 10, 20, 30 and 60 min. The reaction was stopped by addition of acetonitrile:methanol (1:1) containing an internal standard (tolbutamide at 50 nM). Compounds were quantified by LC-MS/MS. Peak area ratios (analyte/internal standard) were converted to % remaining using the area ratio at time 0 as 100%. Half-life ($t_{1/2} = \ln [2]/k$) in minutes and intrinsic clearance ($\text{CL}_{\text{int}} = k \times 1000/0.25$) in $\mu\text{L/min/mg}$ were calculated using a non-linear regression from % remaining versus incubation time. From this plot, the slope (k) was determined. The analysis conditions were: analytical column (Supelco Ascentis express C18 column 3 cm \times 2.1 mm, 5 μM); electrospray ionization source (ESI) in positive and negative mode; mobile phase A (water + 0.1% formic acid) and B (acetonitrile + 0.1% formic acid); flow rate of 0.7 mL/min.

4.8. Parallel artificial membrane permeability assays (PAMPA)

To determine the passive permeability of the compounds, a 96-well

plate containing pre-coated membranes was used (Corning Gentest # 353015). The solutions of the compounds were prepared by diluting the stock solutions (10 mM) in phosphate buffered saline (PBS) pH 6.5 at a final concentration of 10 μM . The solutions diluted in PBS pH 6.5 were then added to the donor portion of the plate (300 $\mu\text{L/well}$), while in the acceptor portion PBS pH 7.4 (200 $\mu\text{L/well}$) was added. The two portions of the plate were then coupled, and the system was incubated for 5 h at 37 °C. Samples of the initial donor solution (T0) were collected and stored at -20 °C. At the end of incubation, samples were collected from the donor and acceptor plates, and then added to plates containing Quench solution (10% water and 90% methanol: acetonitrile (50:50) + 50 nM tolbutamide); the T0 samples were treated similarly. The final concentrations of compounds in the donor, acceptor and T0 wells were quantified by LC-MS/MS. The results were used to calculate an effective permeability (Pe) value. The PAMPA assay was performed in triplicate ($n = 3$).

4.9. Kinetic solubility

To determine kinetic solubility, 10 mM samples of each compound were transferred to a 96-well plate (incubation plate) in duplicate; for each sample on the plate, 195 μL of PBS buffer pH 7.4 and 2.0 (final concentration of 250 μM) was added, and DMSO concentration was 2.5%; the plate was sealed and shaken for 24 ± 1 h (200 rpm, r.t.). The precipitates on the incubation plate were removed by centrifugation (15 min, 3000 rpm, r.t.). The supernatant fractions were quantified by LC-MS/MS. Calibration curves were prepared for each compound by diluting 10 mM samples to reach the desired concentration of 50, 40, 20, 2, and 1 μM . The resulting equation for the calibration curve ($y = mx + b$) was used to calculate the experimental concentration values.

Author contribution

C.O.R.J. took the lead in writing the manuscript; C.O.R.J., R.A.A.F., P.D.G.M., P.J.K. and B.M.S. carried out design and synthetic chemistry efforts; A.M., N.V.P., L.L.G.F., R.C.C. and S.M-D. carried out biological experiments; L.M., G.C., A.D.A., J.M.K., C.E.M. and L.C.D. conceived experiments, provided guidance about data interpretation and design of compounds; S.C. contributed to compound design and interpretation of results; J.M.K, C.E.M. and L.C.D. conceived and planned the project. All authors contributed to manuscript writing.

Declaration of competing interest

The authors declare the following financial interests/personal relationships which may be considered as potential competing interests: Luiz Carlos Dias reports financial support was provided by Fundação de Amparo a Pesquisa do Estado de São Paulo - Fapesp.

Data availability

Data will be made available on request.

Acknowledgments

We thank FAPESP (Grants 2015/50655-9, 2013/07600-3, and 2015/09080-2), CNPq (grant 140551/2017-4) and DNDi for funding; SRBU is the recipient of a senior researcher scholarship from CNPq. We further thank UNICAMP NMR and technical staff for assistance; the Thomson Mass Spectrometry Lab at UNICAMP for use of HRMS equipment; the teams at the Swiss Tropical and Public Health Institute (Dr. Marcel Kaiser) and AbbVie for in kind secondary profiling of compounds, and Dr. Dale Kempf (AbbVie) and Dr. Michael Schrimpf (AbbVie) for helpful discussions; and Dr. André L.B. Formiga for his valuable support in the X-ray crystallographic studies. DNDi is grateful to its donors, public and private, who have provided funding for all DNDi activities since its

inception in 2003. A full list of DNDi's donors can be found at <http://www.dndi.org/donors/donors/>.

Appendix A. Supplementary data

Supplementary data to this article can be found online at <https://doi.org/10.1016/j.ejmech.2022.114925>.

References

- [1] Chagas' disease C. Bern, N. Engl. J. Med. 373 (2015) 456–466.
- [2] Rick L. Tarleton, Ricardo E. Gürtler, Julio A. Urbina, Janine Ramsey, Rodolfo Viotti, Chagas disease and the London declaration on neglected tropical diseases, PLoS Neglected Trop. Dis. 8 (2014) e3219.
- [3] A.I. Porrás, Z.E. Yadon, J. Altchek, C. Britto, G.C. Chaves, L. Flevaud, et al., Target product Profile (TPP) for Chagas Disease point-of-care diagnosis and assessment of response to treatment, PLoS Neglected Trop. Dis. 9 (2015) e0003697.
- [4] D.E. Teixeira, M. Benchimol, P.H. Crepaldi, W. de Souza, Interactive multimedia to teach the life cycle of trypanosoma cruzi, the causative agent of chagas disease, PLoS Neglected Trop. Dis. 6 (2012) e1749.
- [5] Sheba Meymandi, Salvador Hernandez, Sandy Park, Daniel R. Sanchez, Colin Forsyth, Treatment of chagas disease in the United States, Curr. Treat. Options Infect. Dis. 10 (2018) 373–388.
- [6] Eric Chatelain, Chagas disease research and development: is there light at the end of the tunnel? Comput. Struct. Biotechnol. J. 15 (2017) 98–103.
- [7] Jadel Müller Kratz, Drug discovery for chagas disease: a viewpoint, Acta Trop. 198 (2019), 105107.
- [8] João Carlos Pinto Dias, 2nd Brazilian consensus on chagas disease, 2016, Rev. Soc. Bras. Med. Trop. 49 (2015) 3.
- [9] Organization, World Health, Chagas disease (American trypanosomiasis) (2020). Available from: https://www.who.int/health-topics/chagas-disease#tab=tab_1.
- [10] Research Priorities for Chagas Disease, Human African Trypanosomiasis and Leishmaniasis, Organization, World Health, 2012.
- [11] Mark C. Field, David Horn, Alan H. Fairlamb, Michael A.J. Ferguson, David W. Gray, Kevin D. Read, Manu De Rycker, Leah S. Torrie, Paul G. Wyatt, Susan Wyllie, Ian H. Gilbert, Anti-trypanosomatid drug discovery: an ongoing challenge and a continuing need, Nat. Rev. Microbiol. 15 (2017) 217–231.
- [12] R. Viotti, C. Vigliano, B. Lococo, M.G. Alvarez, M. Petti, G. Bertocchi, A. Armenti, Side effects of benznidazole as treatment in chronic Chagas disease: fears and realities, Expert Rev. Anti-infect. Ther. 7 (2009) 157–163.
- [13] Juan Diego Maya, Bruce K. Cassels, Patricio Iturriaga-Vásquez, Jorge Ferreira, Mario Faúndez, Norbel Galanti, Arturo Ferrei, Mode of action of natural and synthetic drugs against Trypanosoma cruzi and their interaction with the mammalian host, Comp. Biochem. Physiol. Mol. Integr. Physiol. 146 (2007) 601–620.
- [14] Fernando Altamura, Rishi Rajesh, M. Carolina, C. Catta-Preta, Nilmar S. Moretti, Igor Cestari, The Current Drug Discovery Landscape for Trypanosomiasis and Leishmaniasis: Challenges and Strategies to Identify Drug Targets, Drug Development Research, 2020, pp. 1–28.
- [15] Eric Chatelain, Chagas disease drug discovery: toward a new era, J. Biomol. Screen 20 (2015) 22–35.
- [16] I. Molina, et al., Randomized trial of posaconazole and benznidazole for chronic Chagas' disease, N. Engl. J. Med. 370 (2014) 1899–1908.
- [17] Cristiane Menezes, Germano Carneiro Costa, Kenneth J. Gollob, Walderez O. Dutra, Clinical aspects of Chagas disease and implications for novel therapies, Drug Dev. Res. 72 (2011) 471–479.
- [18] Lorna M. MacLean, John Thomas, Michael D. Lewis, Ignacio Cotillo, David W. Gray, Manu De Rycker, Development of Trypanosoma cruzi in vitro assays to identify compounds suitable for progression in Chagas' disease drug discovery, PLoS Neglected Trop. Dis. 12 (2018) e0006612.
- [19] Faustino Torrico, Joaquim Gascón, Fabiana Barreira, et al., New Regimens of Benznidazole Monotherapy and in Combination with Fosravuconazole for Treatment of Chagas Disease (BENDITA): a Phase 2, Double-Blind, Randomised Trial, The Lancet Infectious Diseases, 2021.
- [20] M.C. Field, et al., Anti-trypanosomatid drug discovery: an ongoing challenge and a continuing need, Nat. Rev. Microbiol. 15 (2017) 217–231.
- [21] Kei Katsuno, Jeremy N. Burrows, Ken Duncan, Hooft Rob van Huijsduijnen, Takushi Kaneko, Kiyoshi Kita, Charles E. Mowbray, Dennis Schmatz, Peter Warner, B.T. Slingsby, Hit and lead criteria in drug discovery for infectious diseases of the developing world, Nat. Rev. Drug Discov. 14 (2015) 751–758.
- [22] Wunberg Tobias, Hendrix Martin, Hillisch Alexander, Mario Lobell, Heinrich Meier, Carsten Schmeck, Hanno Wild, Berthold Hinzen, Improving the hit-to-lead process: data-driven assessment of drug-like and lead-like screening hits, Drug Discov. Today 11 (2006) 175–180.
- [23] A. Alanine, et al., Lead generation – enhancing the success of drug discovery by investing the hit to lead process, Comb. Chem. High Throughput Screening 6 (2003) 51–66.
- [24] Giulio Vistoli, Alessandro Pedretti, Bernard Testa, Assessing drug-likeness – what are we missing? Drug Discov. Today 13 (2008) 285–294.
- [25] Eric Chatelain, Jean-Robert Ioset, Drug discovery and development for neglected diseases: the DNDi model, Drug Des. Dev. Ther. 5 (2011) 175–181.
- [26] P. Gribbon, A. Sewing, High-throughput drug discovery: what can we expect from HTS? Drug Discov. Today 10 (2005) 17–22.
- [27] G.M. Milne, Pharmaceutical productivity – the imperative for new paradigms, Annu. Rep. Med. Chem. 38 (2003) 383–396.
- [28] I. Peña, M. Pilar Manzano, J. Cantizani, et al., New compound sets identified from high throughput phenotypic screening against three kinetoplastid parasites: an open resource, Sci. Rep. 5 (2015) 8771.
- [29] R.A.A. Ferreira, CdOR. Junior, P.D.G. Martinez, P.J. Koovits, B.M. Soares, L.L. G. Ferreira, et al., 2-aminobenzimidazoles for leishmaniasis: from initial hit discovery to in vivo profiling, PLoS Neglected Trop. Dis. 15 (2) (2021) e0009196.
- [30] Nicole McNamara, Raphael Rahmani, Melissa L. Sykes, Vicky M. Avery, Jonathan Baell, Hit-to-lead optimization of novel benzimidazole phenylacetamides as broad spectrum trypanosomacides, RSC Med. Chem. 11 (2020) 685–695.
- [31] Michael J. Waring, Lipophilicity in drug discovery, Expert Opin. Drug Discov. 5 (2010) 235–248.
- [32] A.F. Nassar, A.M. Kamel, C. Clarimont, Improving the decision-making process in the structural modification of drug candidates: enhancing metabolic stability, Drug Discov. Today 9 (2004) 1020–1028.
- [33] Di Li, Edward H. Kerns, Guy T. Carter, Drug-like property concepts in pharmaceutical design, Curr. Pharmaceut. Des. 15 (2009) 2184–2194.
- [34] Randy R. Miller, et al., Integrating the impact of lipophilicity on potency and pharmacokinetic parameters enables the use of diverse chemical space during small molecule drug optimization, J. Med. Chem. 63 (2020) 12156–12170.
- [35] Minoru Ishikawa, Yuichi Hashimoto, Improvement in aqueous solubility in small molecule drug discovery programs by disruption of molecular planarity and symmetry, J. Med. Chem. 54 (2011) 1539–1554.
- [36] Swapna Varghese, et al., Discovery of potent N-ethylurea pyrazole derivatives as dual inhibitors of trypanosoma brucei and trypanosoma cruzi, ACS Med. Chem. Lett. 11 (2020) 278–285.

SUPPORTING INFORMATION

Hit-to-lead optimization of a 2-aminobenzimidazole series as new candidates for Chagas disease.

Celso de Oliveira Rezende Júnior^{‡1}, Pablo David Grigol Martinez^{‡1}, Rafael Augusto Alves Ferreira^{‡1}, Paul John Koovits¹, Bruna Miranda Soares¹, Leonardo L. G. Ferreira², Simone Michelan-Duarte², Rafael Consolin Chelucci², Adriano D. Andricopulo², An Matheeussen⁴, Natascha Van Pelt⁴, Guy Caljon⁴, Louis Maes⁴, Simon Campbell⁵, Jadel M. Kratz⁵, Charles E. Mowbray⁵, Luiz Carlos Dias¹

¹Institute of Chemistry, University of Campinas (UNICAMP), Campinas-SP, 13083-861, Brazil

²Laboratory of Medicinal and Computational Chemistry, Physics Institute of São Carlos, University of São Paulo (USP), São Carlos-SP, 13563-120, Brazil

⁴Laboratory of Microbiology, Parasitology and Hygiene (LMPH), Universiteitsplein 1, 2610 Antwerpen, Belgium

⁵Drugs for Neglected Diseases *initiative* (DNDⁱ), 15 Chemin Camille-Vidart, 1202 Geneva, Switzerland

[‡] These authors contributed equally

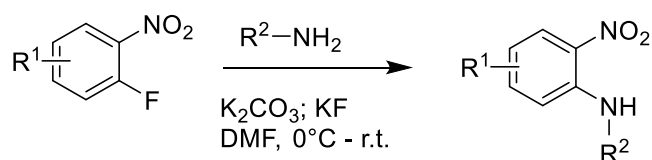
*To whom correspondence should be addressed. L.C.D.: telephone: + 55 19 3521 3097; email: ldias@unicamp.br

Synthetic Chemistry

Unless noted, all reactions were performed under an atmosphere of argon with dry solvents and magnetic stirring. Dichloromethane (DCM) and triethylamine (Et₃N) were distilled from CaH₂. Tetrahydrofuran (THF) was distilled from sodium/benzophenone. Dimethyl formamide (DMF) was purchased from Aldrich (anhydrous) and used without further purification. Yields refer to homogeneous materials obtained after purification of reaction products by flash column chromatography using silica gel (200-400 mesh), liquid-liquid extraction or recrystallization. Analytical thin-layer chromatography was performed on silica-gel 60 and GF (5-40 μ m thickness) plates, and visualization was accomplished using UV light, basic potassium permanganate staining or ninhydrine solution followed by heating. ¹H and proton-decoupled ¹³C NMR spectra were acquired in CDCl₃, CD₃OD or *d*₆-DMSO at 250 MHz (¹H) and 62.5 MHz (¹³C) (Bruker DPX250), at 400 MHz (¹H) and 100 MHz (¹³C) (Bruker Avance 400), at 500 MHz (¹H) and 125 MHz (¹³C) (Varian Inova 500), or at 600 MHz (¹H) and 150 MHz (¹³C) (Bruker Avance 600). Chemical shifts (δ) are reported in ppm using residual undeuterated solvent as an internal standard (CDCl₃ at 7.26 ppm, CD₃OD at 3.31 ppm, *d*₆-DMSO at 2.50 ppm, and TMS at 0.00 ppm for ¹H NMR spectra and CDCl₃ at 77.16 ppm, CD₃OD at 49.0 ppm, *d*₆-DMSO at 39.52 ppm for ¹³C NMR spectra). Multiplicity data are reported as follows: s = singlet, d = doublet, t = triplet, q = quartet, br s = broad singlet, dd = doublet of doublets, dt = doublet of triplets, ddd = doublet of doublet of doublets, tt = triplet of triplets, app d = apparent doublet, app t = apparent triplet, m = multiplet, and br m = broad multiplet. The multiplicity is followed by the coupling constant(s) in Hz and integration. High resolution mass spectrometry (HRMS) was measured using electrospray ionization (ESI) (waters

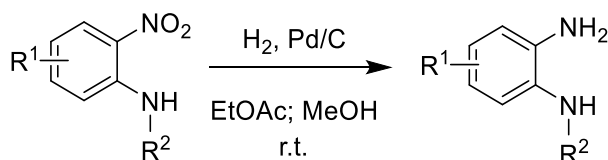
xevo Q-tof, thermo LTQ-FT ultra, or thermos Q exactive) or using electron ionization (EI) (GCT premier waters). The synthesis and description of compounds **2**, **12-14**, **16-24**, **41**, **45-48**, **50**, **51** and **53** were previously reported (1). All presented compounds were synthesized, characterized and tested within the development of this work. Details of synthetic and characterization data present only in the supporting information are available upon request.

Method A: Nucleophilic substitution reactions with amines



To a stirring solution of 2-fluoronitrobenzene derivatives in DMF (concentration of 0.5 mol.L⁻¹) was added K₂CO₃ (1.0 equiv.), KF (1.0 equiv.) and corresponding primary amines (1.1 equiv.) at 0°C. The reaction was stirred at room temperature until the consumption of the 2-fluoronitrobenzene. Water (15-fold DMF amount) was added at room temperature and the formed solid was filtered and washed with water. The solid was dried in the high vacuum, generating the desired aniline. When a solid was not formed after water addition, the solution was extracted with diethyl ether. The organic layer was dried with magnesium sulfate, filtered and evaporated, giving the aniline product.

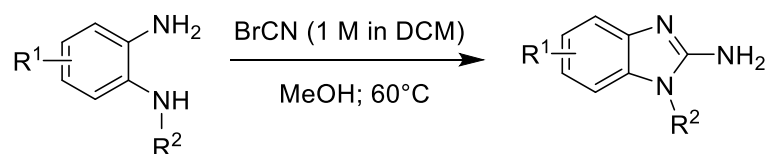
Method B: Reduction reaction of nitro groups



To a stirring solution of nitrobenzene derivatives in mixture of EtOAc and MeOH (1:1, concentration of 0.2 mol.L⁻¹) was added 10% Pd/C (10 mol %) at room temperature.

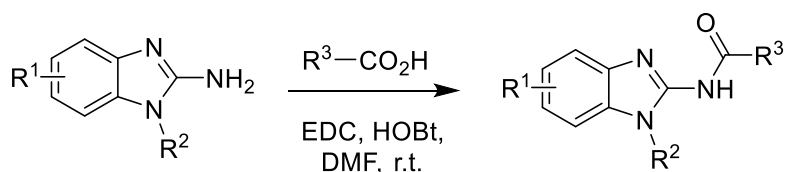
Hydrogen gas (1 bar) was added until the consumption of the nitrobenzene derivative. The solution was filtered through celite and evaporated under reduced pressure, generating the phenylenediamine derivatives.

Method C: Construction of aminobenzimidazole fragment



To a stirring solution of phenylenediamine derivatives in methanol (concentration of 1.0 mol.L⁻¹) in a sealed tube, was added a 1.0 mol.L⁻¹ fresh solution of cyanogen bromine (1.5 equiv.) at room temperature. The reaction was stirred at 60°C until the consumption of phenylenediamine derivative. The reaction was quenched at room temperature with a solution of NaOH (2.0 mol.L⁻¹). The organic layer was separated and washed with brine. The DCM layer was dried with magnesium sulfate, filtered and evaporated under reduced pressure, giving the desired aminobenzimidazole fragment.

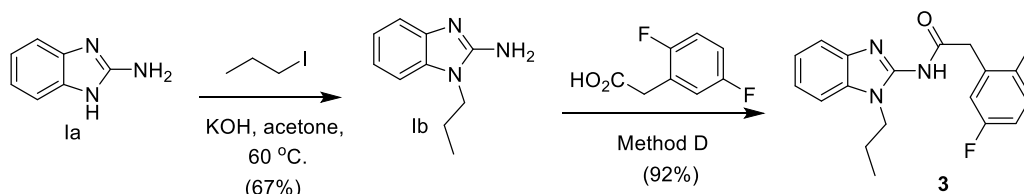
Method D: EDC-coupling reaction



To a stirring solution of aminobenzimidazole in a minimal possible amount of DMF was added EDC (1.2 equiv.), HOBt (1.0 equiv.) and the corresponding carboxylic acid (1.1 equiv.) at room temperature. The reaction was stirred until the consumption of aminobenzimidazole. Excess of water was added and the mixture was stirred for 15 minutes at room temperature. The solid was filtered and washed with water and dried in

the high vacuum, generating the desired acyl aminobenzimidazole. A flash chromatography column was performed for some final compounds.

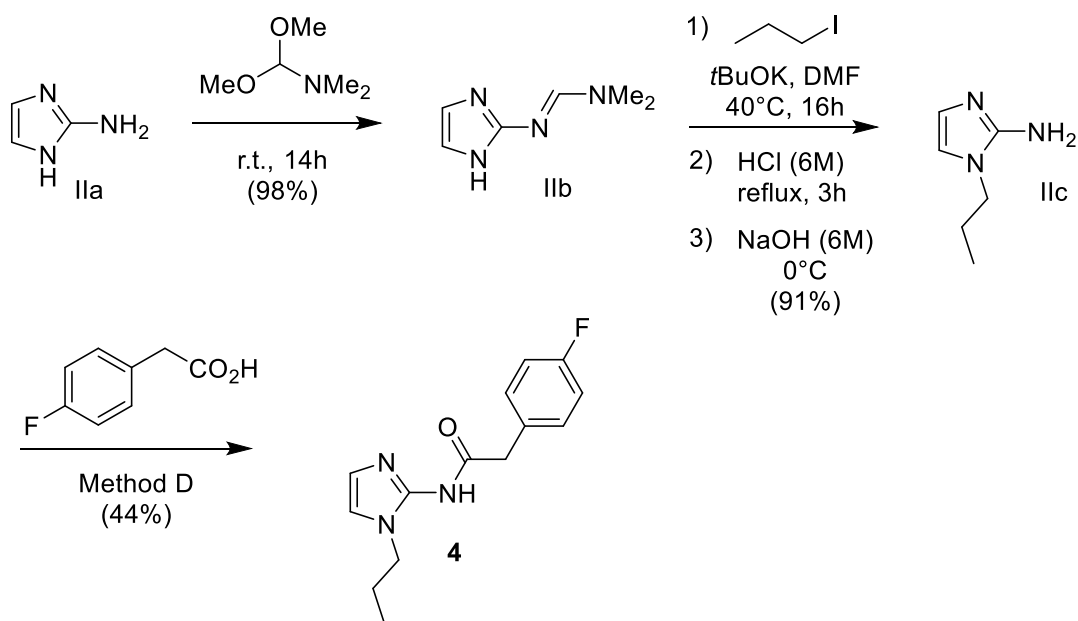
2-(2,5-difluorophenyl)-*N*-(1-propyl-1*H*-benzo[d]imidazol-2-yl)acetamide (**3**)



To a stirred solution of 2-aminobenzimidazole **1a** (531 mg; 4 mmol) in acetone PA (20 mL), KOH (450 mg; 8 mmol) and then Pr-I (0.39 mL; 4 mmol) were added. After 3 h at 60°C (oil bath temperature) the volatiles were removed, and water (1 mL) was added. The product was extracted with EtOAc (4 × 8 mL), dried over Na₂SO₄ and purified by flash column chromatography (DCM:MeOH 9:1) to yield 468 mg (67%) of the desired alkylated compound **1b**. The compound **3** was prepared in 92% yield using the method D.

3; ¹H NMR (500 MHz, CDCl₃) δ 7.30 – 7.17 (m, 4H), 7.09 (ddd, *J* = 8.8, 5.7, 3.2 Hz, 1H), 6.99 (td, *J* = 8.9, 4.6 Hz, 1H), 6.93 – 6.85 (m, 1H), 4.02 (t, *J* = 7.2 Hz, 2H), 3.81 (s, 2H), 1.94 – 1.62 (m, 2H), 0.92 (t, *J* = 7.4 Hz, 3H). ¹³C NMR (126 MHz, CDCl₃) δ 181.71, 158.58 (d, *J* = 241.0 Hz), 157.48 (d, *J* = 243.5 Hz), 153.47, 129.61, 128.24, 126.65 (dd, *J* = 18.9, 8.2 Hz), 123.19, 123.08, 118.21 (dd, *J* = 24.0, 4.9 Hz), 115.90 (dd, *J* = 25.3, 8.8 Hz), 114.24 (dd, *J* = 24.0, 8.5 Hz), 111.32, 109.51, 43.82, 40.41, 21.77, 11.34. HRMS *m/z* calculated for C₁₈H₁₈F₂N₃O⁺ [M+H]⁺ 330.1412, found 330.1407.

2-(4-fluorophenyl)-*N*-(1-propyl-1*H*-imidazol-2-yl)acetamide (**4**)



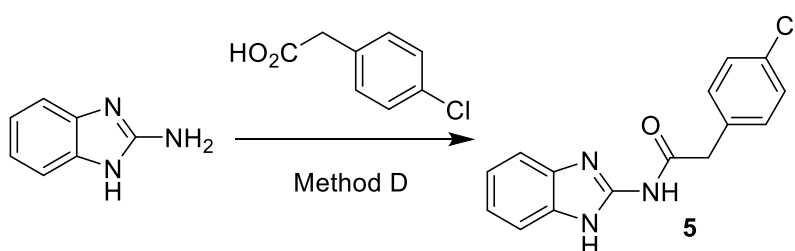
A solution of **IIa** (3 mmol) in *N,N*-dimethylformamide dimethyl acetal (5 mL) was stirred at room temperature for 14h. The mixture was evaporated under reduced pressure and the residue was purified by flash chromatographic column (3 DCM : 1 Et₃N) giving **IIb** in 98% yield (2).

To a solution of **IIb** (270 mg; 1.95 mmol) in DMF (10 mL) was added *n*-propyl iodide (0.29 mL; 2.93 mmol) and potassium *tert*-butoxide (0.44 g; 3.91 mmol) at room temperature. The mixture was stirred for 16 h at 40°C. Then, it was added water (15 mL) at room temperature, and the mixture was extracted with EtOAc (3 × 30 mL), the organic layer was dried with magnesium sulfate, filtered and evaporated under reduced pressure. To the crude was added HCl (6 M) and the solution was stirred at reflux for 3h. Then, NaOH (6 M) was added at 0°C until pH 7. The mixture was extracted with DCM (4 × 40 mL), the organic layer was dried with magnesium sulfate, filtered and evaporated under reduced pressure giving **IIc** in 91% yield.

The compound **4** was prepared in 44% yield from **IIc** using the Method D.

4; ¹H NMR (500 MHz, DMSO) δ 10.22 (s, 1H), 7.44 – 7.35 (m, 2H), 7.16 (t, *J* = 8.8 Hz, 2H), 7.06 (s, 1H), 6.76 (s, 1H), 3.60 (s, 2H), 3.56 (t, *J* = 7.6 Hz, 2H), 1.60 – 1.49 (m, H), 0.71 (t, *J* = 7.3 Hz, 3H). **¹³C NMR (126 MHz, DMSO)** δ 162.55, 160.63, 132.67, 131.45, 131.41, 131.35, 119.16, 115.54, 115.37, 115.22, 46.89, 23.43, 11.27. **HRMS** *m/z* calculated for C₁₄H₁₇FN₃O⁺ [M+H]⁺ 262.1350, found 262.1351.

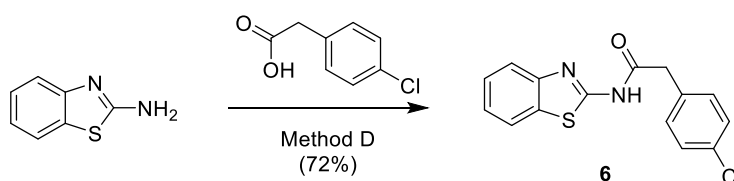
***N*-(1*H*-benzo[*d*]imidazol-2-yl)-2-(4-chlorophenyl)acetamide (5)**



The compound **5** was prepared in 73% yield using the Method D.

5; ¹H NMR (400 MHz, DMSO) δ 12.02 (s, 1H), 11.79 (s, 1H), 7.61 – 7.26 (m, 3H), 7.07 (dd, *J* = 6.0, 3.1 Hz, 1H), 3.79 (s, 2H). **¹³C NMR (101 MHz, DMSO)** δ 170.05, 146.47, 134.20, 131.54, 131.17, 128.31, 123.72, 121.03, 115.14, 41.48.

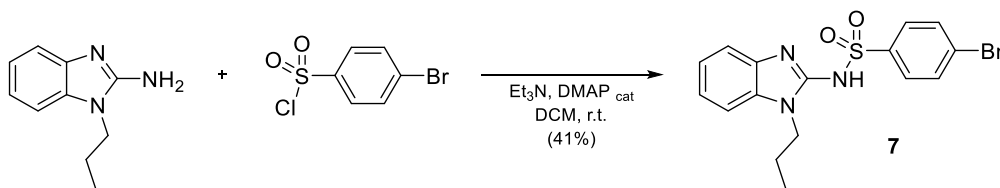
***N*-(benzo[*d*]thiazol-2-yl)-2-(4-chlorophenyl)acetamide (6)**



The compound **6** was prepared in 72% yield using the Method D.

6; ¹H NMR (500 MHz, CDCl₃) δ 9.99 (s, 1H), 7.84 (d, *J* = 7.9 Hz, 1H), 7.74 (d, *J* = 8.1 Hz, 1H), 7.49 – 7.39 (m, 1H), 7.32 (d, *J* = 8.4 Hz, 2H), 7.17 (d, *J* = 8.3 Hz, 2H), 3.80 (s, 2H). **¹³C NMR (126 MHz, CDCl₃)** δ 168.94, 158.50, 148.10, 134.26, 132.25, 131.25, 130.90, 129.57, 126.61, 124.40, 121.75, 120.89, 42.86.

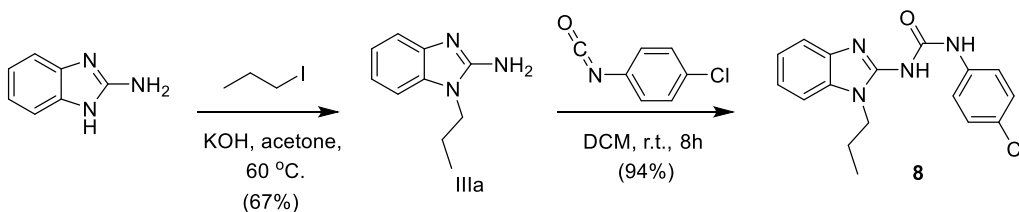
4-bromo-*N*-(1-propyl-1*H*-benzo[*d*]imidazol-2-yl)benzenesulfonamide (7)



To a solution of 1-propyl-1*H*-benzo[*d*]imidazol-2-amine (40 mg, 0.23 mmol) and DMAP (5.6 mg; 0.046 mmol, 20 mmol%) in dichloromethane (1.18 mL), 4-bromobenzenesulfonyl chloride (64 mg, 0.25 mmol, 1.1 eq) and triethylamine (0.095 mL, 0.69 mmol, 3.0 eq) were added at room temperature. The yellow reaction mixture was stirred overnight and then 0.5 mL of water was added. The product was extracted with DCM (3x3 mL) and the combined organic extracts were dried with MgSO_4 and filtrated. Removal of volatiles afforded 99.5 mg of white solid. The crude product was purified by flash column chromatography (Hex:AcOEt 35%) to yield 37 mg (41%) of the desired sulfonamide as a white solid.

7; ^1H NMR (250 MHz, CDCl_3) δ 10.36 (s, 1H), 7.83 (d, $J = 8.6$ Hz, 2H), 7.57 (d, $J = 8.4$ Hz, 2H), 7.33 – 7.10 (m, 4H), 3.96 (t, $J = 7.3$ Hz, 2H), 1.86 – 1.65 (m, 2H), 0.88 (t, $J = 7.4$ Hz, 3H). **^{13}C NMR (63 MHz, CDCl_3)** δ 149.66, 142.87, 132.04, 129.93, 128.32, 127.70, 126.46, 123.46, 123.32, 111.23, 109.44, 43.89, 21.58, 11.29.

1-(4-chlorophenyl)-3-(1-propyl-1*H*-benzo[*d*]imidazol-2-yl)urea (8)



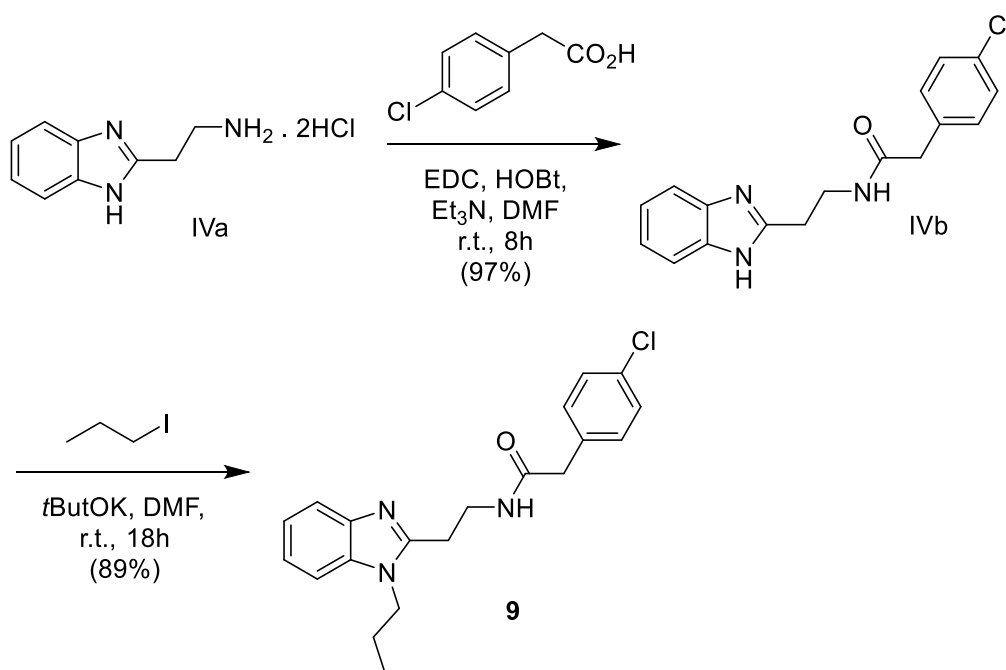
To a stirred solution of 2-aminobenzimidazole (531 mg; 4 mmol) in acetone PA (20 mL), KOH (450 mg; 8 mmol) and then *n*-propyl iodide (0.39 mL; 4 mmol) were added. After 3 h at 60 °C the volatiles were removed and water (1 mL) was added. The product was

extracted with EtOAc (4×8 mL), dried over Na_2SO_4 and purified by flash column chromatography (DCM:MeOH 9:1) to yield 468 mg (67%) of the desired alkylated compound **IIIa**.

To a solution of **IIIa** (85 mg; 0.49 mmol) in DCM (3 mL) was added 1-chloro-4-isocyanatobenzene (82 mg; 0.53 mmol) at room temperature. After 8h, the solution was washed with water (2×3 mL), the organic layer was dried with magnesium sulfate, filtered and evaporated under reduced pressure. The mixture was purified by flash column chromatography (EtOAc:Hex 1:1) to yield 131 (94%).

8; $^1\text{H NMR}$ (400 MHz, CDCl_3) δ 11.60 (s, 1H), 7.49 (d, $J = 8.4$ Hz, 2H), 7.31 – 7.08 (m, 7H), 4.00 (t, $J = 7.3$ Hz, 2H), 1.83 (m, 2H), 0.99 (t, $J = 7.3$ Hz, 3H). $^{13}\text{C NMR}$ (101 MHz, CDCl_3) δ 162.57, 153.51, 148.29, 138.57, 129.94, 128.80, 128.63, 126.98, 122.40, 122.36, 119.77, 110.36, 108.77, 43.40, 40.04, 21.57, 11.37, 0.01. **HRMS** m/z calculated for $\text{C}_{17}\text{H}_{18}\text{ClN}_4\text{O}^+$ $[\text{M}+\text{H}]^+$ 329.1164, found 329.1171.

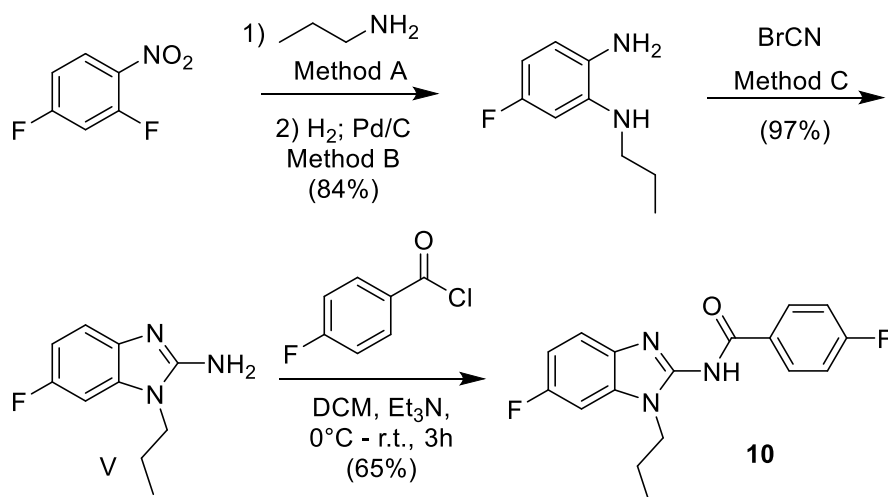
2-(4-chlorophenyl)-N-(2-(1-propyl-1H-benzo[d]imidazol-2-yl)ethyl)acetamide (9)



To a stirring solution of amine **IVa** (0.2 g; 0.85 mmol) in DMF (5 mL) were added EDC (0.2 g; 1.02 mmol), HOBt (0.14 g; 1.02 mmol), Et₃N (0.35 mL) and the corresponding carboxylic acid (0.16 g; 0.94 mmol) at room temperature. After 8h, excess of water (50 mL) was added, and the mixture was stirred for 15 minutes at room temperature. The solid was filtered and washed with water and dried in the high vacuum, generating **IVb** in 97% yield. To a stirring solution of **IVb** (0.05g; 0.16 mmol) in DMF (2 mL) were added tBuOK (0.018 g; 0.16 mmol) and propyl iodide (0.041 g; 0.24 mmol) at room temperature. After 18 h, water was added (8 mL) and the mixture was extracted with EtOAc (3 × 6 mL). The organic layer was dried with magnesium sulfate, filtered and evaporated under reduced pressure. The mixture was purified by flash column chromatography (EtOAc:Hex 1:1) to give **9** in 89% yield

9; ¹H NMR (400 MHz, CDCl₃) δ 7.79 – 7.45 (m, 1H), 7.36 – 7.24 (m, 3H), 7.21 – 7.05 (m, 5H), 4.05 – 3.97 (t, *J* = 5.9 Hz, 2H), 3.83 (dd, *J* = 11.9, 6.0 Hz, 2H), 3.48 (s, 2H), 3.00 (t, *J* = 5.9 Hz, 2H), 1.90 – 1.71 (m, 2H), 0.94 (t, *J* = 7.4 Hz, 3H). ¹³C NMR (101 MHz, CDCl₃) δ 170.70, 152.54, 142.22, 134.91, 133.34, 133.01, 130.69, 128.86, 122.33, 122.04, 119.04, 109.47, 45.08, 43.11, 36.47, 26.75, 23.06, 11.37. HRMS *m/z* calculated for C₂₀H₂₃ClN₃O⁺ [M+H]⁺ 356.1524, found 356.1529.

4-fluoro-*N*-(6-fluoro-1-propyl-1*H*-benzo[*d*]imidazol-2-yl)benzamide (10)

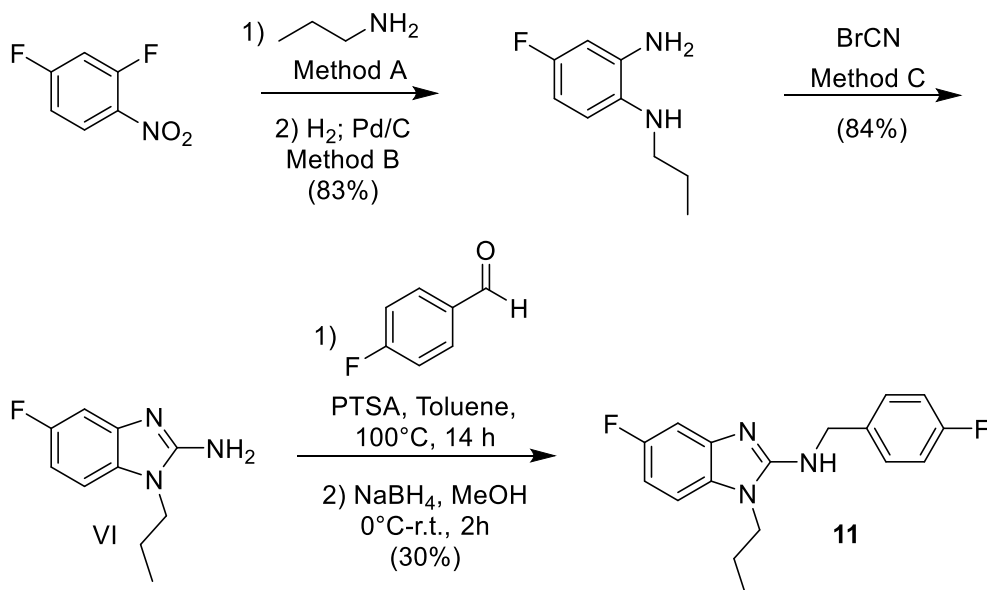


The aminobenzimidazole **V** was prepared in 82% yield using the methods A, B and C.

To a solution of **V** (61 mg; 0.32 mmol) in anhydrous DCM (3 mL) was added Et₃N (0.5 mL) and 4-fluorobenzoyl chloride (102 mg; 0.64 mmol) at 0°C. The solution was stirred at room temperature for 3h. DCM (10 mL) was added at room temperature and the mixture was washed with water (2 × 10 mL). The organic layer was dried with magnesium sulfate, filtered and evaporated under reduced pressure. The mixture was purified by flash column chromatography (EtOAc:Hex 1:1) to give **10** in 65% yield.

10; ¹H NMR (600 MHz, CDCl₃) δ 12.38 (s, 1H), 8.45 – 8.28 (m, 2H), 7.23 (dd, *J* = 8.6, 4.4 Hz, 1H), 7.14 – 7.08 (m, 2H), 7.01 – 6.91 (m, 2H), 4.18 (t, *J* = 7.4 Hz, 2H), 1.98 – 1.88 (m, 2H), 1.04 (t, *J* = 7.4 Hz, 3H). ¹³C NMR (151 MHz, CDCl₃) δ 175.52, 165.86, 164.19, 160.36, 158.76, 154.79, 134.14, 131.56, 131.50, 130.47, 130.39, 124.46, 114.89, 114.74, 111.72, 111.65, 110.22, 110.05, 97.28, 97.09, 44.05, 21.69, 11.45. HRMS *m/z* calculated for C₁₇H₁₆F₂N₃O⁺ [M+H]⁺ 316.1256, found 316.1265.

5-fluoro-*N*-(4-fluorobenzyl)-1-propyl-1*H*-benzo[*d*]imidazol-2-amine (**11**)



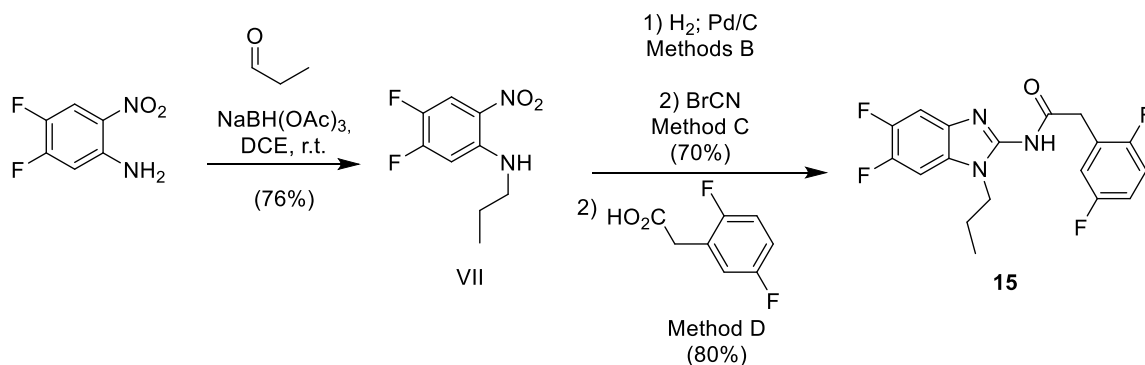
The aminobenzimidazole **VI** was prepared in 68% yield using the methods A, B and C. To a solution of **VI** (98 mg; 0.51 mmol) in anhydrous toluene (15 mL) was added PTSA (18 mg; 0.1 mmol; 20 mol%). The solution was stirred at 100°C for 14h. EtOAc (25 mL) was added at room temperature and the mixture was washed with water (20 mL). The organic layer was dried with magnesium sulfate, filtered and evaporated under reduced pressure. The mixture was purified by flash column chromatography (Et₂O:DCM 1:5) to give the corresponding imine (55 mg).

To a solution of this imine in MeOH (5 mL) was added NaBH₄ (9 mg; 0.23 mmol) at 0°C. After 2h at room temperature, water (5 mL) was added and the mixture was extracted with EtOAc (2 × 10 mL), dried over Na₂SO₄ and evaporated giving **11** in 30% yield.

11; ¹H NMR (500 MHz, CDCl₃) δ 7.39 (dd, *J* = 8.5, 5.4 Hz, 2H), 7.20 (dd, *J* = 9.6, 2.4 Hz, 1H), 7.04 (t, *J* = 8.7 Hz, 2H), 6.97 (dd, *J* = 8.6, 4.5 Hz, 1H), 6.87 – 6.78 (m, 1H), 4.73 (s, 2H), 3.85 (t, *J* = 7.3 Hz, 2H), 1.79 (h, *J* = 7.3 Hz, 2H), 0.98 (t, *J* = 7.4 Hz, 3H). ¹³C NMR (126 MHz, CDCl₃) δ 163.33, 161.37, 160.09, 158.22, 154.49, 134.25, 134.22, 130.81, 129.62, 129.55, 115.69, 115.52, 107.36, 107.27, 107.06, 106.86, 103.21, 103.01,

46.77, 44.09, 22.27, 11.44. **HRMS** m/z calculated for $C_{17}H_{16}F_2N_3O^+$ $[M+H]^+$ 316.1256, found 316.1569.

***N*-(5,6-difluoro-1-propyl-1*H*-benzo[*d*]imidazol-2-yl)-2-(2,5-difluorophenyl)acetamide (**15**)**

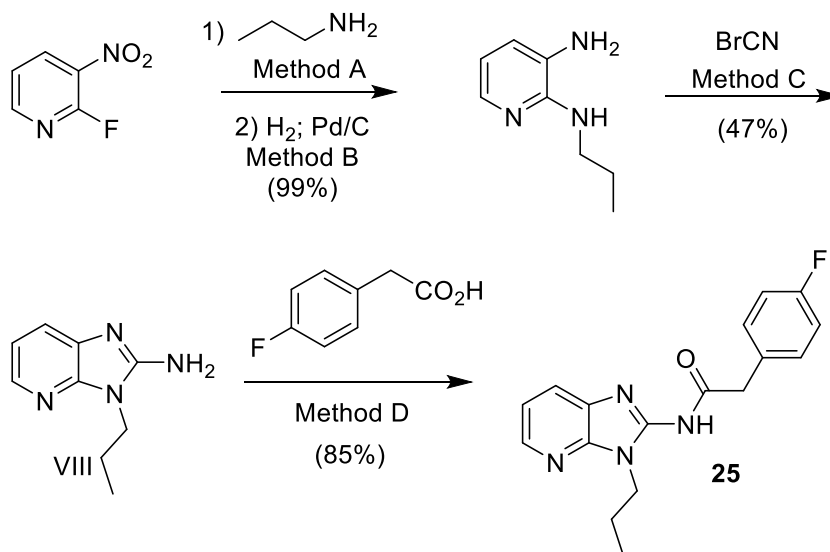


To a solution of nitroaniline (350 mg; 2 mmol) in DCE (2.4 mL), propanal (0.30 mL; 4.2 mmol) was added. After 10 min at rt, $NaBH(OAc)_3$ (1189 mg; 5.6 mmol) was added in five portions for 10 min. After stirring for 24 h at rt, DCE (4 mL), propanal (0.30 mL; 4.2 mmol) and $NaBH(OAc)_3$ (1165 mg; 5.5 mmol) were added again. The reaction mixture was allowed to stir additional 36 h and then quenched with NaOH 2 M (5 mL). The product was extracted with DCM, dried over $MgSO_4$, concentrated and purified by flash column chromatography (Hexanes:AcOEt 9:1) to yield 329 mg (76%) of the desired compound **VII**. The compound **15** was prepared in 56% yield using the methods B, C and D.

15; 1H NMR (500 MHz, $CDCl_3$) δ 12.12 (s, 1H), 7.15 – 6.95 (m, 4H), 6.94 – 6.85 (m, 1H), 4.03 – 3.89 (m, 2H), 3.79 (s, 2H), 1.83 – 1.70 (m, 2H), 0.91 (t, $J = 7.4$ Hz, 3H). **^{13}C NMR (126 MHz, $CDCl_3$)** δ 181.37, 158.58 (d, $J = 241.2$ Hz), 157.45 (d, $J = 241.0$ Hz), 154.16, 147.80 (dd, $J = 243.2$, 14.0 Hz), 147.51 (dd, $J = 243.0$, 14.1 Hz), 126.29, 125.42, 124.10, 118.18 (dd, $J = 24.0$, 4.8 Hz), 115.98 (dd, $J = 25.2$, 8.8 Hz), 114.43 (dd, $J = 23.9$, 8.2 Hz), 100.82 (d, $J = 21.8$ Hz), 98.68 (d, $J = 23.9$ Hz), 44.24, 40.30, 21.65, 11.29.

HRMS m/z calculated for $C_{18}H_{16}F_4N_3O^+$ $[M+H]^+$ 366.1224, found 366.1215.

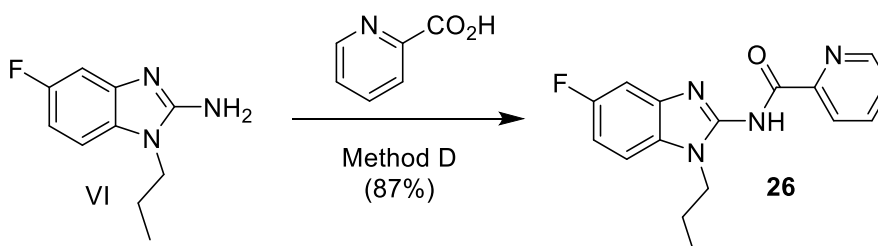
2-(4-fluorophenyl)-N-(3-propyl-3H-imidazo[4,5-b]pyridin-2-yl)acetamide (25)



The compound **25** was prepared in 40% yield using the methods A, B, C and D.

25; ^1H NMR (500 MHz, CDCl_3) δ 12.14 (s, 1H), 8.27 (d, $J = 4.9$ Hz, 1H), 7.48 (d, $J = 7.7$ Hz, 1H), 7.38 (dd, $J = 8.2, 5.6$ Hz, 2H), 7.15 (dd, $J = 7.8, 5.1$ Hz, 1H), 7.03 (t, $J = 8.7$ Hz, 2H), 4.18 (t, $J = 7.4$ Hz, 2H), 3.80 (s, 2H), 1.89 (m, 2H), 0.99 (t, $J = 7.4$ Hz, 3H). ^{13}C NMR (126 MHz, CDCl_3) δ 183.98, 162.70, 160.76, 153.55, 143.51, 143.18, 132.83, 131.01, 122.10, 118.27, 117.69, 115.07, 114.90, 46.68, 42.69, 21.65, 11.23. HRMS m/z calculated for $\text{C}_{17}\text{H}_{18}\text{FN}_4\text{O}^+$ $[\text{M}+\text{H}]^+$ 313.1459, found 313.1470.

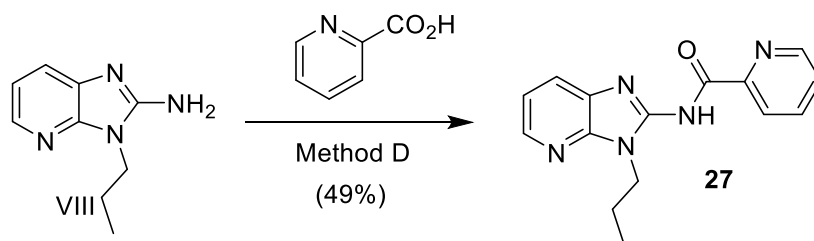
N-(5-fluoro-1-propyl-1H-benzo[d]imidazol-2-yl)picolinamide (26)



The aminobenzimidazole VI was prepared in 70% yield as reported in the synthesis of **11**. The compound **26** was prepared in 87% yield using the method D.

26; ^1H NMR (400 MHz, CDCl_3) δ 8.73 (d, J = 4.3 Hz, 1H), 8.38 (d, J = 7.8 Hz, 1H), 7.87 (t, J = 7.6 Hz, 1H), 7.50 – 7.42 (m, 1H), 7.38 (d, J = 8.8 Hz, 1H), 7.23 (dd, J = 8.8, 4.3 Hz, 1H), 7.02 (td, J = 9.1, 2.3 Hz, 1H), 4.22 (t, J = 7.3 Hz, 2H), 1.99 – 1.80 (m, 2H), 0.99 (t, J = 7.4 Hz, 3H). ^{13}C NMR (101 MHz, CDCl_3) δ 160.64, 158.27, 149.00, 137.07, 126.13, 123.86, 110.62, 110.37, 109.92, 109.83, 102.32, 45.55, 22.14, 11.39. HRMS m/z calculated for $\text{C}_{16}\text{H}_{16}\text{FN}_4\text{O}^+$ $[\text{M}+\text{H}]^+$ 299.1303, found 299.1312.

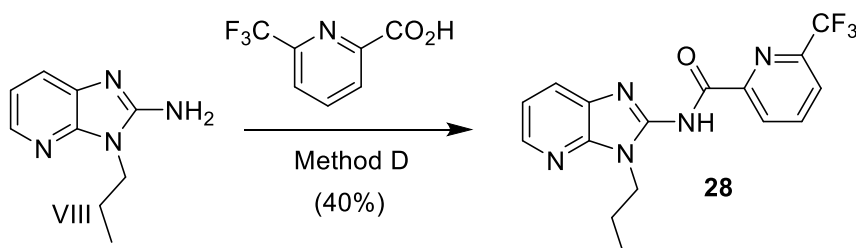
***N*-(3-propyl-3*H*-imidazo[4,5-*b*]pyridin-2-yl)picolinamide (27)**



The aminobenzimidazole VIII was prepared in 47% yield as reported in the synthesis of **25**. The compound **27** was prepared in 49% yield from **i**, using the method D.

27; ^1H NMR (500 MHz, CDCl_3) δ 10.54 (s, 1H), 8.74 (s, 3H), 8.40 (s, 1H), 8.34 (d, J = 4.5 Hz, 1H), 7.93 (s, 2H), 7.53 (s, 1H), 7.23 (dd, J = 7.7, 5.0 Hz, 1H), 4.38 (t, J = 7.3 Hz, 2H), 2.10 – 1.91 (m, 2H), 1.02 (t, J = 7.2 Hz, 3H). HRMS m/z calculated for $\text{C}_{15}\text{H}_{16}\text{N}_5\text{O}^+$ $[\text{M}+\text{H}]^+$ 282.1349, found 282.1357.

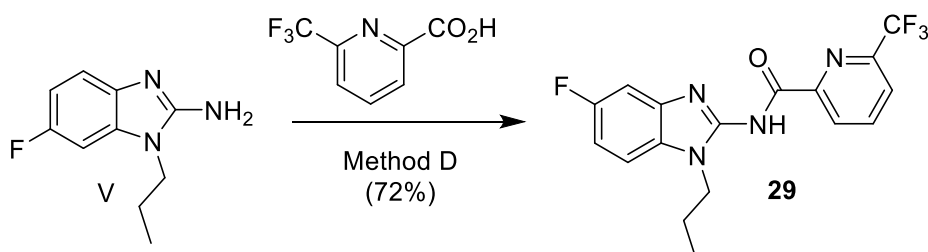
***N*-(3-propyl-3*H*-imidazo[4,5-*b*]pyridin-2-yl)-6-(trifluoromethyl)picolinamide (28)**



The aminobenzimidazole VIII was prepared in 47% yield as reported in the synthesis of **25**. The compound **28** was prepared in 40% yield from **i**, using the method D.

28; ^1H NMR (500 MHz, CDCl_3) δ 12.69 (s, 1H), 8.62 (d, $J = 5.7$ Hz, 1H), 8.34 (d, $J = 4.2$ Hz, 1H), 8.10 (s, 1H), 8.03 (d, $J = 6.9$ Hz, 1H), 7.87 (s, 1H), 7.24 (s, 1H), 4.38 (t, $J = 6.9$ Hz, 1H), 2.13 – 1.95 (m, 1H), 1.05 (t, $J = 7.3$ Hz, 1H). HRMS m/z calculated for $\text{C}_{16}\text{H}_{15}\text{F}_3\text{N}_5\text{O}^+$ $[\text{M}+\text{H}]^+$ 350.1223, found 350.1223.

***N*-(5-fluoro-1-propyl-1*H*-benzo[*d*]imidazol-2-yl)-6-(trifluoromethyl)picolinamide (29)**

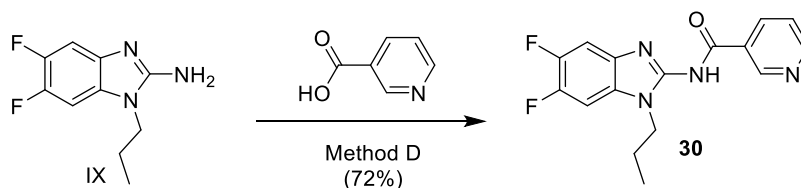


The aminobenzimidazole V was prepared in 82% yield as reported in the synthesis of **10**.

The compound **29** was prepared in 72% yield using the method D.

29; ^1H NMR (500 MHz, CDCl_3) δ 12.55 (s, 1H), 8.55 (d, $J = 7.8$ Hz, 1H), 8.03 (s, 1H), 7.80 (d, $J = 6.9$ Hz, 1H), 7.54 (dd, $J = 7.0, 3.5$ Hz, 1H), 7.13 – 6.73 (m, 2H), 4.19 (t, $J = 7.2$ Hz, 2H), 2.03 – 1.72 (m, 2H), 1.02 (t, $J = 7.4$ Hz, 3H). ^{13}C NMR (126 MHz, CDCl_3) δ 160.68, 158.77, 148.06, 147.77, 138.26, 126.74, 122.50, 122.07, 120.32, 113.41, 110.83, 110.64, 97.19, 96.97, 44.62, 21.91, 11.40. HRMS m/z calculated for $\text{C}_{17}\text{H}_{15}\text{F}_4\text{N}_4\text{O}^+$ $[\text{M}+\text{H}]^+$ 367.1177, found 367.1192.

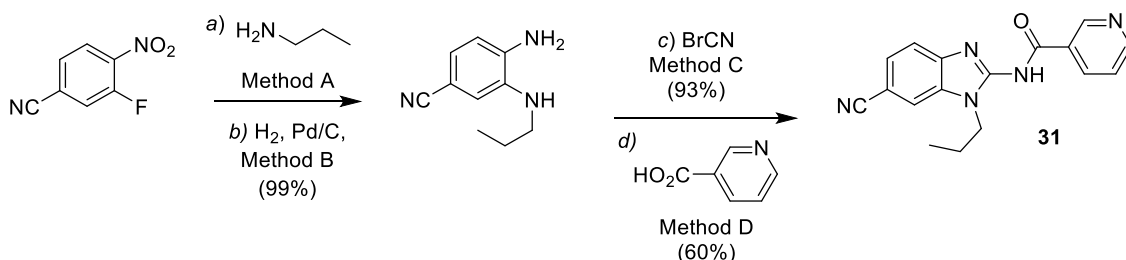
***N*-(5,6-difluoro-1-propyl-1*H*-benzo[*d*]imidazol-2-yl)nicotinamide (30)**



The aminobenzimidazole IX was prepared in 53% yield as reported in the synthesis of **15**. The compound **30** was prepared in 72% yield using the method D.

30; ^1H NMR (600 MHz, CDCl_3) δ 12.44 (s, 1H), 9.53 (d, J = 1.6 Hz, 1H), 8.71 (dd, J = 4.8, 1.7 Hz, 1H), 8.51 (dt, J = 7.9, 1.9 Hz, 1H), 7.37 (dd, J = 7.9, 5.0 Hz, 1H), 7.17 (dd, J = 9.2, 6.7 Hz, 1H), 7.11 (dd, J = 9.4, 6.5 Hz, 1H), 4.19 (t, J = 7.2 Hz, 2H), 1.97 – 1.87 (m, 2H), 1.03 (t, J = 7.4 Hz, 3H). ^{13}C NMR (151 MHz, CDCl_3) δ 175.08, 154.91, 152.03, 151.34 (d, J = 3.4 Hz), 147.96 (dd, J = 243.9, 14.0 Hz), 147.68 (dd, J = 243.9, 14.4 Hz), 136.64, 133.15, 125.45 (d, J = 10.2 Hz), 123.61 (d, J = 10.6 Hz), 123.13, 100.72 (d, J = 23.5 Hz), 98.89 (d, J = 23.8 Hz), 44.43, 21.84, 11.54. HRMS m/z calculated for $\text{C}_{16}\text{H}_{15}\text{F}_2\text{N}_4\text{O}^+$ $[\text{M}+\text{H}]^+$ 317.1208, found 317.1194.

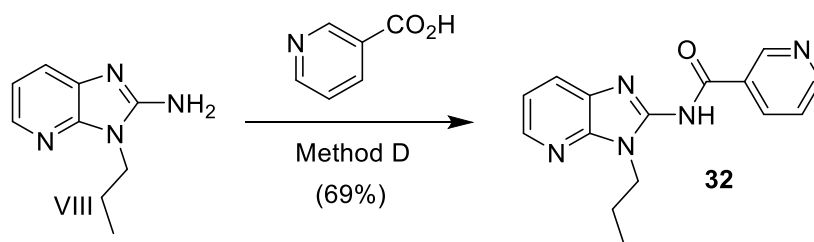
***N*-(6-cyano-1-propyl-1*H*-benzo[*d*]imidazol-2-yl)nicotinamide (31)**



The compound **31** was prepared in 55% yield using the method A, followed by B, C and D.

31; ^1H NMR (500 MHz, $\text{DMSO}-d_6$) δ 13.09 (s, 1H), 9.37 (s, 1H), 8.71 (d, J = 3.9 Hz, 1H), 8.48 (d, J = 7.8 Hz, 1H), 8.17 (s, 1H), 7.78 – 7.58 (m, 2H), 7.52 (dd, J = 7.5, 4.9 Hz, 1H), 4.26 (t, J = 7.0 Hz, 2H), 1.84 (dd, J = 14.3, 7.2 Hz, 2H), 0.94 (t, J = 7.3 Hz, 3H). ^{13}C NMR (126 MHz, $\text{DMSO}-d_6$) δ 172.38, 152.99, 151.80, 150.20, 136.14, 132.85, 132.44, 129.65, 127.02, 123.36, 119.35, 113.91, 112.81, 104.73, 43.52, 21.20, 11.02. HRMS m/z calculated for $\text{C}_{17}\text{H}_{16}\text{N}_5\text{O}^+$ $[\text{M}+\text{H}]^+$ 306.1349, found 306.1326.

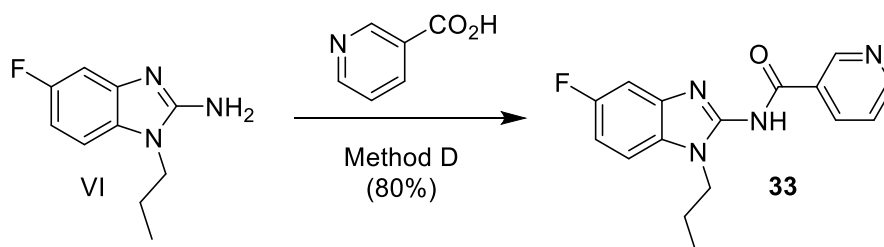
***N*-(3-propyl-3*H*-imidazo[4,5-*b*]pyridin-2-yl)nicotinamide (32)**



The aminobenzimidazole VIII was prepared in 47% yield as reported in the synthesis of **25**. The compound **32** was prepared in 69% yield from **i**, using the method D.

32; ^1H NMR (500 MHz, CDCl_3) δ 12.42 (s, 1H), 9.58 (d, $J = 1.1$ Hz, 1H), 8.75 (dd, $J = 4.7, 1.4$ Hz, 1H), 8.57 (d, $J = 7.9$ Hz, 1H), 8.33 (d, $J = 4.3$ Hz, 1H), 7.59 (d, $J = 7.8$ Hz, 1H), 7.42 (dd, $J = 7.8, 4.8$ Hz, 1H), 7.22 (dd, $J = 7.8, 5.1$ Hz, 1H), 4.37 (t, $J = 7.3$ Hz, 2H), 2.14 – 1.91 (m, 2H), 1.07 (t, $J = 7.4$ Hz, 3H). ^{13}C NMR (126 MHz, CDCl_3) δ 175.58, 154.12, 152.02, 151.30, 143.51, 136.64, 123.04, 118.58, 117.81, 42.92, 21.82, 11.41. HRMS m/z calculated for $\text{C}_{15}\text{H}_{16}\text{N}_5\text{O}^+$ $[\text{M}+\text{H}]^+$ 282.1349, found 282.1360.

***N*-(5-fluoro-1-propyl-1*H*-benzo[*d*]imidazol-2-yl)nicotinamide (33)**

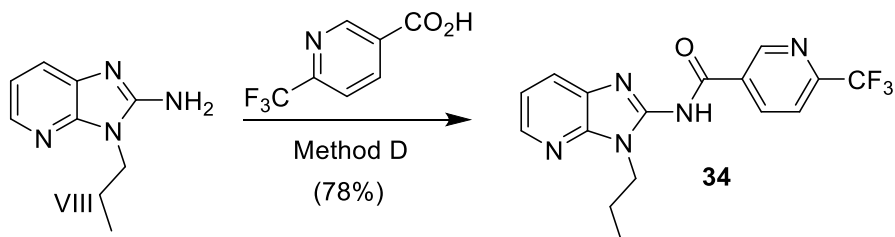


The aminobenzimidazole VI was prepared in 70% yield as reported in the synthesis of **11**. The compound **33** was prepared in 80% yield using the method D.

33; ^1H NMR (600 MHz, CDCl_3) δ 12.43 (s, 1H), 9.56 (d, $J = 1.4$ Hz, 1H), 8.72 (dd, $J = 4.8, 1.7$ Hz, 1H), 8.54 (dt, $J = 7.9, 1.9$ Hz, 1H), 7.40 (dd, $J = 7.9, 4.9$ Hz, 1H), 7.22 (dd, $J = 8.7, 4.2$ Hz, 1H), 7.09 (dd, $J = 8.1, 2.4$ Hz, 1H), 7.07 – 7.02 (m, 1H), 4.33 – 4.09 (m, 2H), 2.03 – 1.89 (m, 2H), 1.05 (t, $J = 7.4$ Hz, 3H). ^{13}C NMR (151 MHz, CDCl_3) δ 174.93, 160.30, 158.70, 154.37, 151.76, 151.21, 136.50, 133.20, 128.64, 128.56, 125.99, 122.97,

110.73, 110.56, 110.01, 109.95, 99.17, 98.98, 44.07, 21.81, 11.43. **HRMS** m/z calculated for $C_{16}H_{16}FN_4O^+$ $[M+H]^+$ 299.1303, found 299.1305.

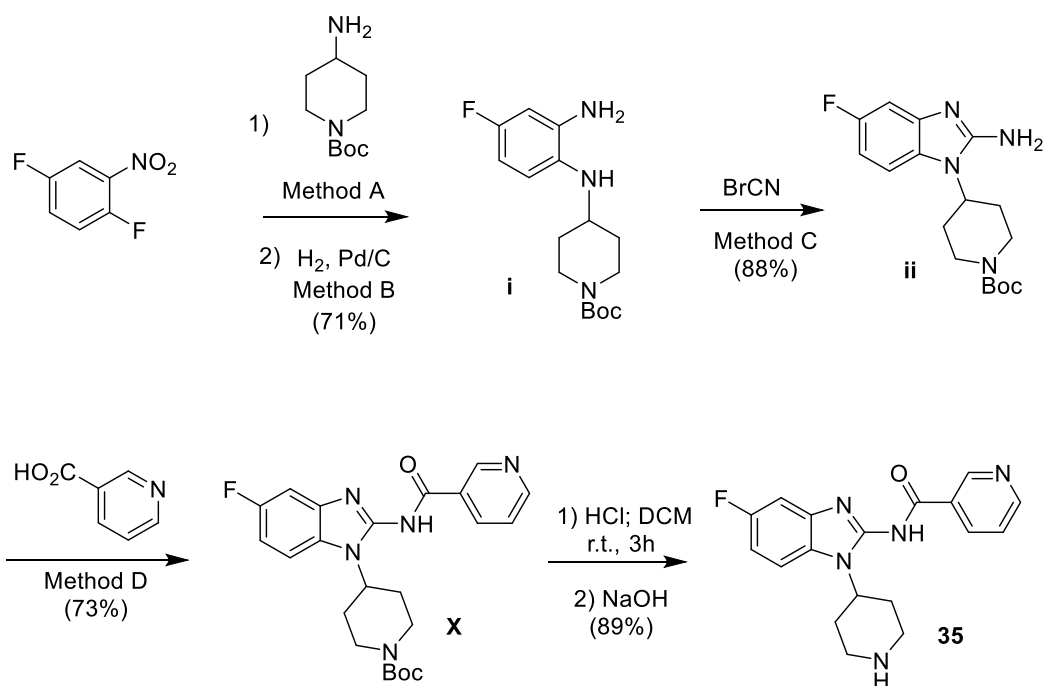
***N*-(3-propyl-3*H*-imidazo[4,5-*b*]pyridin-2-yl)-6-(trifluoromethyl)nicotinamide (34)**



The aminobenzimidazole VIII was prepared in 47% yield as reported in the synthesis of **25**. The compound **34** was prepared in 78% yield from **i**, using the method D.

34; **1H NMR (500 MHz, $CDCl_3$)** δ 12.36 (s, 1H), 9.66 (s, 1H), 8.72 (dd, $J = 8.0, 1.3$ Hz, 1H), 8.35 (dd, $J = 5.0, 1.2$ Hz, 1H), 7.80 (s, 1H), 7.63 (d, $J = 1.2$ Hz, 1H), 7.24 (dd, $J = 7.9, 5.0$ Hz, 1H), 4.49 – 4.26 (m, 2H), 2.15 – 1.90 (m, 2H), 1.06 (t, $J = 7.4$ Hz, 3H). **^{13}C NMR (126 MHz, $CDCl_3$)** δ 173.93, 154.00, 151.39, 150.16, 149.89, 149.61, 149.34, 143.84, 143.27, 138.02, 135.54, 122.67, 121.57, 120.53, 119.88, 118.82, 118.10, 43.05, 21.83, 11.36. **HRMS** m/z calculated for $C_{16}H_{14}F_3N_5NaO^+$ $[M+Na]^+$ 372.1043, found 372.1035.

***N*-(5-fluoro-1-(piperidin-4-yl)-1*H*-benzo[*d*]imidazol-2-yl)nicotinamide (35)**

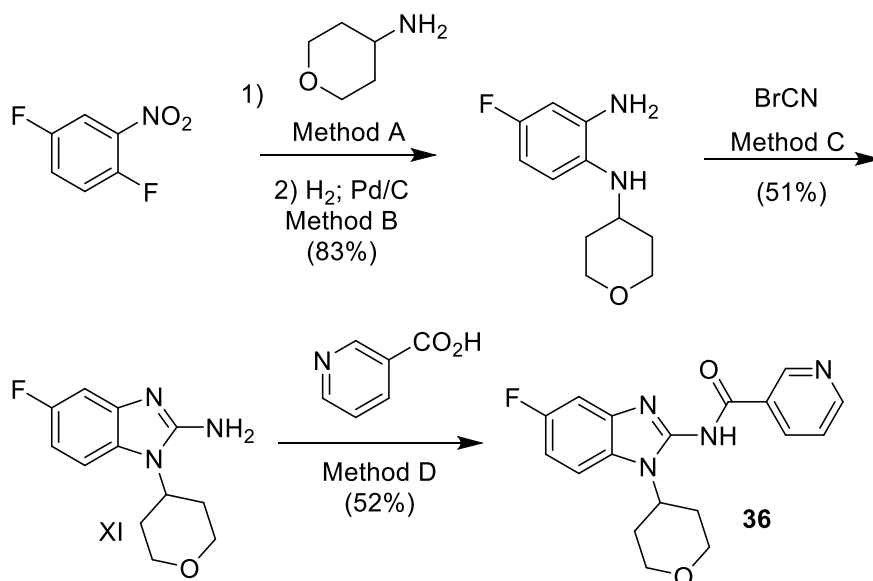


The intermediate **X** was prepared in 46% yield by Method A, followed by B, C and D. To a solution of **X** (45 mg; 0.14 mmol) in DCM (10 mL) was added HCl (2 M in EtOAc, 5 mL) at room temperature. The solution was stirred for 3h, then the solvents were removed under reduced pressure and the residual solid was solubilized in MeOH (1 mL). To this solution was added NaOH (1.0 M, until pH 8) and the mixture was extracted with EtOAc (2×10 mL). The organic layer was extracted with brine and dried with magnesium sulfate. The solution was filtered and evaporated under reduced pressure, generating **35** in 89% yield.

35; ^1H NMR (500 MHz, DMSO) δ 10.03 (d, $J = 9.7$ Hz, 1H), 9.70 (s, 1H), 9.44 (d, $J = 9.8$ Hz, 1H), 9.36 (d, $J = 8.0$ Hz, 1H), 9.01 (d, $J = 5.3$ Hz, 1H), 8.13 (dd, $J = 7.8, 5.8$ Hz, 1H), 8.02 (dd, $J = 8.8, 4.2$ Hz, 1H), 7.44 (dd, $J = 8.7, 2.5$ Hz, 1H), 7.22 (td, $J = 9.4, 2.5$ Hz, 1H), 5.26 (s, 1H), 3.47 (d, $J = 12.0$ Hz, 2H), 3.26 (dd, $J = 23.7, 12.3$ Hz, 2H), 3.00 (dd, $J = 22.4, 12.4$ Hz, 2H), 2.00 (d, $J = 12.1$ Hz, 2H). ^{13}C NMR (126 MHz, DMSO) δ 169.05, 160.11, 158.22, 152.61, 145.38, 144.65, 143.74, 136.43, 130.26, 127.30, 125.28, 112.89, 110.93, 110.73, 100.48, 100.25, 50.15, 43.15, 25.86.

***N*-(5-fluoro-1-(tetrahydro-2*H*-pyran-4-yl)-1*H*-benzo[*d*]imidazol-2-yl)nicotinamide**

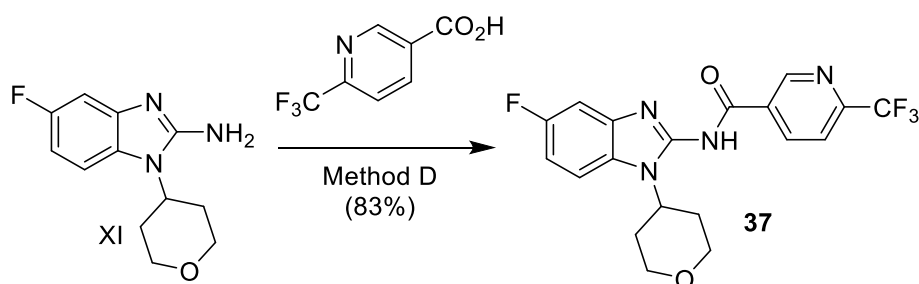
(36)



The compound **36** was prepared in 22% yield using the methods A, B, C and D.

36; $^1\text{H NMR}$ (400 MHz, CDCl_3) δ 12.58 (sl, 1H), 9.54 (sl, 1H), 8.72 (d, $J = 3.8$ Hz, 1H), 8.52 (d, $J = 7.8$ Hz, 1H), 7.42 (m, 2H), 7.09 (dd, $J = 8.1, 2.4$ z, 1H), 7.02 (td, $J = 9.1, 2.4$ Hz, 1H), 5.15 (tt, $J = 12.5, 4.3$ Hz, 1H), 4.22 (dd, $J = 11.6, 4.5$ Hz, 2H), 3.66 (td, $J = 11.9, 1.5$ Hz, 2H), 2.65 (qd, $J = 12.6, 4.7$ Hz, 2H), 1.89 (dd, $J = 12.5, 2.7$ Hz, 2H). $^{13}\text{C NMR}$ (100 MHz, CDCl_3) δ 160.6, 158.2, 153.5 (d. $J = 296.7$ Hz), 151.9, 136.5, 133.0, 128.9, 124.6, 123.0, 111.7 (d. $J = 9.5$ Hz), 110.5 (d. $J = 24.6$ Hz), 99.2 (d. $J = 27.9$ Hz), 67.5, 51.5, 30.1. **HRMS** m/z calculated for $\text{C}_{18}\text{H}_{17}\text{FN}_4\text{O}_2^+$ $[\text{M}+\text{H}]^+$ 341.1408, found 341.1423.

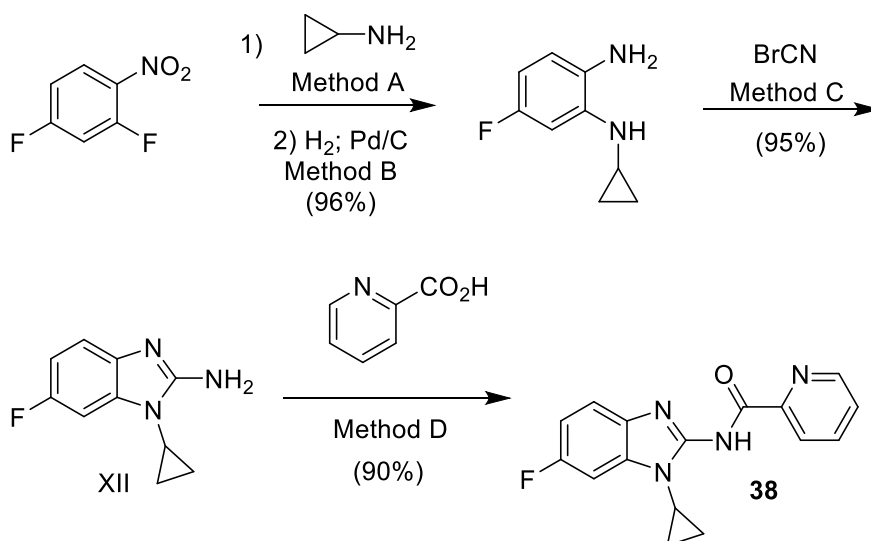
***N*-(5-fluoro-1-(tetrahydro-2*H*-pyran-4-yl)-1*H*-benzo[*d*]imidazol-2-yl)-6-(trifluoromethyl)nicotinamide (37)**



The aminobenzimidazole XI was prepared in 43% yield as reported in the synthesis of **36**. The compound **37** was prepared in 83% yield using the method D.

37; $^1\text{H NMR}$ (500 MHz, CDCl_3) δ 12.52 (sl, 1H), 9.63 (s, 1H), 8.67 (dd, $J = 8.1, 1.2$ Hz, 1H), 7.78 (d, $J = 8.0$ Hz, 1H), 7.46 (dd, $J = 8.9, 4.2$ Hz, 1H), 7.12 (dd, $J = 8.0, 2.4$ Hz, 1H), 7.05 (td, $J = 9.0, 2.5$ Hz, 1H), 5.11 (tt, $J = 12.5, 4.3$ Hz, 1H), 4.22 (dd, $J = 11.8, 4.6$ Hz, 2H), 3.63 (m, 2H), 2.66 (qd, $J = 12.5, 4.6$ Hz, 2H), 1.89 (dd, $J = 12.6, 2.7$ Hz, 2H). $^{13}\text{C NMR}$ (125 MHz, CDCl_3) δ 173.3, 160.4, 158.5, 153.9, 151.3, 149.6 (q, $J = 34.1$ Hz), 137.9, 135.6, 128.9 (d, $J = 13.1$ Hz), 124.6, 121.5 (q, $J = 274.0$ Hz), 119.9, 111.9 (d, $J = 9.0$ Hz), 110.9 (d, $J = 25.1$ Hz), 99.3 (d, $J = 28.1$ Hz), 67.5, 51.8, 30.1.

***N*-(1-cyclopropyl-6-fluoro-1*H*-benzo[*d*]imidazol-2-yl)picolinamide (**38**)**

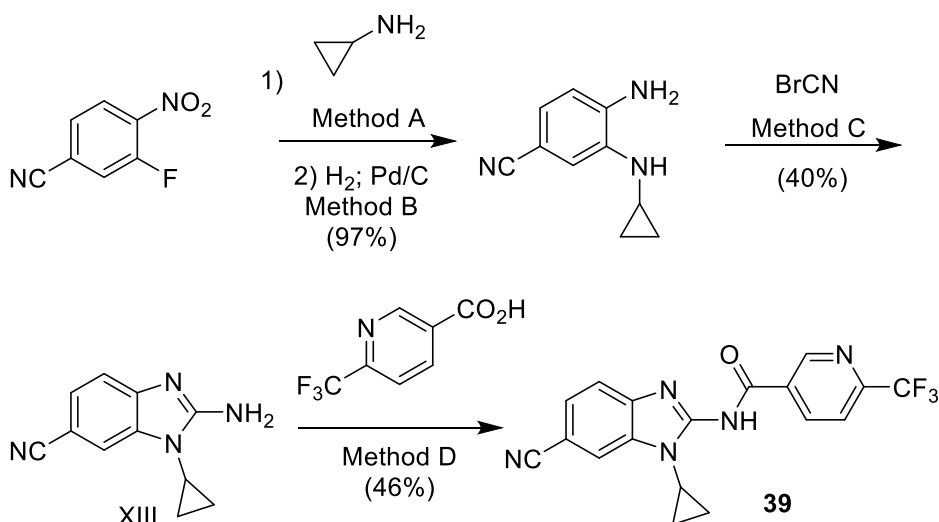


The compound **38** was prepared in 82% yield using the methods A, B, C and D.

38; $^1\text{H NMR}$ (500 MHz, CDCl_3) δ 12.42 (s, 1H), 9.59 (d, $J = 1.5$ Hz, 1H), 8.74 (dd, $J = 4.8, 1.6$ Hz, 1H), 8.57 (dt, $J = 7.9, 1.8$ Hz, 1H), 7.41 (dd, $J = 7.8, 4.8$ Hz, 1H), 7.27 – 7.20 (m, 2H), 7.00 (td, $J = 9.1, 2.4$ Hz, 1H), 3.26 – 3.11 (m, 1H), 1.40 – 1.32 (m, 2H), 1.31 – 1.24 (m, 2H). $^{13}\text{C NMR}$ (126 MHz, CDCl_3) δ 174.98, 160.55, 158.63, 155.70, 151.84, 151.21, 136.55, 133.21, 131.41, 131.31, 124.09, 123.02, 111.81, 111.73, 110.68, 110.49,

98.46, 98.23, 24.12, 6.85. **HRMS** m/z calculated for $C_{16}H_{14}FN_4O^+$ $[M+H]^+$ 297.1146, found 297.1153.

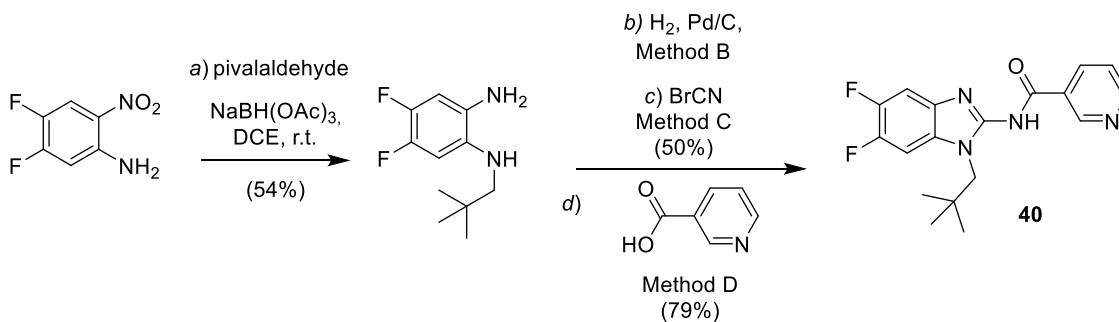
***N*-(6-cyano-1-cyclopropyl-1*H*-benzo[*d*]imidazol-2-yl)-6-(trifluoromethyl)nicotinamide (39)**



The compound **39** was prepared in 19% yield using the methods A, B, C and D.

39; ^1H NMR(500 MHz, DMSO) δ 13.03 (sl, 1H), 9.50 (s, 1H), 8.73 (sl, 1H), 8.03 (m, 2H), 7.66 (m, 2H), 3.25 (sl, 1H), 1.28 (sl, 2H), 1.16 (sl, 1H). ^{13}C NMR (125 MHz, DMSO) δ 171.1, 154.8, 150.9, 148.7 (q. $J = 34.1$ Hz), 138.6, 136.5, 133.8, 131.6, 127.5, 122.1 (q. $J = 274.1$ Hz), 120.8, 118.9, 114.6, 114.0, 105.6, 25.1, 6.8.

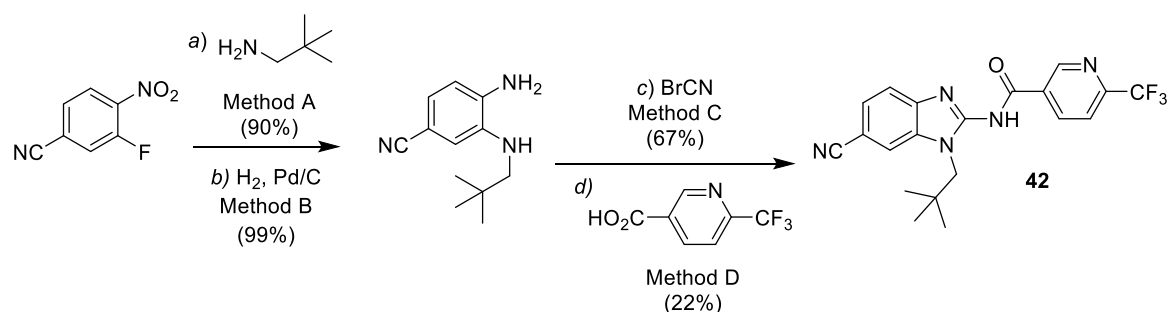
***N*-(5,6-difluoro-1-neopentyl-1*H*-benzo[*d*]imidazol-2-yl)nicotinamide (40)**



To a solution of nitroaniline (350 mg; 2 mmol) in DCE (2.4 mL), pivalaldehyde (4.2 mmol) was added. After 10 min at rt, NaBH(OAc)₃ (1189 mg; 5.6 mmol) was added in five portions for 10 min. After stirring for 24 h at rt, DCE (4 mL), pivalaldehyde (4.2 mmol) and NaBH(OAc)₃ (1165 mg; 5.5 mmol) were added again. The reaction mixture was allowed to stir additional 36 h and then quenched with NaOH 2 M (5 mL). The product was extracted with DCM, dried over MgSO₄, concentrated and purified by flash column chromatography (Hexanes:AcOEt 9:1) to yield 54% of the desired compound. The compound **40** was prepared in 40% yield using the methods B, C and D.

40; ¹H NMR (600 MHz, CDCl₃) δ 12.65 (s, 1H), 9.52 (d, *J* = 1.2 Hz, 1H), 8.70 (dd, *J* = 4.7, 1.4 Hz, 1H), 8.49 (dt, *J* = 7.9, 1.8 Hz, 1H), 7.37 (dd, *J* = 7.7, 4.8 Hz, 1H), 7.14 (dt, *J* = 9.7, 6.5 Hz, 2H), 4.02 (s, 2H), 1.11 (s, 9H). **¹³C NMR (151 MHz, CDCl₃)** δ 174.80 , 155.89, 151.96 , 151.27 , 147.71 (dd, *J* = 243.1, 13.6 Hz), 147.58 (dd, *J* = 243.9, 14.0 Hz), 136.60, 133.20, 126.68 (d, *J* = 10.3 Hz), 123.71 (d, *J* = 10.3 Hz), 123.15, 100.48 (d, *J* = 23.3 Hz), 100.10 (d, *J* = 24.1 Hz), 54.20 , 35.00 , 28.80 . **HRMS** *m/z* calculated for C₁₈H₁₉F₂N₄O⁺ [M+H]⁺ 345.1521, found 345.1523.

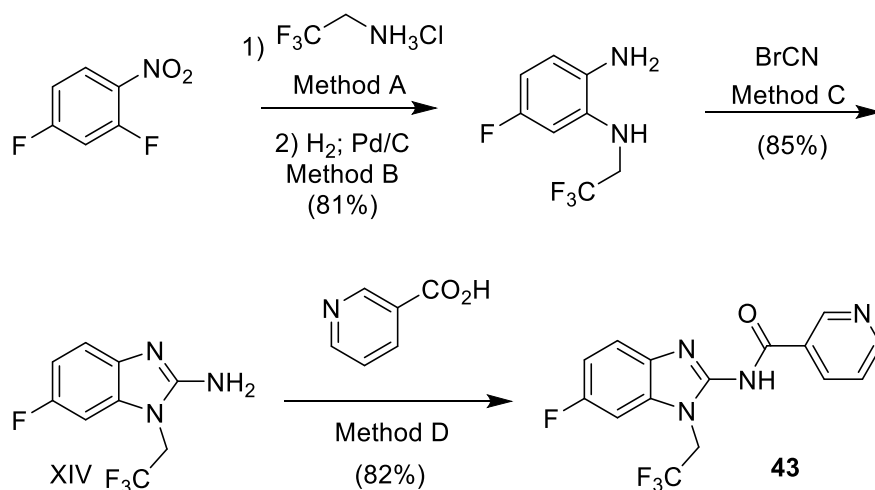
***N*-(6-cyano-1-neopentyl-1*H*-benzo[*d*]imidazol-2-yl)-6-(trifluoromethyl)nicotinamide (**42**)**



The compound **42** was prepared in 13% yield using the methods A, B, C and D.

42; ^1H NMR (500 MHz, CDCl_3) δ 12.65 (s, 1H), 9.63 (s, 1H), 8.67 (d, $J = 7.9$ Hz, 1H), 7.78 (d, $J = 8.1$ Hz, 1H), 7.62 (s, 1H), 7.59 (d, $J = 8.3$ Hz, 1H), 7.44 (d, $J = 8.2$ Hz, 1H), 4.09 (s, 2H), 1.14 (s, 9H). ^{13}C NMR (126 MHz, CDCl_3) δ 173.96 (s), 155.95 (s), 151.48 (s), 150.06 (q, $J = 34.3$ Hz), 138.20 (s), 135.45 (s), 131.40 (s), 131.21 (s), 127.81 (s), 121.64 (q, $J = 274.5$ Hz), 120.12 (d, $J = 2.1$ Hz), 118.88 (s), 114.73 (s), 112.07 (s), 107.03 (s), 54.38 (s), 35.09 (s), 28.81 (s).

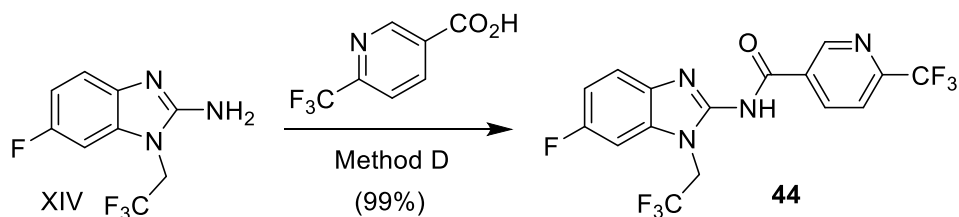
***N*-(6-fluoro-1-(2,2,2-trifluoroethyl)-1*H*-benzo[*d*]imidazol-2-yl)nicotinamide (43)**



The compound **43** was prepared in 57% yield using the methods A, B, C and D.

43; ^1H NMR (500 MHz, CDCl_3) δ 12.34 (s, 1H), 9.53 (d, $J = 1.2$ Hz, 1H), 8.75 (dd, $J = 4.7, 1.4$ Hz, 1H), 8.53 (d, $J = 7.9$ Hz, 1H), 7.41 (dd, $J = 7.8, 4.9$ Hz, 1H), 7.31 (dd, $J = 8.6, 4.3$ Hz, 1H), 7.14 – 7.04 (m, 2H), 4.88 (q, $J = 8.4$ Hz, 2H). ^{13}C NMR (126 MHz, CDCl_3) δ 175.26, 160.86, 158.93, 155.02, 152.13, 151.14, 136.68, 132.57, 129.70, 129.60, 126.70, 124.56, 124.47, 123.07, 122.32, 120.14, 112.29, 112.22, 111.68, 111.49, 98.06, 97.83, 44.01, 43.72, 43.42, 43.13. **HRMS** m/z calculated for $\text{C}_{15}\text{H}_{11}\text{F}_4\text{N}_4\text{O}^+$ $[\text{M}+\text{H}]^+$ 339.0864, found 339.0872.

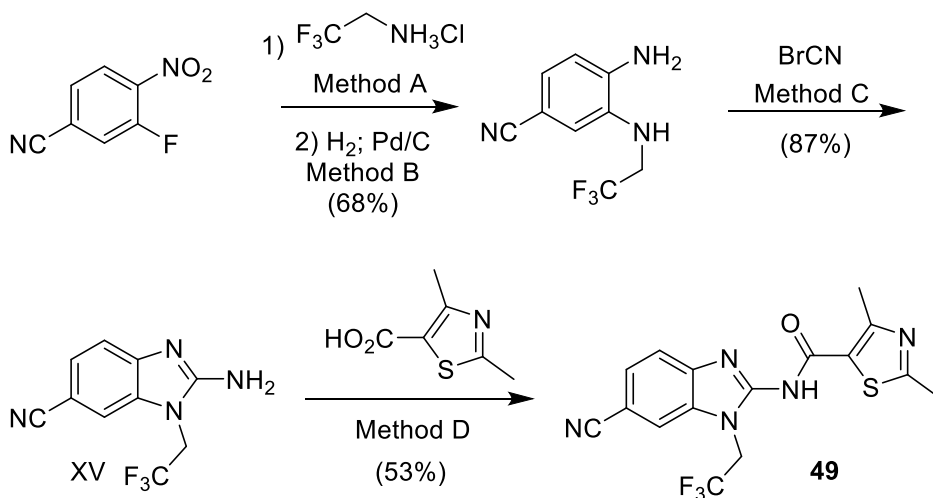
***N*-(6-fluoro-1-(2,2,2-trifluoroethyl)-1*H*-benzo[*d*]imidazol-2-yl)-6-(trifluoromethyl)nicotinamide (44)**



The aminobenzimidazole XIV was prepared in 69% yield as reported in the synthesis of **43**. The compound **44** was prepared in quantitative yield using the method D.

44; ^1H NMR (400 MHz, DMSO) δ 13.07 (s, 1H), 9.55 (s, 1H), 8.80 – 8.72 (m, 1H), 8.04 (d, J = 8.1 Hz, 1H), 7.64 (dd, J = 9.0, 2.0 Hz, 1H), 7.57 (dd, J = 8.8, 4.7 Hz, 1H), 7.18 (td, J = 9.8, 2.4 Hz, 1H), 5.32 (q, J = 9.0 Hz, 2H).

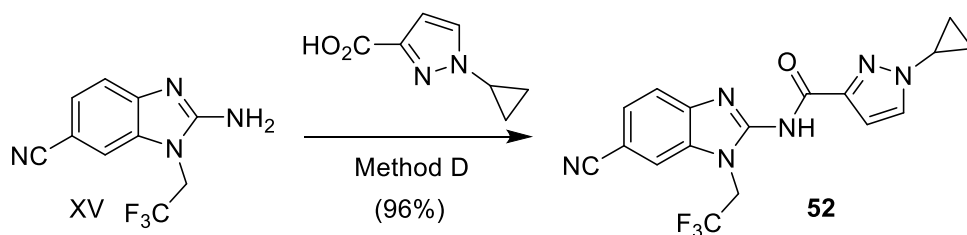
***N*-(6-cyano-1-(2,2,2-trifluoroethyl)-1*H*-benzo[*d*]imidazol-2-yl)-2,4-dimethylthiazole-5-carboxamide (49)**



The compound **49** was prepared in 31% yield using the methods A, B, C and D.

49; ^1H NMR (500 MHz, DMSO) δ 13.10 (s, 1H), 8.15 (s, 1H), 7.72 (dd, J = 8.3, 1.4 Hz, 1H), 7.63 (d, J = 8.3 Hz, 1H), 5.09 (q, J = 9.0 Hz, 2H), 2.70 (s, 3H), 2.60 (s, 3H). ^{13}C NMR (126 MHz, DMSO) δ 170.05, 167.77, 156.38, 153.07, 133.29, 131.98, 130.81, 129.67, 128.40, 127.89, 125.74, 123.48, 121.18, 119.56, 114.42, 113.43, 105.45, 43.64, 43.37, 43.09, 42.81, 19.37, 17.52. **HRMS** m/z calculated for $\text{C}_{16}\text{H}_{13}\text{F}_3\text{N}_5\text{OS}^+ [\text{M}+\text{H}]^+$ 380.0787, found 380.0807.

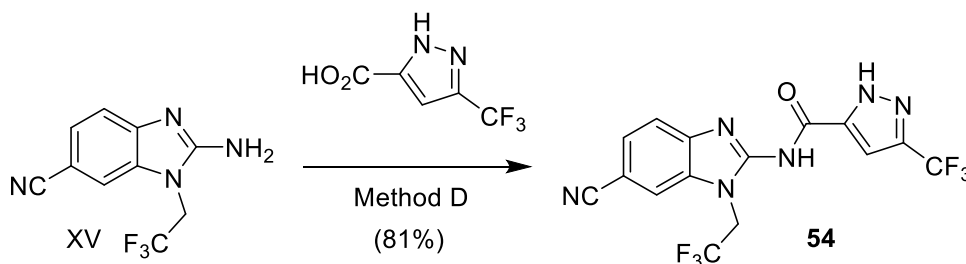
***N*-(6-cyano-1-(2,2,2-trifluoroethyl)-1*H*-benzo[*d*]imidazol-2-yl)-1-cyclopropyl-1*H*-pyrazole-3-carboxamide (**52**)**



The aminobenzimidazole **XV** was prepared in 59% yield as reported in the synthesis of **49**. The compound **52** was prepared in 96% yield using the method D.

52; ¹H NMR (500 MHz, DMSO) δ 12.81 (sl, 1H), 8.18 (s, 1H), 7.85 (s, 1H), 7.70 (m, 2H), 6.84 (d, J = 2.4 Hz, 1H), 5.22 (m, 2H), 3.84 (m, 1H), 1.12 (m, 2H), 1.03 (m, 2H). ¹³C NMR (125 MHz, DMSO) δ 131.5, 127.9, 125.7, 123.5, 119.8, 114.7, 108.5, 105.1, 33.8, 7.0. HRMS m/z calculated for C₁₇H₁₄N₆O⁺ [M+Na]⁺ 397.0995, found 397.0983.

***N*-(6-cyano-1-(2,2,2-trifluoroethyl)-1*H*-benzo[*d*]imidazol-2-yl)-3-(trifluoromethyl)-1*H*-pyrazole-5-carboxamide (**54**)**

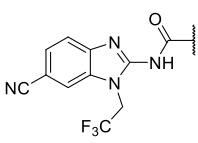


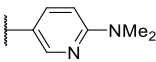
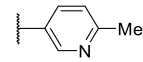
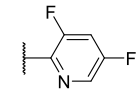
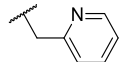
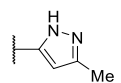
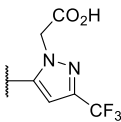
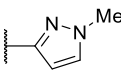
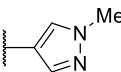
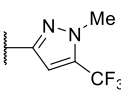
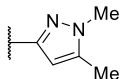
The aminobenzimidazole **XV** was prepared in 59% yield as reported in the synthesis of **49**. The compound **54** was prepared in 81% yield using the method D.

54; ¹H NMR (500 MHz, DMSO) δ 14.38 (s, 1H), 13.17 (s, 1H), 8.16 (s, 1H), 7.75 (d, J = 8.3 Hz, 1H), 7.68 (d, J = 8.3 Hz, 1H), 7.23 (s, 1H), 5.40 (q, J = 8.9 Hz, 2H). ¹³C NMR (126 MHz, DMSO) δ 165.61, 153.51, 143.35, 141.96 (q, J = 37.6 Hz), 133.31, 129.74, 128.45, 128.10, 125.87, 125.16, 123.63, 123.02, 121.40, 120.89, 119.51, 118.76, 114.89,

113.76, 106.09, 105.69, 79.88, 79.42, 79.16, 42.92 (q, $J = 34.1$ Hz). **HRMS** m/z calculated for $C_{15}H_9F_6N_6O^+$ $[M+H]^+$ 403.0737, found 403.0754.

Table S1 Evaluation of antitrypanosomal activity, selectivity and initial ADME properties for additional compounds with introduction of heteroaromatic groups at acyl fragment.



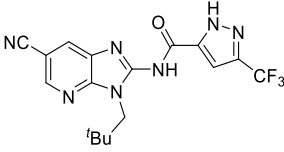
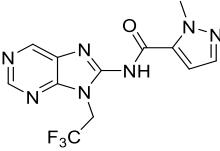
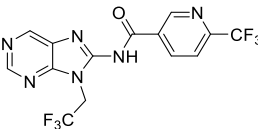
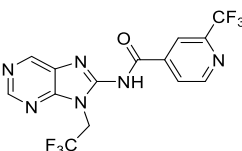
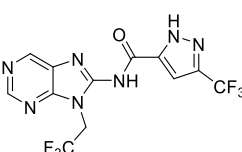
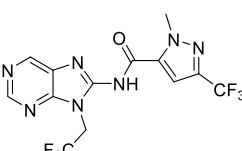
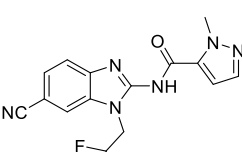
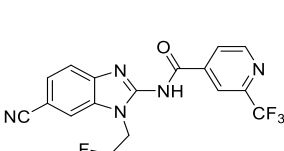
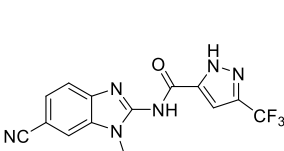
Code	Substituent	T. cruzi IC ₅₀ ^a (SD)	SI	MLM Cl _{int} in vitro ^b	eLogD
55		8.6 (7.23)	>7	ND	6.1
56		64	1	ND	3.0 ^c
57		17 (18.2)	3	253	4.4
58		9.3 (0.47)	>7	236	3.9
59		36 (0.52)	1	ND	4.7
60		64	1	ND	0.9 ^c
61		64	1	73	4.2
62		64	1	ND	2.5 ^c
63		64	1	77	5.2
64		64	1	181	4.3

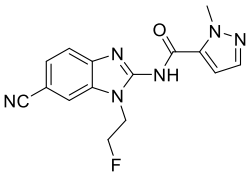
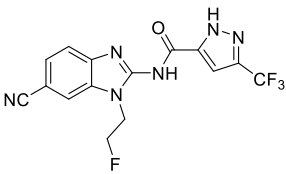
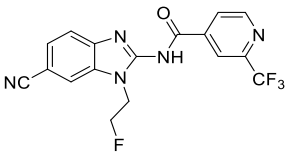
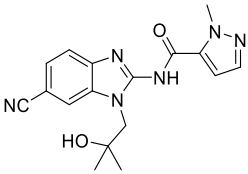
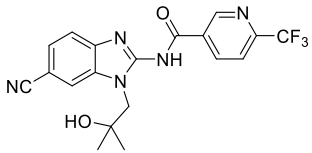
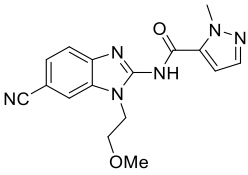
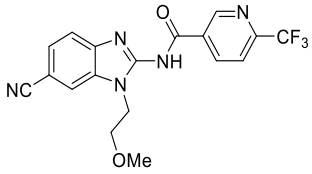
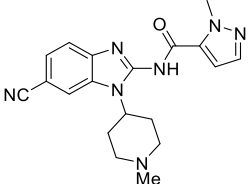
65		24 (39.1)	>3	ND	4.0
66		64	1	ND	2.1 ^c
67		64	1	141	4.0
68		11 (4.92)	>6	25	2.8
69		50 (17.3)	>1	23	2.6
70		6.6 (3.69)	9	36	3.0

ND: not determined; **SD: standard deviation of the analyses**; SI: Selectivity index relative to MRC-5 cells (CC_{50} / IC_{50}); MLM: Mouse Liver Microsome; ^a IC_{50} represented in μ M, ^b Intrinsic clearance represented in μ L/min/mg; ^c calculated logD. IC_{50} of Benznidazole (reference validation) was 2.1 μ M.

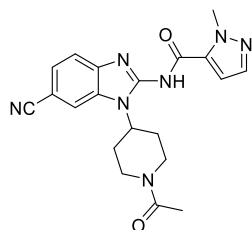
Table S2 Evaluation of antitrypanosomal activity, selectivity and initial ADME properties for additional compounds.

Code	Compound	<i>T. cruzi</i> IC_{50}^a (SD)	SI	MLM Cl_{int} in vitro ^b	eLogD
71		2.2 (ND)	6	ND	2.1 ^c
72		0.55 (0.03)	5	23	2.9 ^c
73		8.1 (0.18)	2	23	1.8 ^c

83		1.5 (8.68)	3	23	4.6
84		8.2 (0.17)	3	24	1.8 ^c
85		0.51 (0.02)	6	ND	2.7 ^c
86		1.1 (1.15)	5	ND	2.7 ^c
87		7.5 (0.43)	4	ND	2.2 ^c
88		0.59 (0.06)	7	ND	2.7 ^c
89		2.4 (0.73)	5	383	1.9 ^c
90		0.51 (ND)	24	ND	3.0 ^c
91		0.49 (0.01)	11	70	2.4 ^c

92		8.4(0.39)	2	154	1.3 ^c
93		2.1 (ND)	11	39	1.9 ^c
94		49 (18.6)	1	ND	2.5 ^c
95		13 (8.55)	>5	23	1.7 ^c
96		37 (1.26)	1	23	2.9 ^c
97		8.8 (0.13)	>7	98	1.3 ^c
98		64	1	ND	2.6 ^c
99		34 (1.71)	>2	72	1.0 ^c

100



64

1

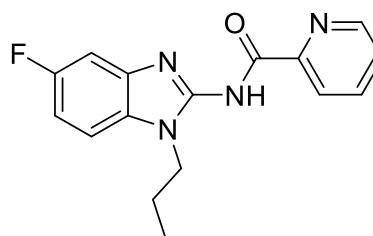
23

1.6^c

ND: not determined; **SD: standard deviation of the analyses**; SI: Selectivity index relative to MRC-5 cells (CC_{50} / IC_{50}); MLM: Mouse Liver Microsome; ^a IC_{50} represented in μM , ^b Intrinsic clearance represented in $\mu L/min/mg$; ^c calculated logD. IC_{50} of Benznidazole (reference validation) was 2.1 μM .

Metabolite ID data for compound 26

Metabolite ID report Metabolic soft spot ID	
property	value
Concentration	10 μM
Incubation Date	20170419
Incubation Time (h)	1hr
Matrix	S9 Fraction
Species	human, mouse
Project	Neglected Tropical Diseases DNDi_GEN



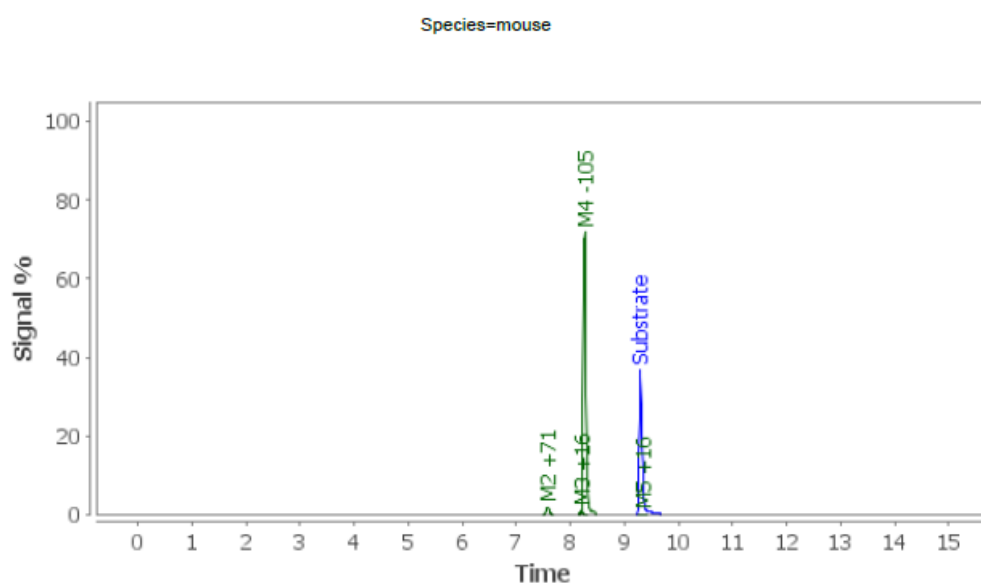
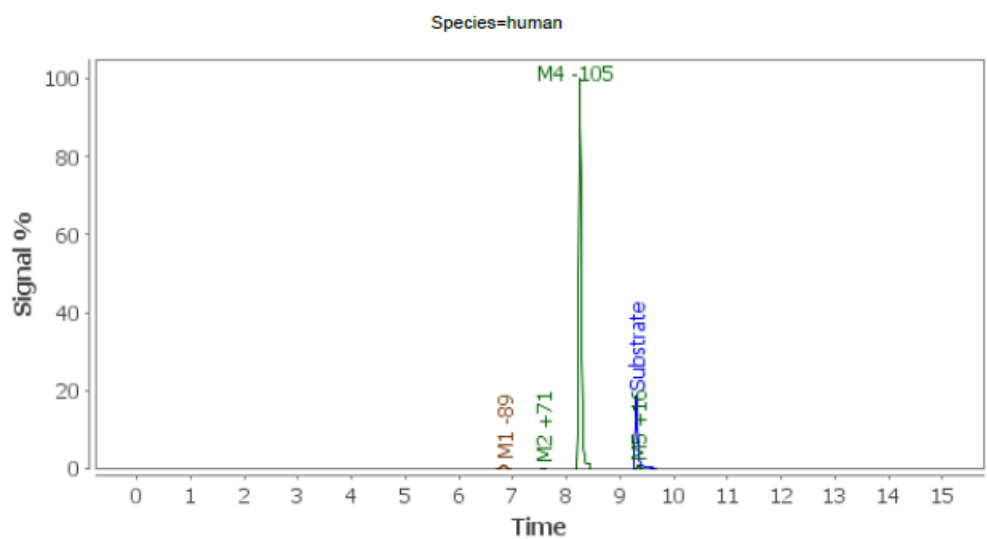
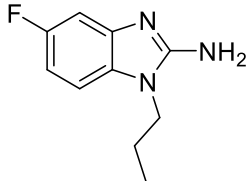
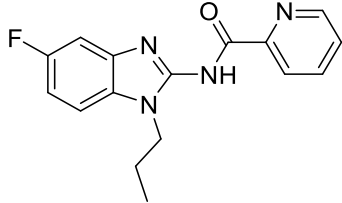
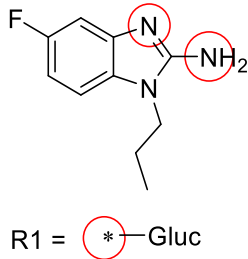
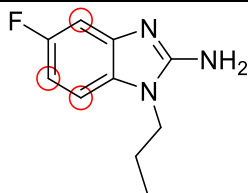
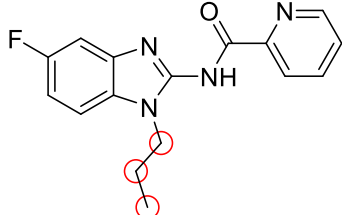
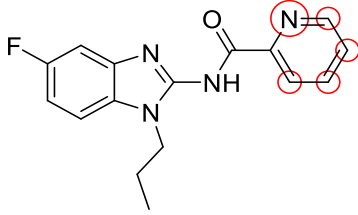


Table S3. Metabolite ID data for compound **26**

Peak Name	Proposed Structure	Retention Time (min)	m/z	Area (%)	
				Mouse	Human
M4 (-105)		8.25	194.1089	62.84	80.61

Substrate 26			299.1303	33.84	17.22
M2 (+71)	 R1 = (*)-Gluc	7.58	370.1414	2.10	0.22
M1 (-89)	 R1 = (*)-OH	6.85	210.1039	-	1.32
M3 (+16)	 R1 = (*)-OH	8.20	315.1255	1.02	-
M5 (+16)	 R1 = (*)-OH	9.34	315.1262	0.2	0.63

Metabolite ID data for compound 33

Metabolite ID report	
Metabolic soft spot ID	
property	value
Concentration	10µM
Incubation Date	20170419
Incubation Time (h)	1hr
Matrix	S9 Fraction
Species	human, mouse
Project	Neglected Tropical Diseases DNDi_GEN

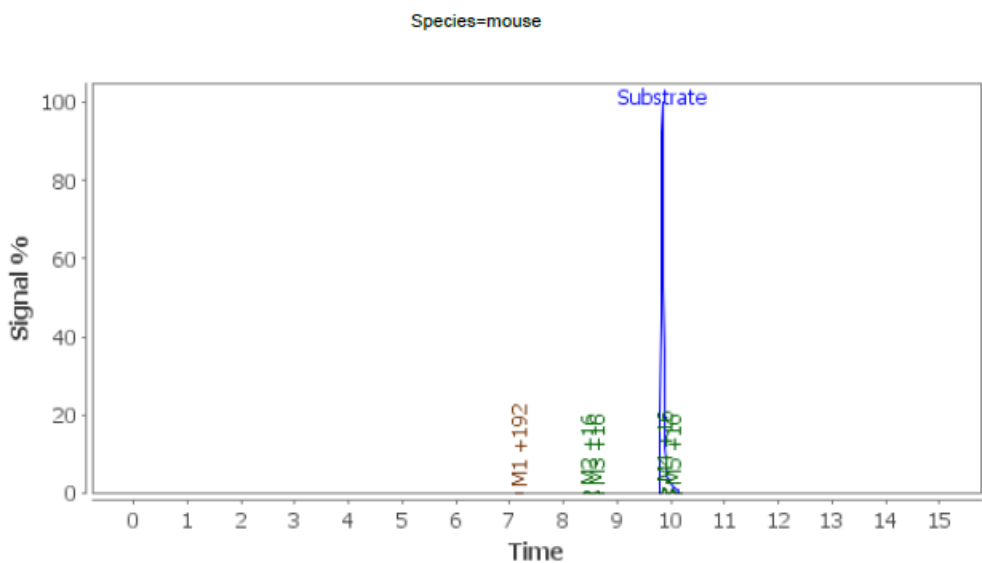
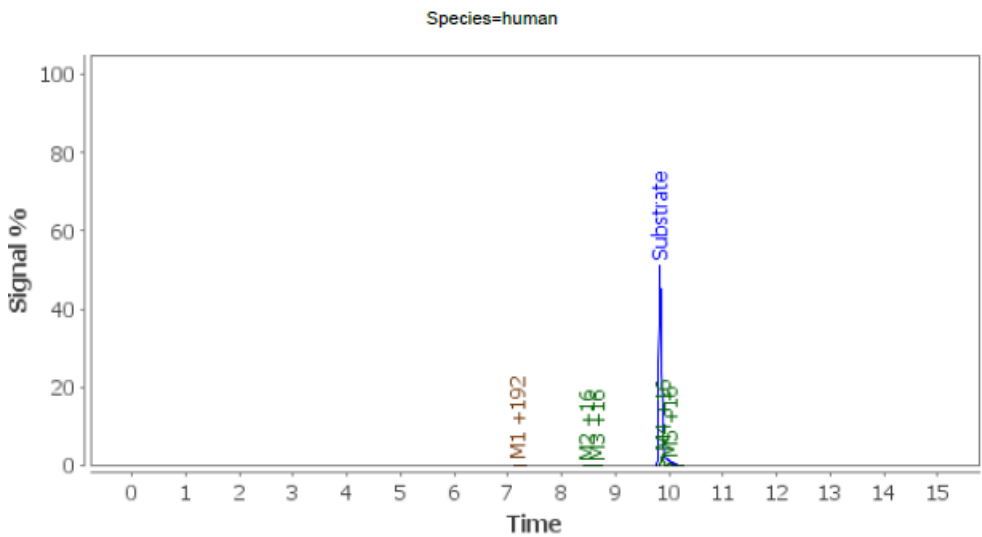
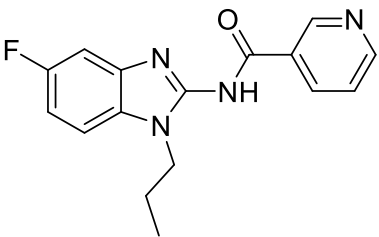
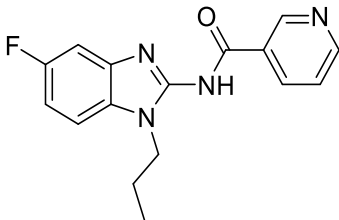
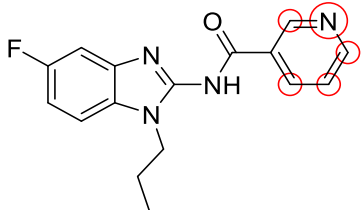

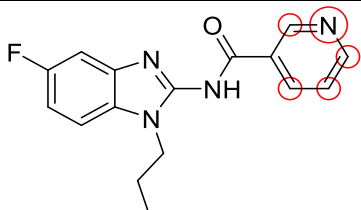

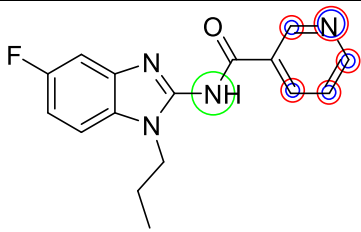



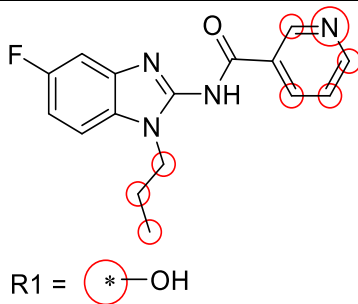

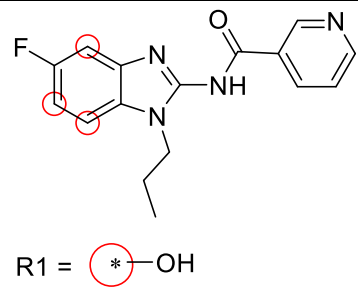



Table S4. Metabolite ID data for compound **33**

Peak Name	Proposed Structure	Retention Time (min)	m/z	Area (%)	
				Mouse	Human
Substrate 33			299.1297	98.09	94.29
M4 (+16)	 R1 =  -OH	9.87	315.1245	0.69	3.93
M5 (+16)	 R1 =  -OH	10.02	315.1246	0.44	1.23
M1 (+192)	 R1 =  -Gluc R2 =  -OGluc R3 =  -OH	7.18	491.1563	0.09	0.46

M2 (+16)	 <p>R1 = -OH</p>	8.44	315.1249	0.36	0.04
M3 (+16)	 <p>R1 = -OH</p>	8.63	315.1248	0.33	0.04

X-ray crystallographic data of **54**

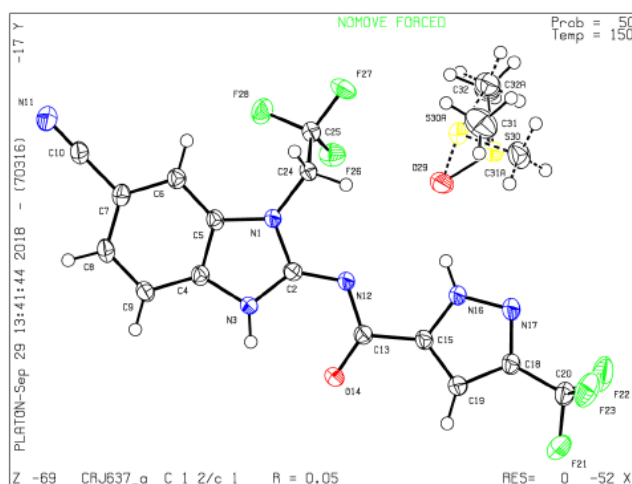
The crystals were obtained by solubilizing 8 mg of the compound **54** in 2 ml of DMSO, followed by refrigeration at 2 degrees for 72 h.

Summary of Data CCDC 1870932

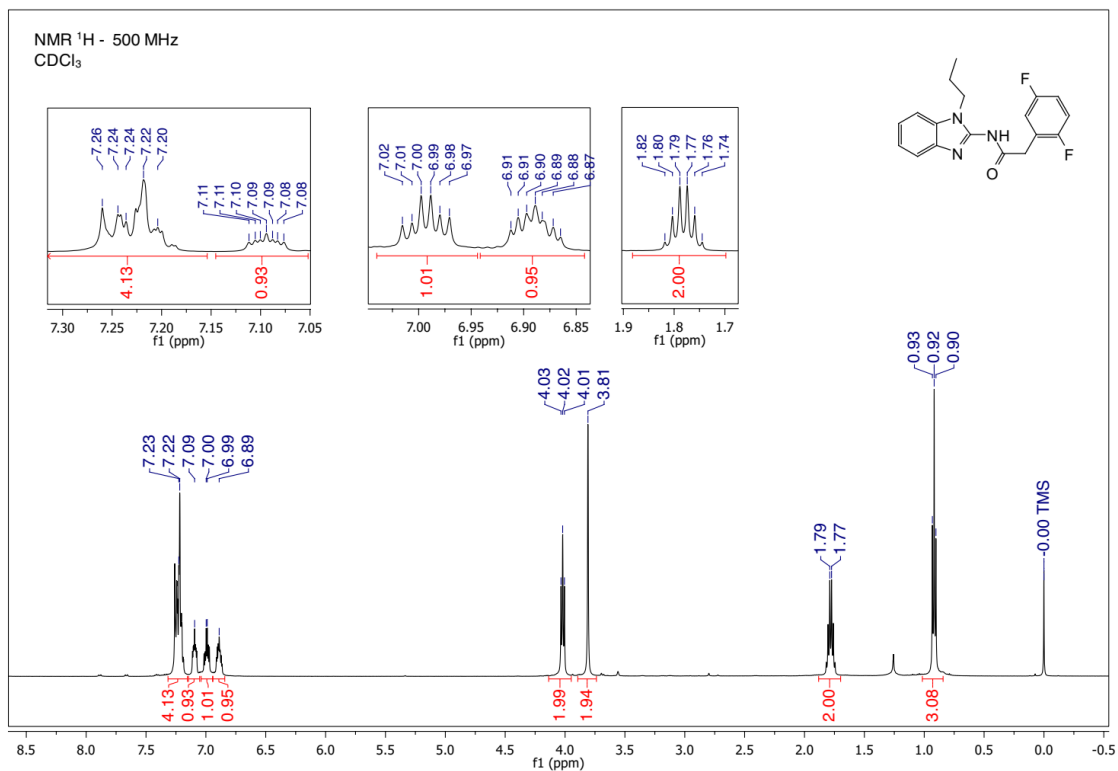
Formula: C₁₅ H₈ F₆ N₆ O₁ C₂ H₆ O₁ S₁

Unit Cell Parameters: a 35.724(4) b 4.8349(5) c 24.352(3) C2/c

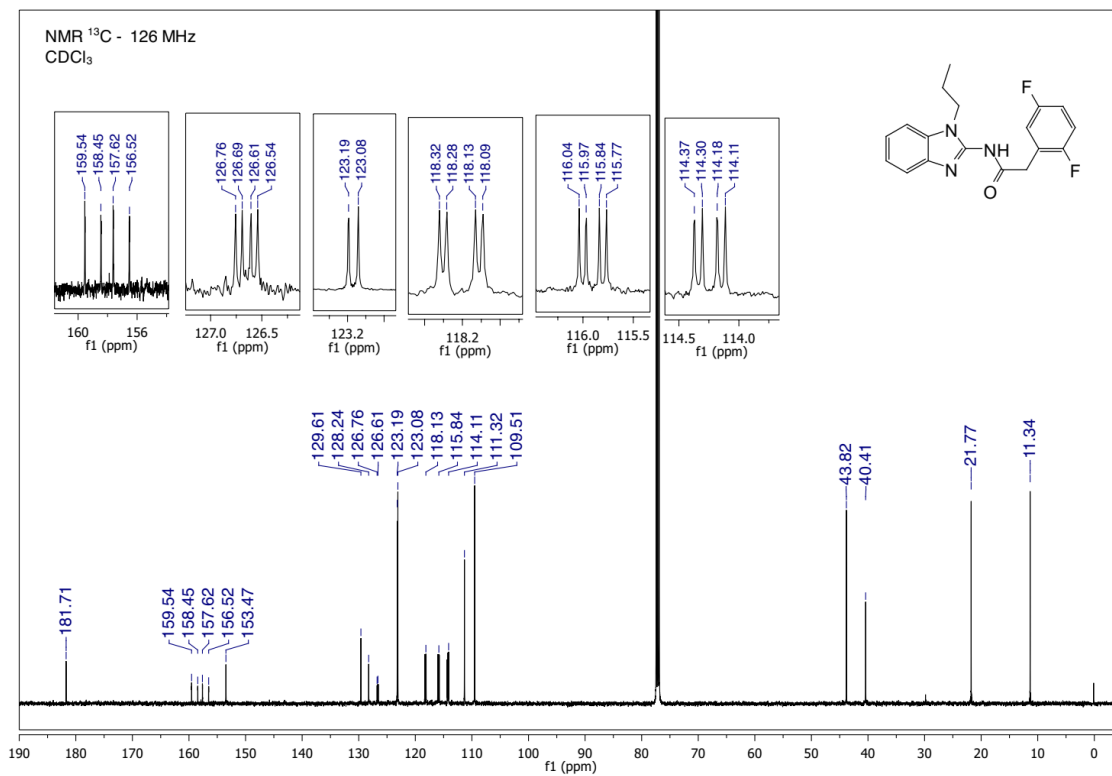
Bond precision:	C-C = 0.0030 Å	Wavelength=1.54178	
Cell:	a=35.724 (4)	b=4.8349 (5)	c=24.352 (3)
	alpha=90	beta=112.773 (5)	gamma=90
Temperature:	150 K		
	Calculated	Reported	
Volume	3878.2 (8)	3878.3 (7)	
Space group	C 2/c	C 1 2/c 1	
Hall group	: -C 2yc	-C 2yc	
Moiety formula	C ₁₅ H ₈ F ₆ N ₆ O, C ₂ H ₆ O S	C ₁₅ H ₈ F ₆ N ₆ O, C ₂ H ₆ O S	
Sum formula	C ₁₇ H ₁₄ F ₆ N ₆ O ₂ S	C ₁₇ H ₁₄ F ₆ N ₆ O ₂ S	
Mr	480.40	480.40	
Dx, g cm ⁻³	1.646	1.645	
Z	8	8	
Mu (mm ⁻¹)	2.298	2.298	
F ₀₀₀	1952.0	1962.9	
F ₀₀₀ '	1962.50		
h,k,lmax	42,5,29	41,5,28	
Nref	3572	3470	
Tmin,Tmax	0.811,0.938	0.527,0.753	
Tmin'	0.326		
Correction method=	# Reported T Limits: Tmin=0.527 Tmax=0.753		
AbsCorr =	MULTI-SCAN		
Data completeness=	0.971	Theta(max)= 68.670	
R(reflections)=	0.0472 (3099)	wR2(reflections)= 0.1386 (3470)	
S =	1.047	Npar= 321	



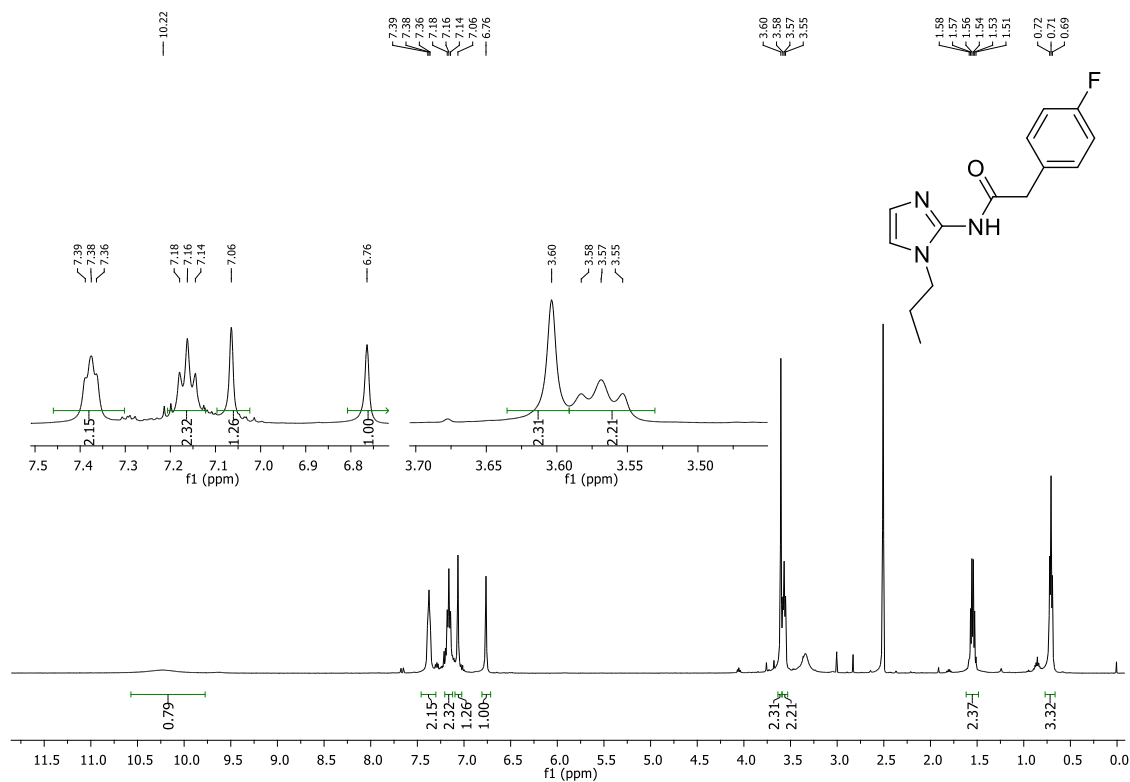
NMR spectra



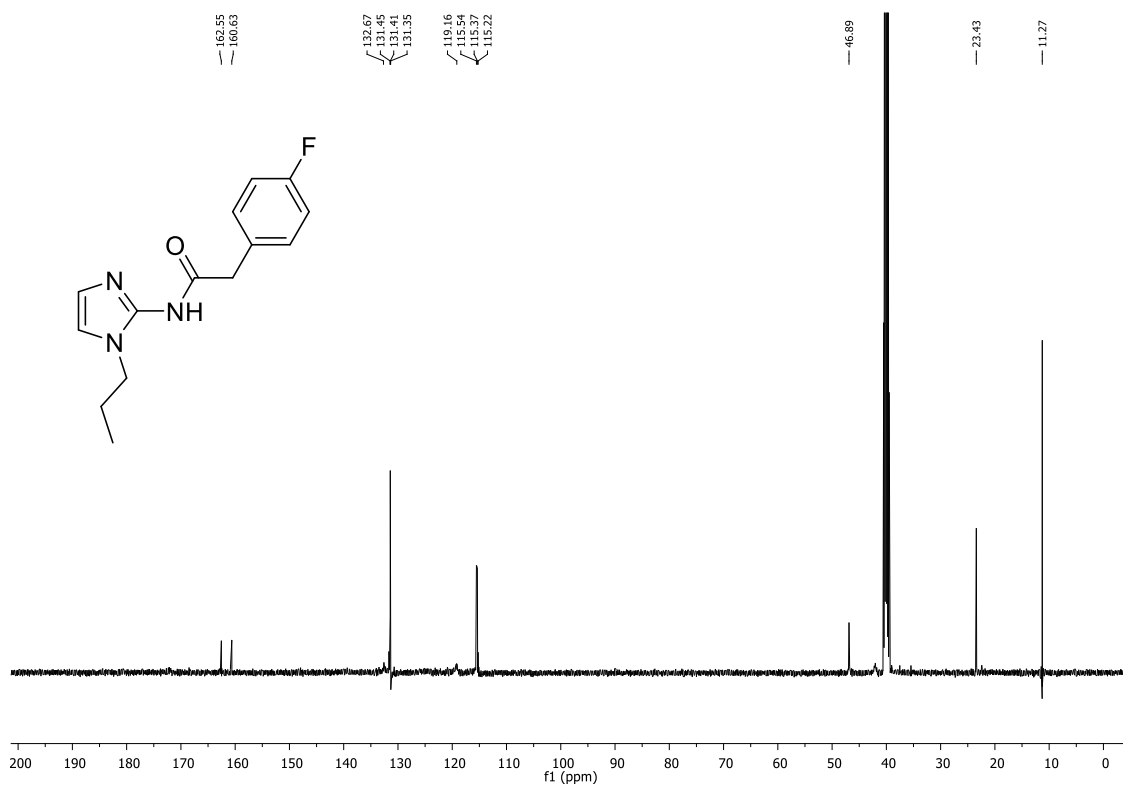
^1H NMR of **3** (500 MHz, CDCl_3)



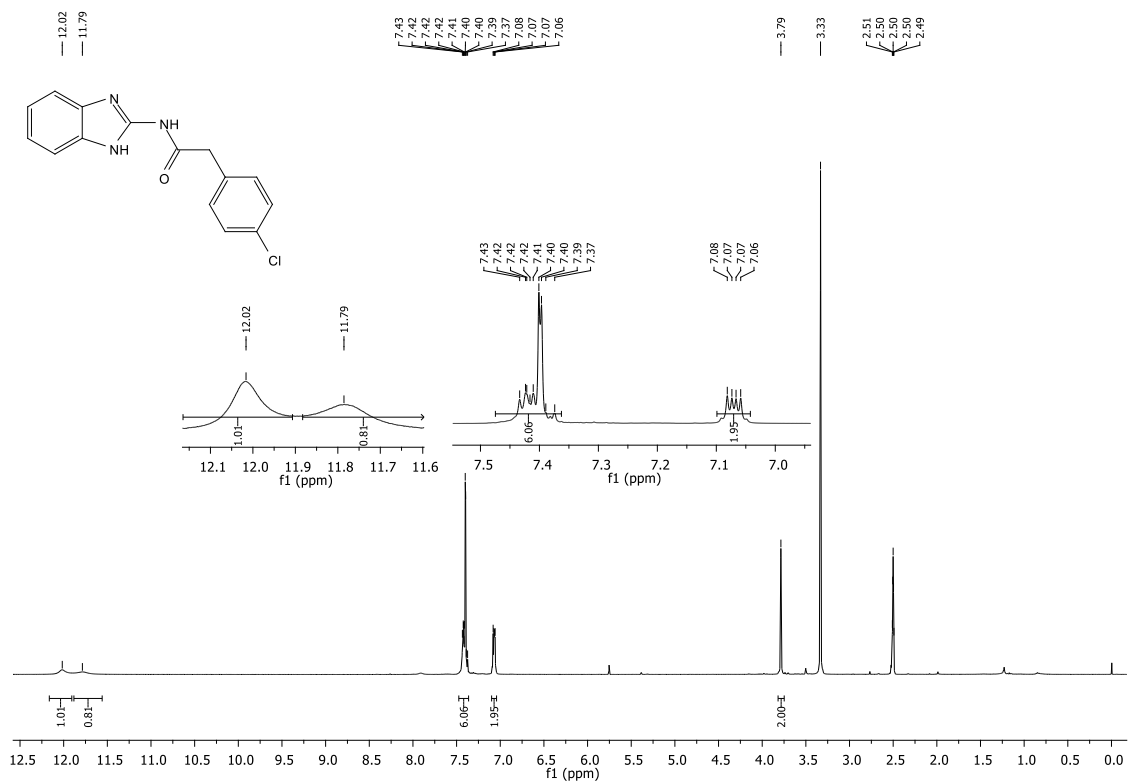
^{13}C NMR of **3** (126 MHz, CDCl_3)



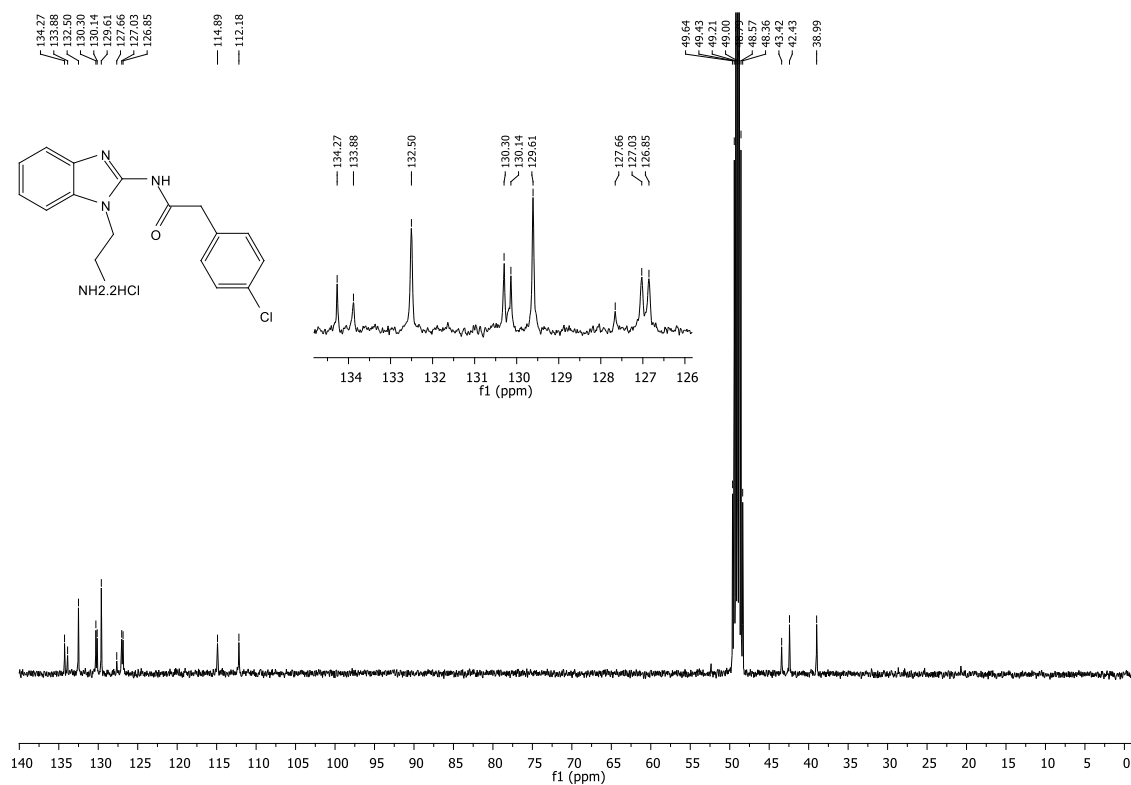
¹H NMR of 4 (500 MHz, DMSO)



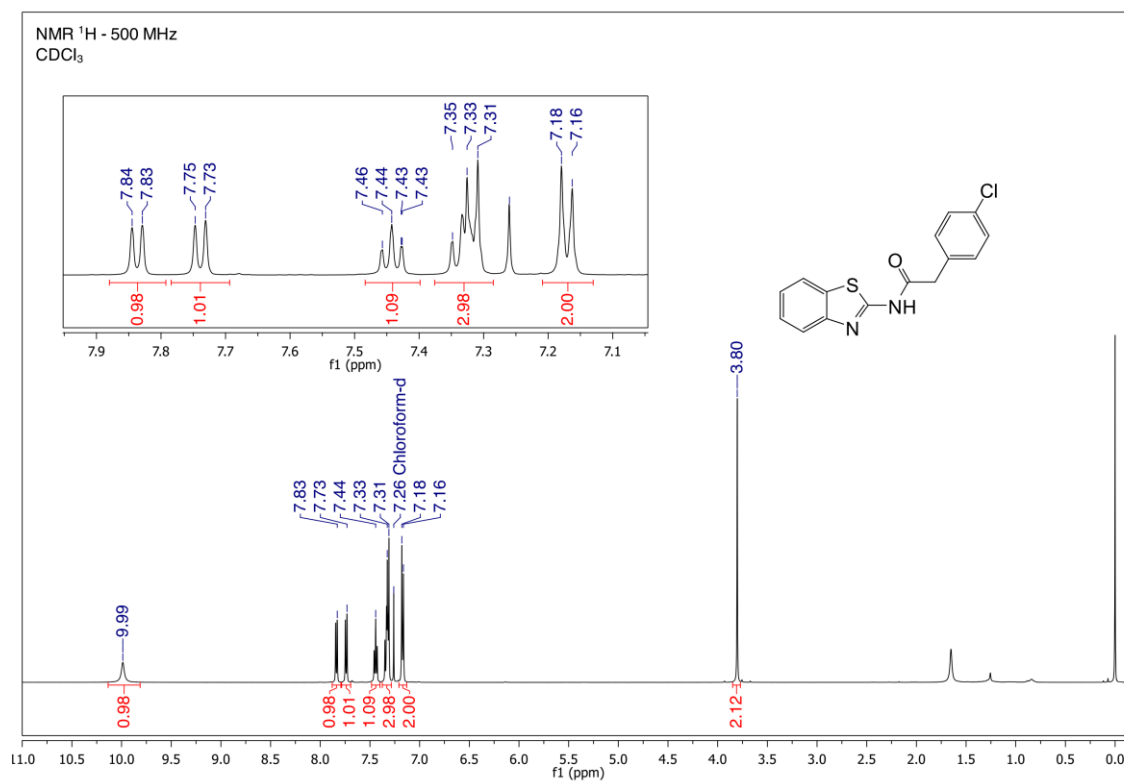
¹³C NMR of 4 (126 MHz, DMSO)



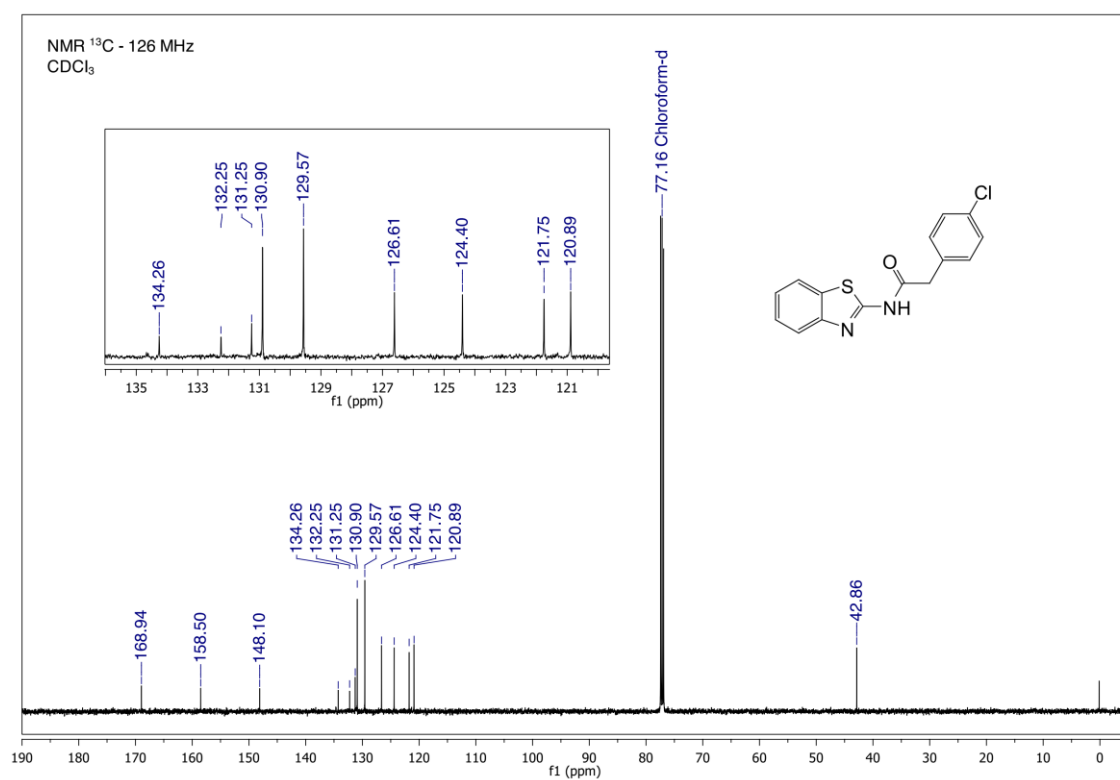
¹H NMR of 5 (400 MHz, DMSO)



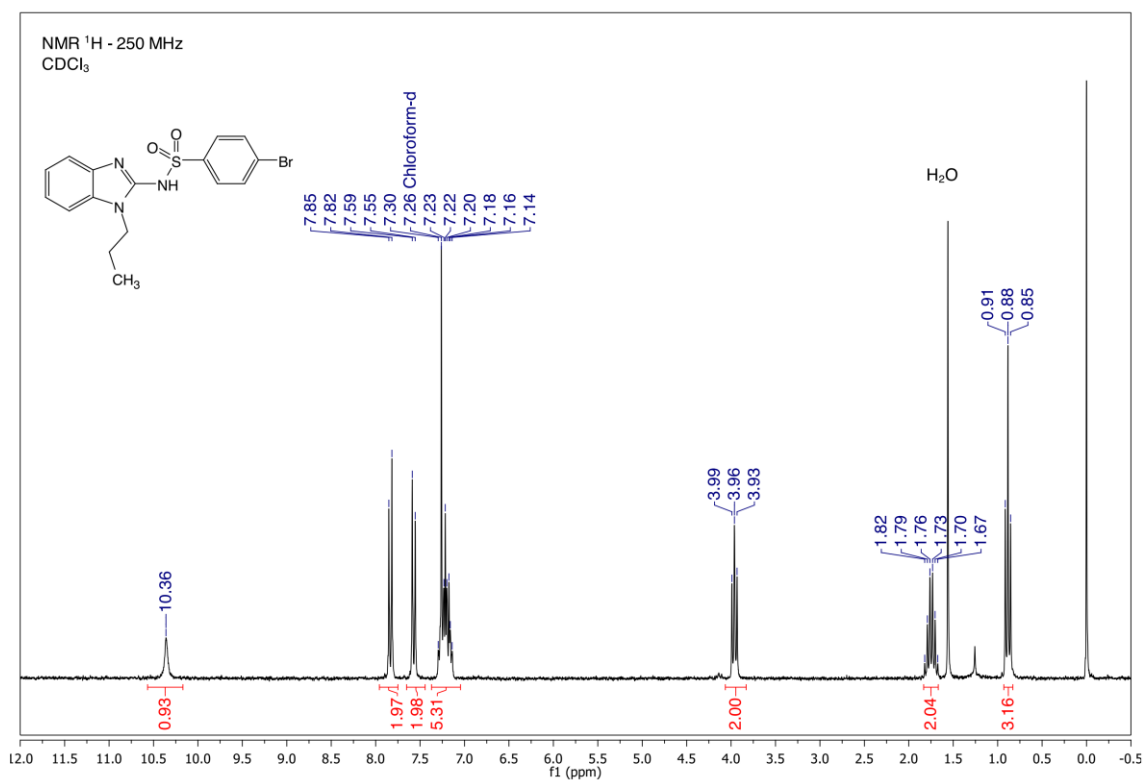
¹³C NMR of 5 (101 MHz, DMSO)



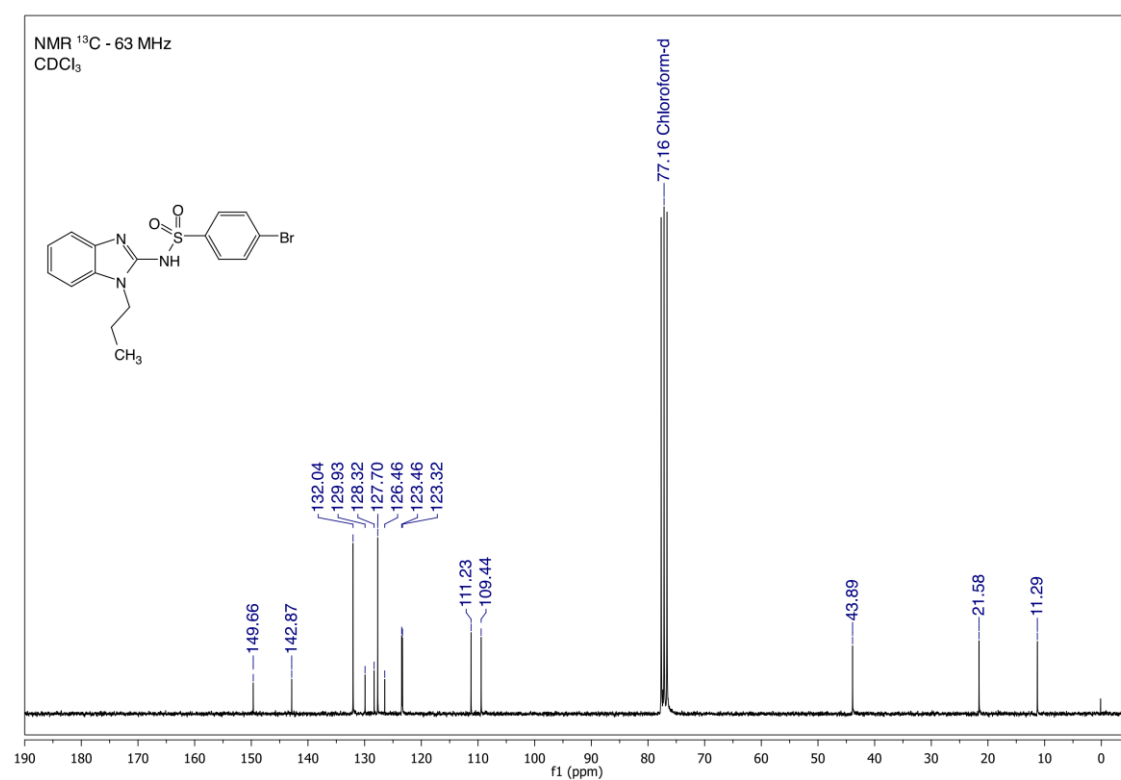
^1H NMR of 6 (500 MHz, CDCl_3)



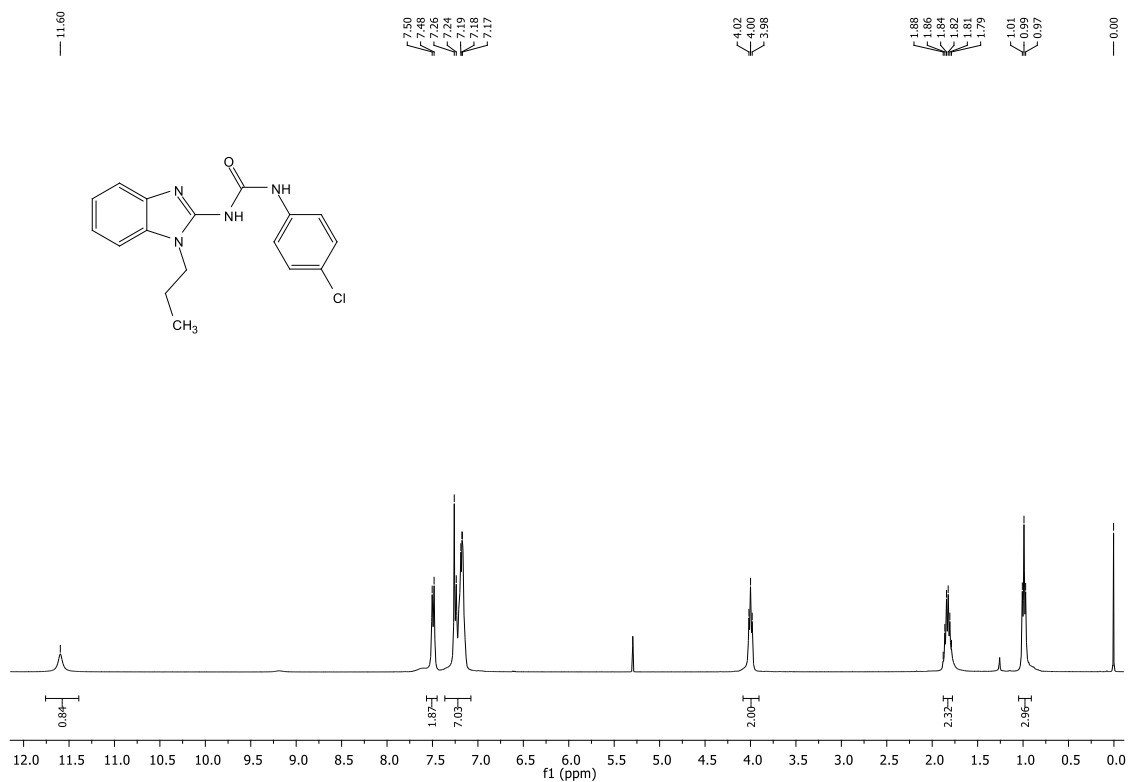
^{13}C NMR of 6 (126 MHz, CDCl_3)



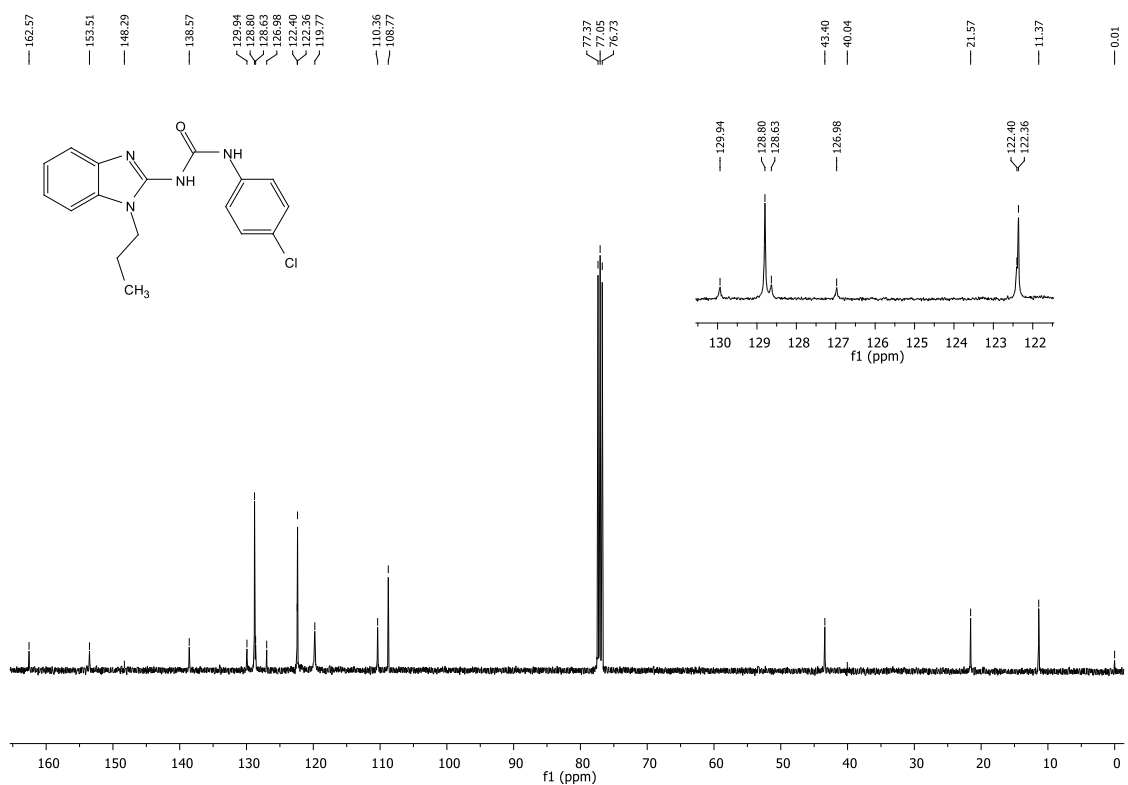
^1H NMR of 7 (250 MHz, CDCl_3)



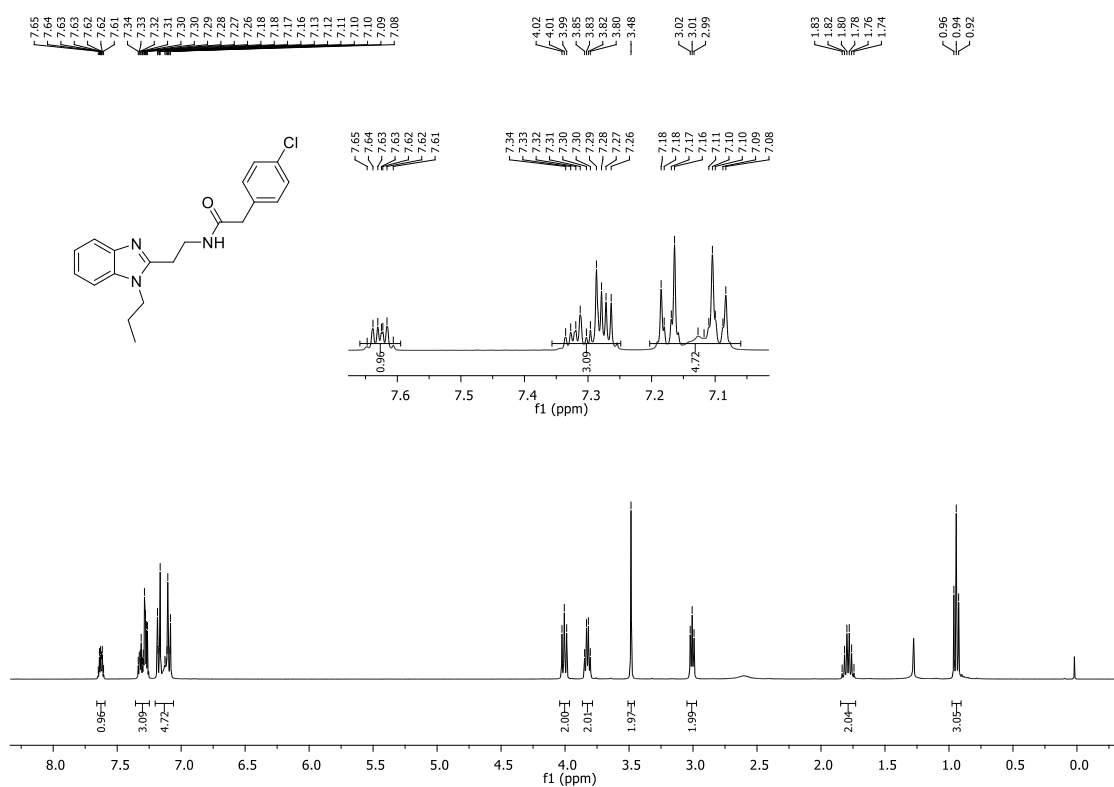
^{13}C NMR of 7 (63 MHz, CDCl_3)



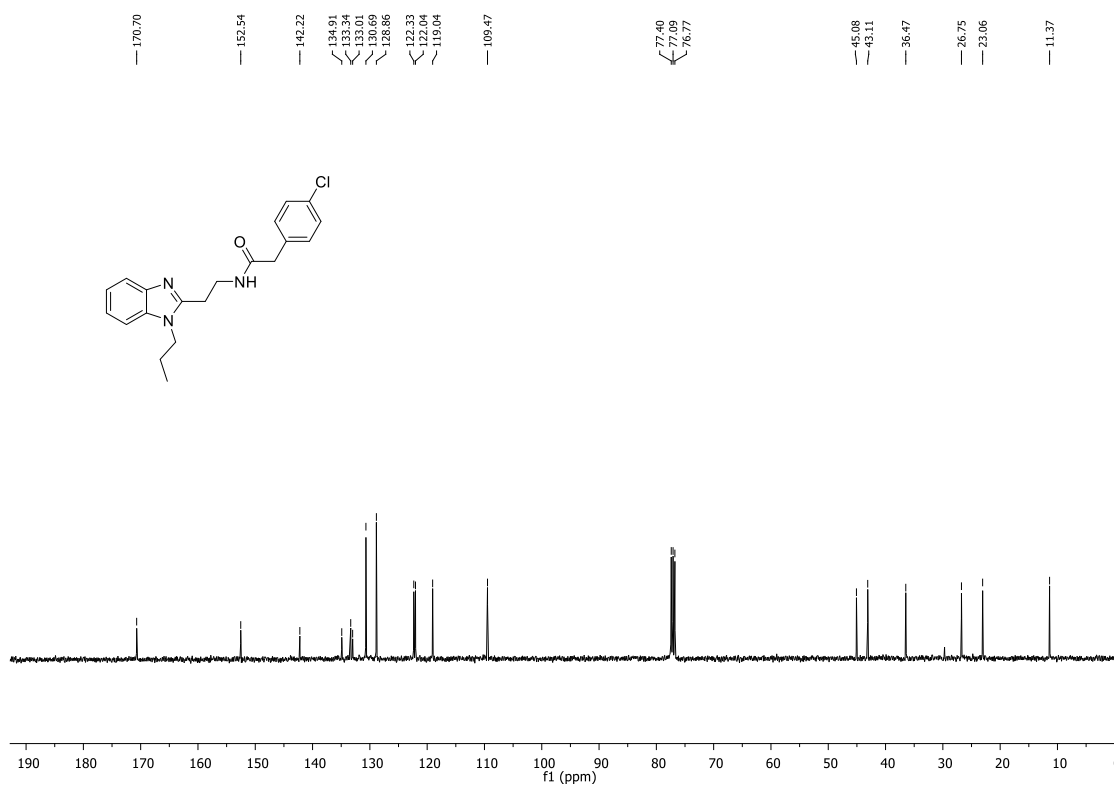
¹H NMR of 8 (400 MHz, CDCl₃)



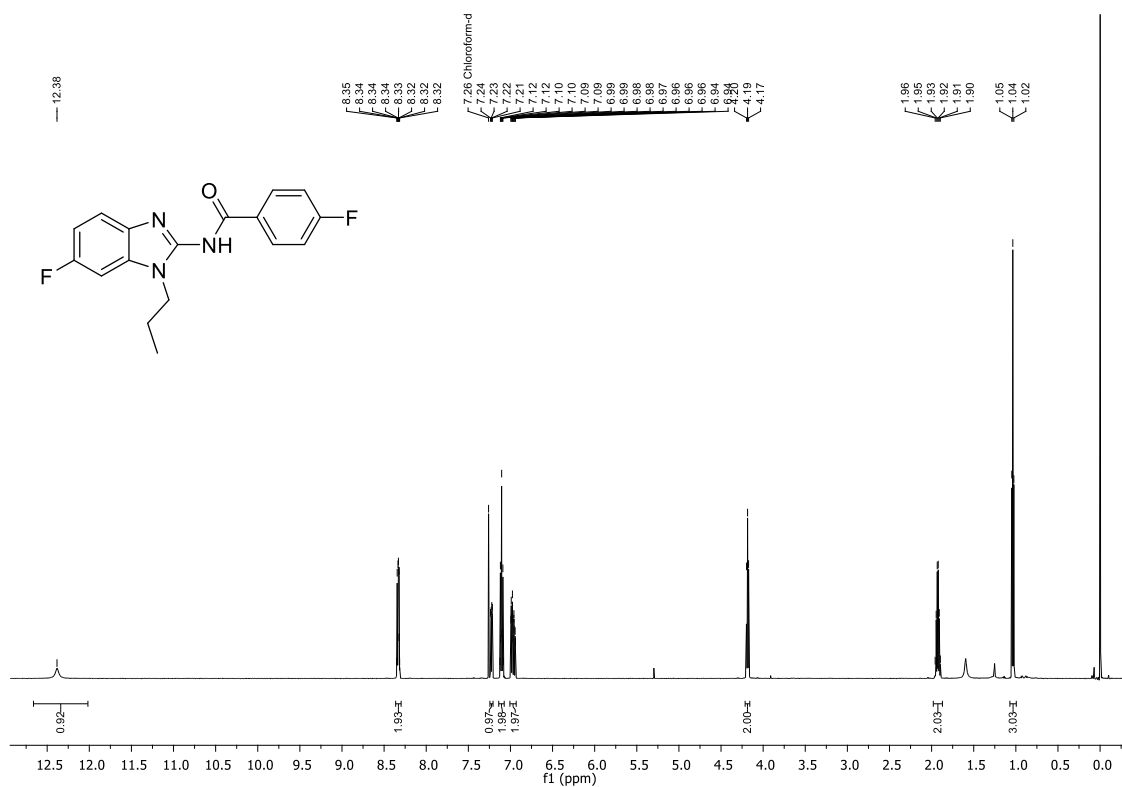
¹³C NMR of 8 (101 MHz, CDCl₃)



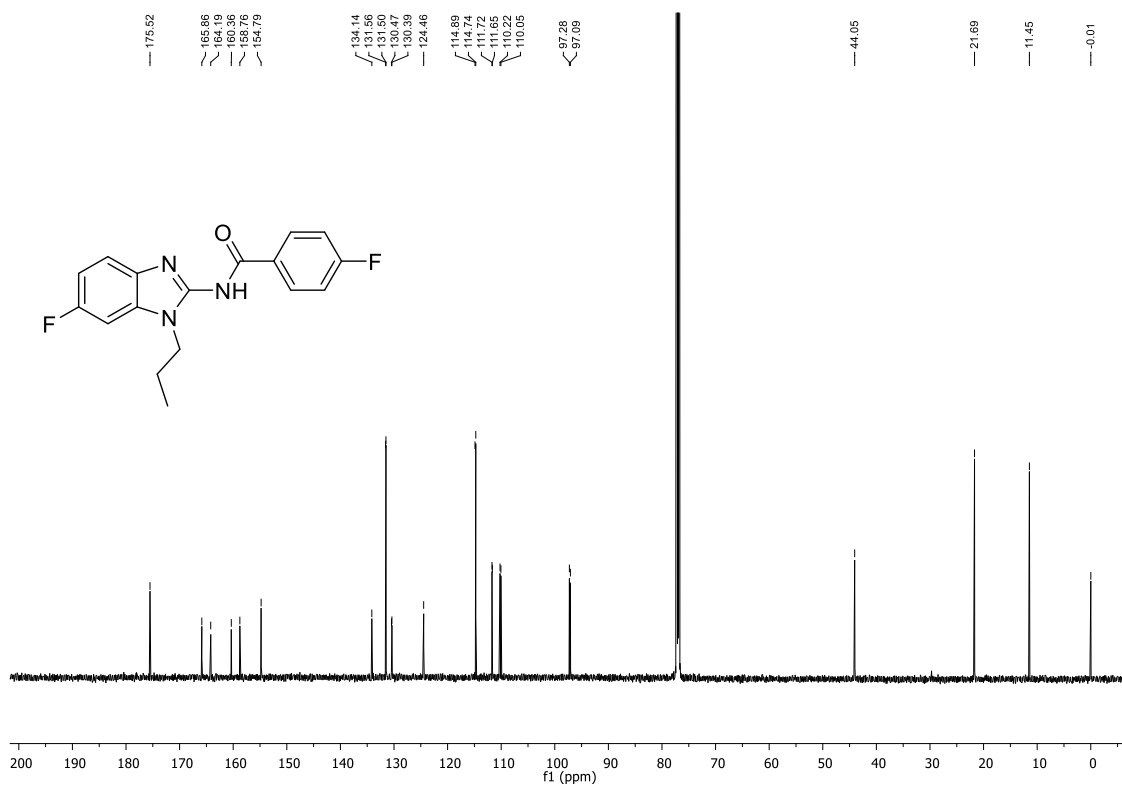
¹H NMR of 9 (400 MHz, CDCl₃)



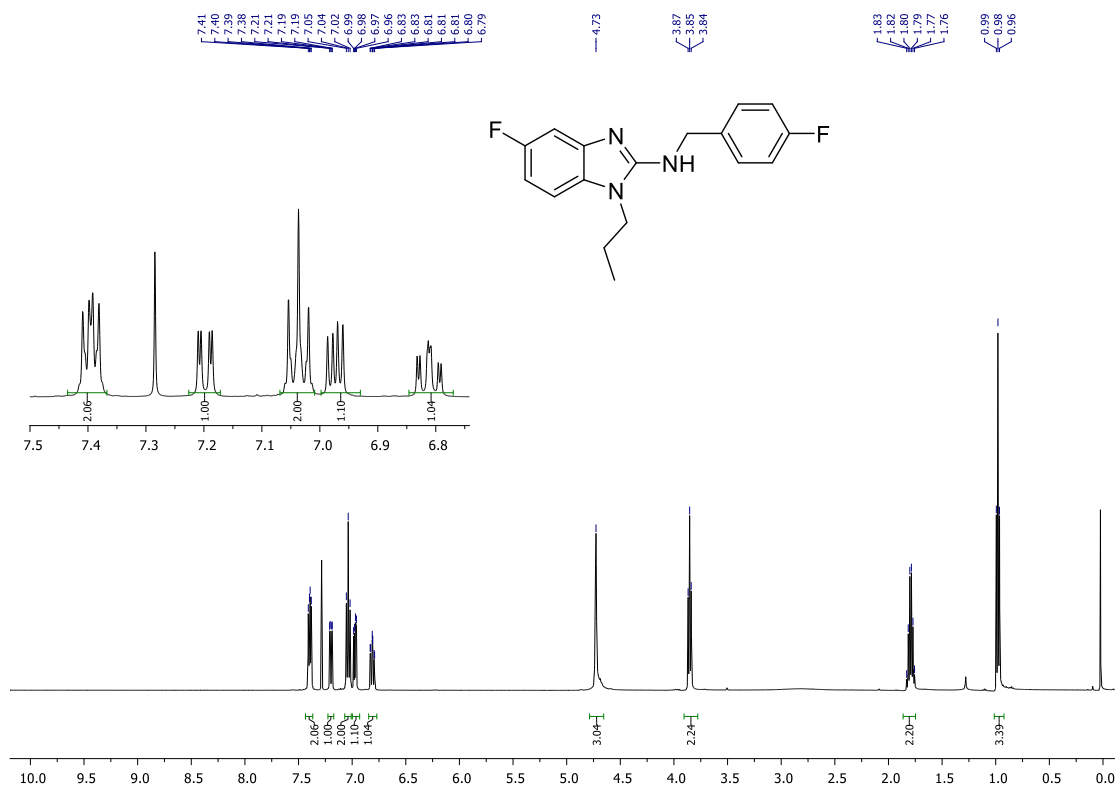
¹³C NMR of 9 (101 MHz, CDCl₃)



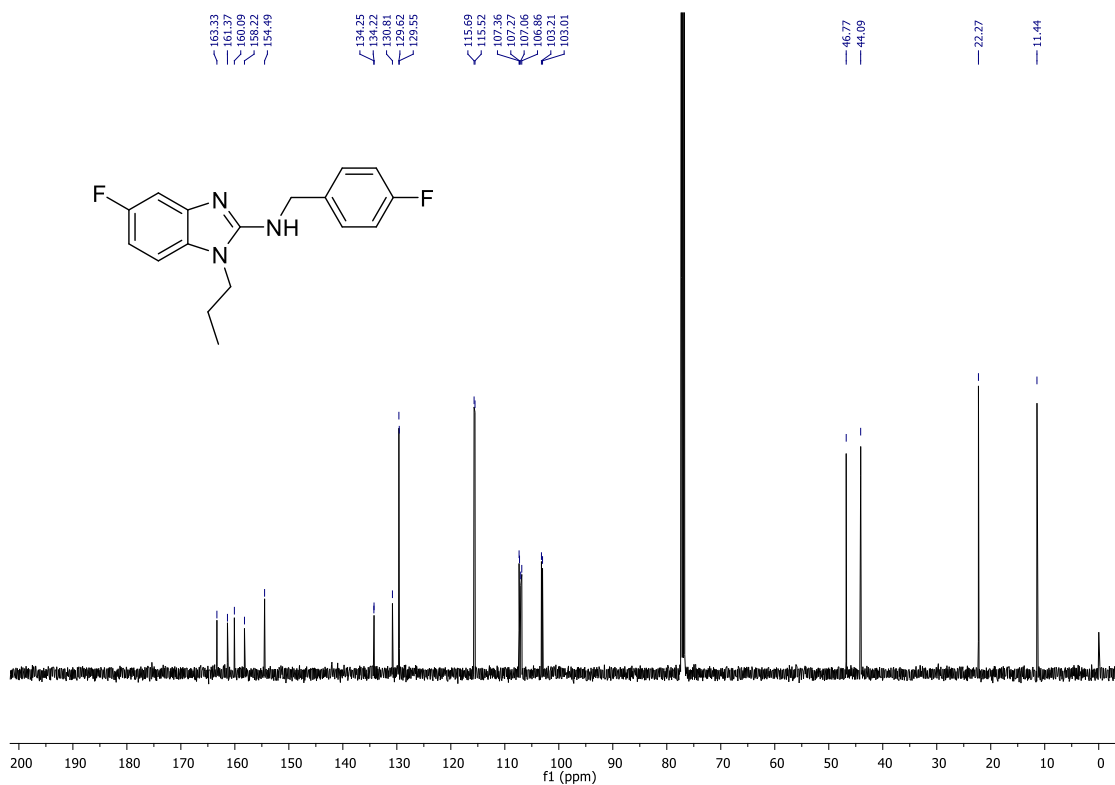
¹H NMR of 10 (600 MHz, CDCl₃)



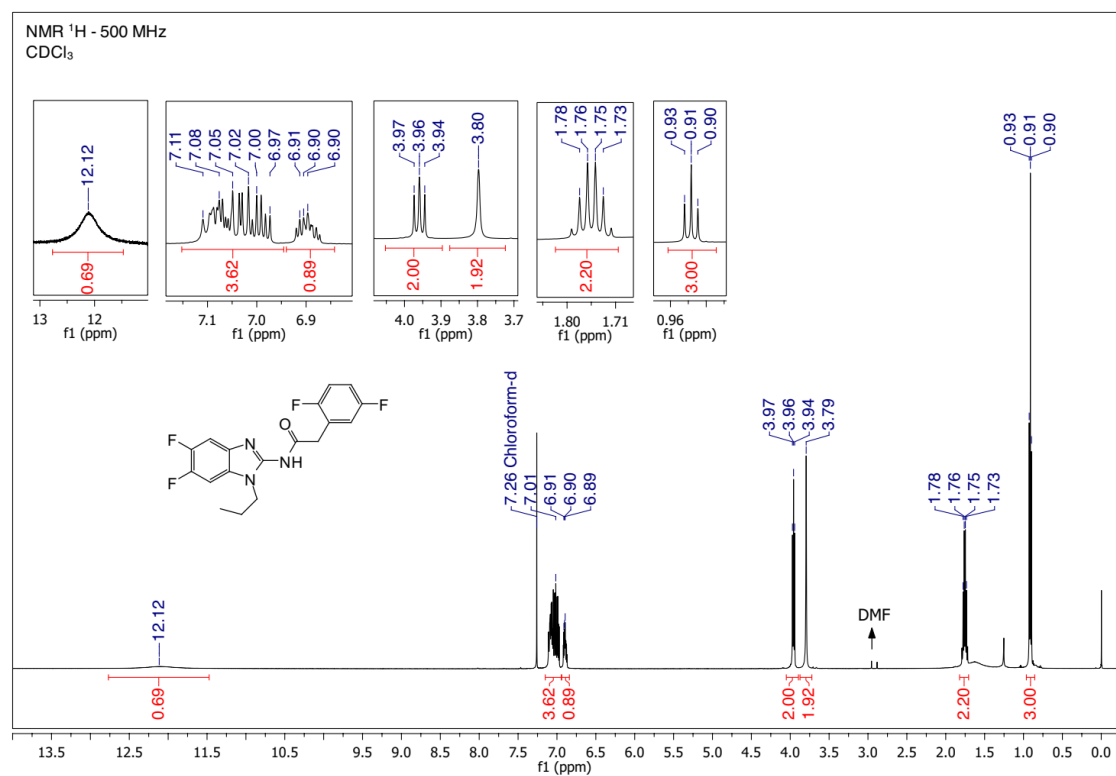
¹³C NMR of 10 (151 MHz, CDCl₃)



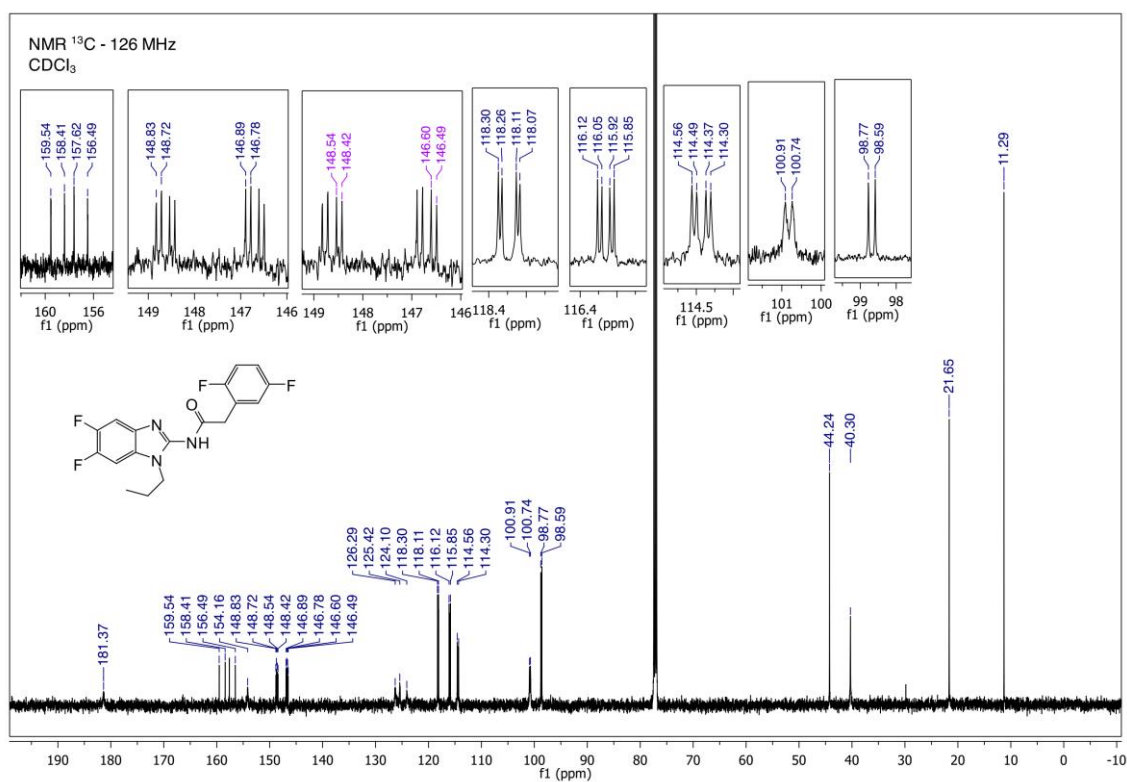
¹H NMR of 11 (500 MHz, CDCl₃)



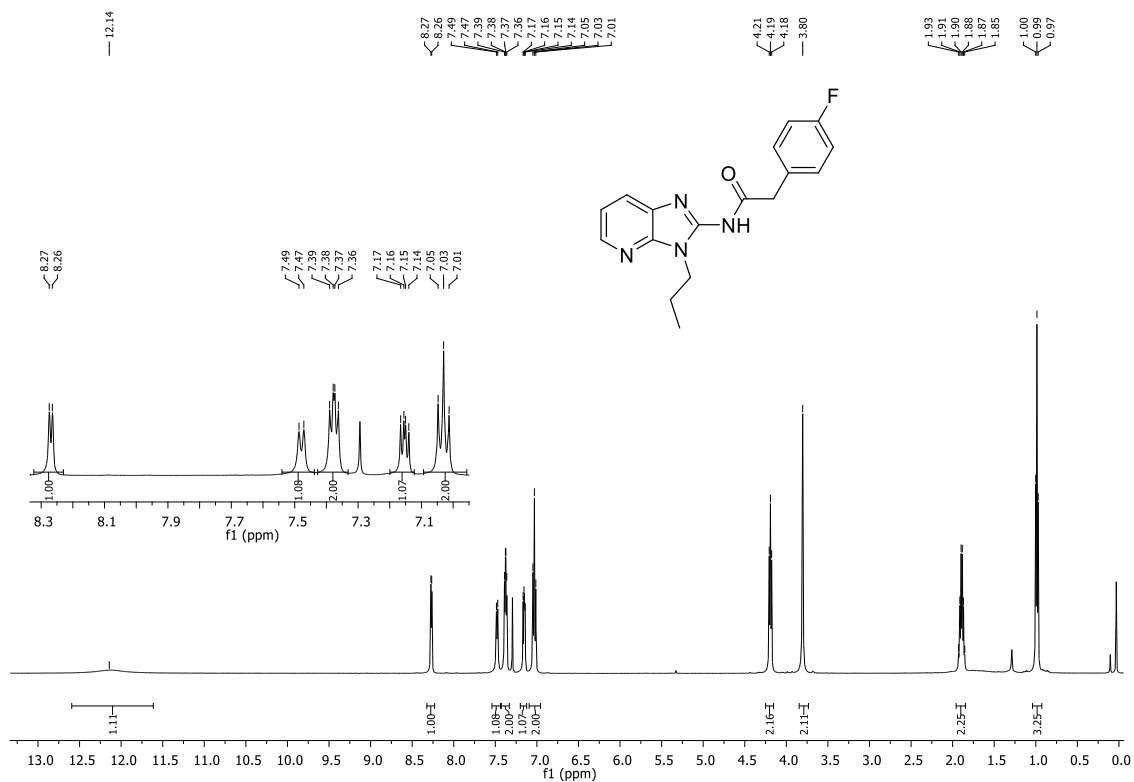
¹³C NMR of 11 (126 MHz, CDCl₃)



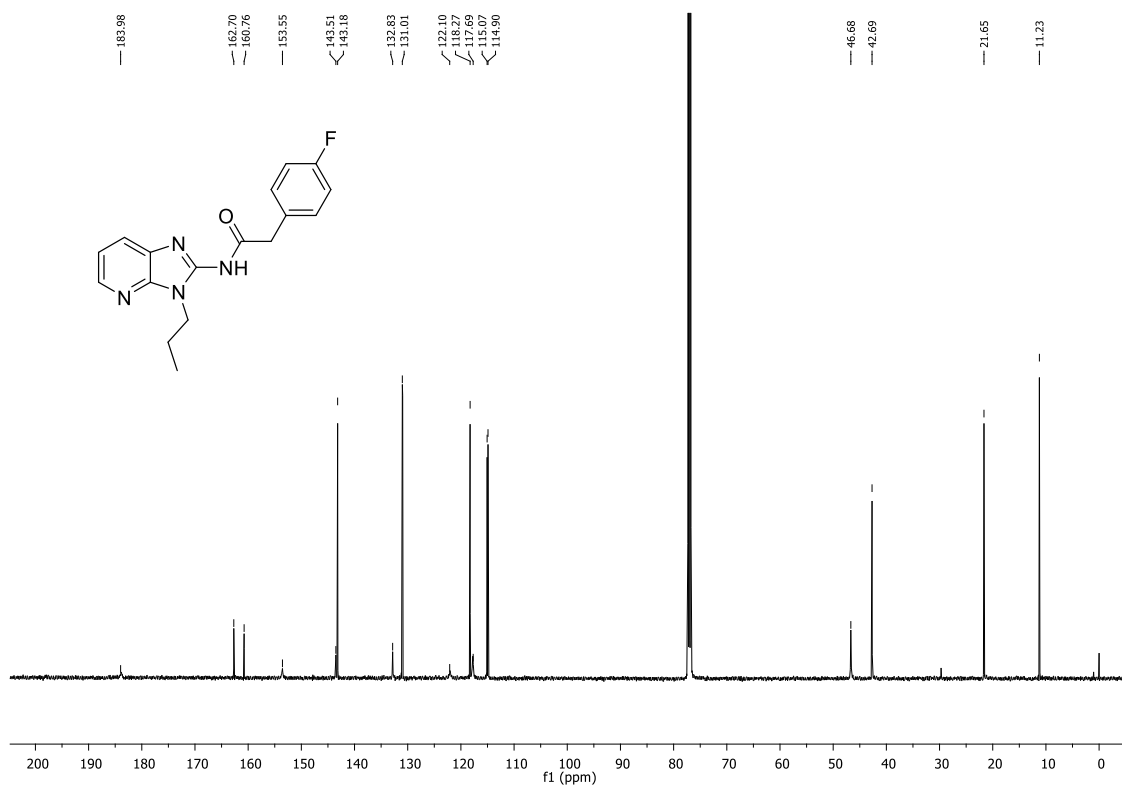
^1H NMR of 15 (500 MHz, CDCl₃)



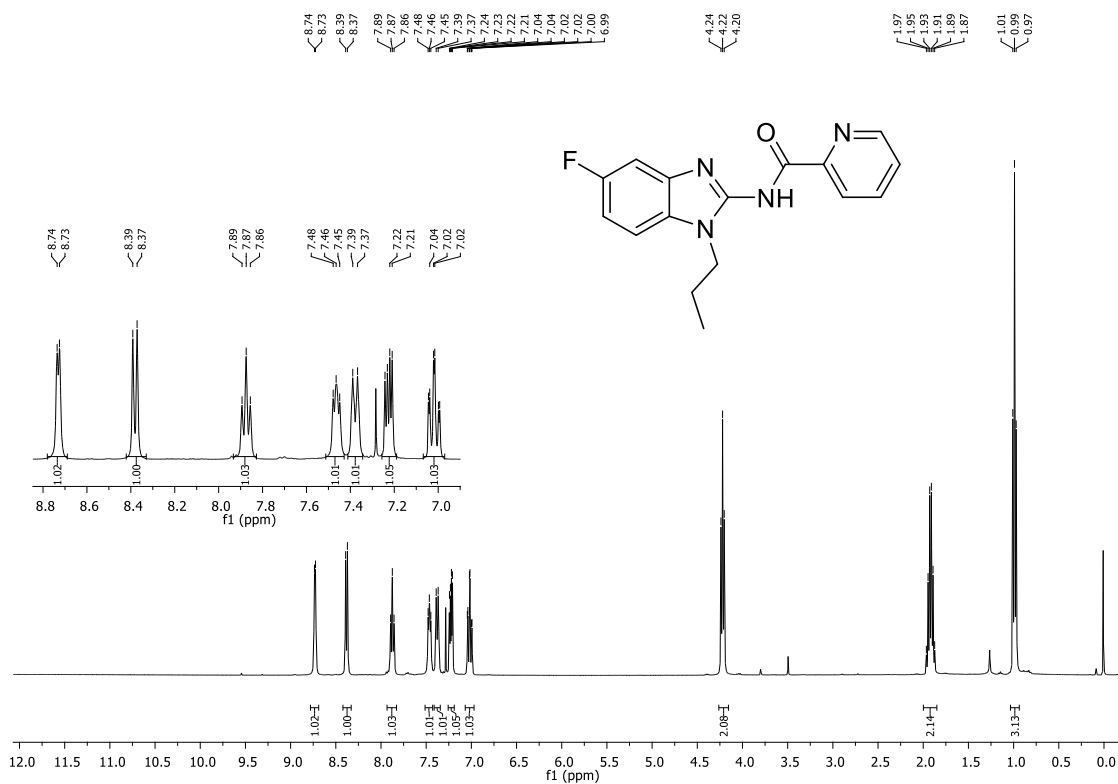
^{13}C NMR of 15 (126 MHz, CDCl₃)



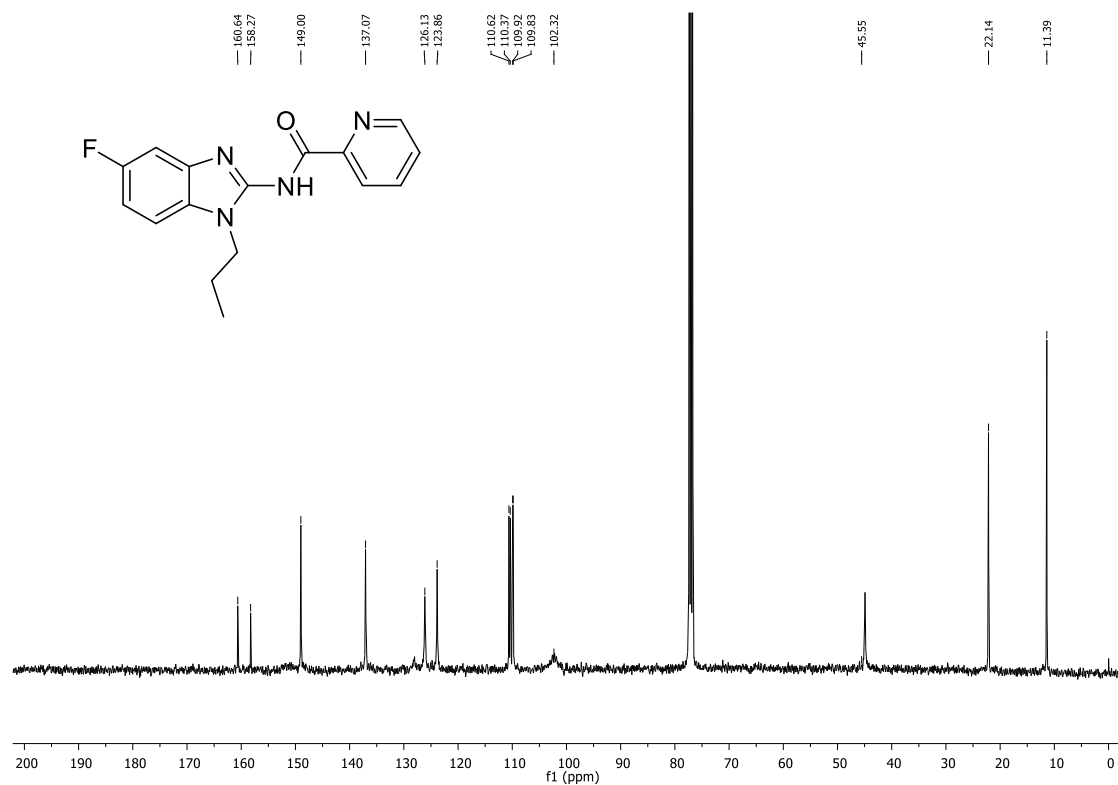
¹H NMR of 25 (500 MHz, CDCl₃)



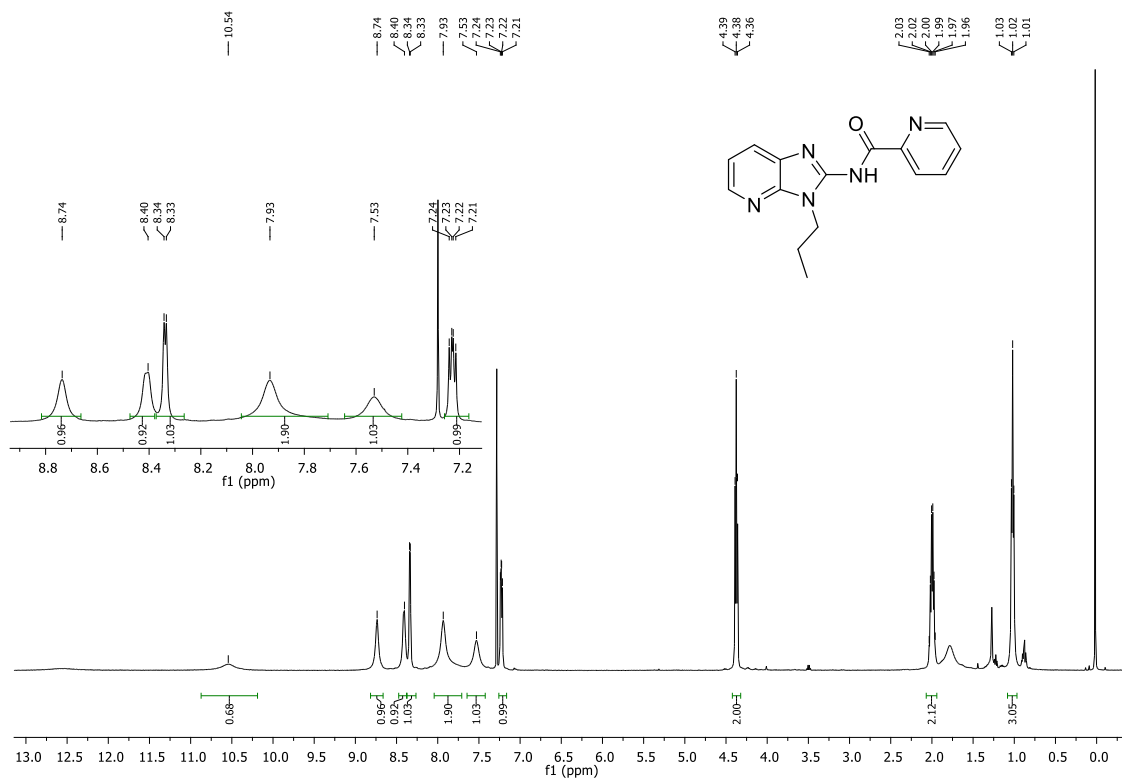
¹³C NMR of 25 (126 MHz, CDCl₃)



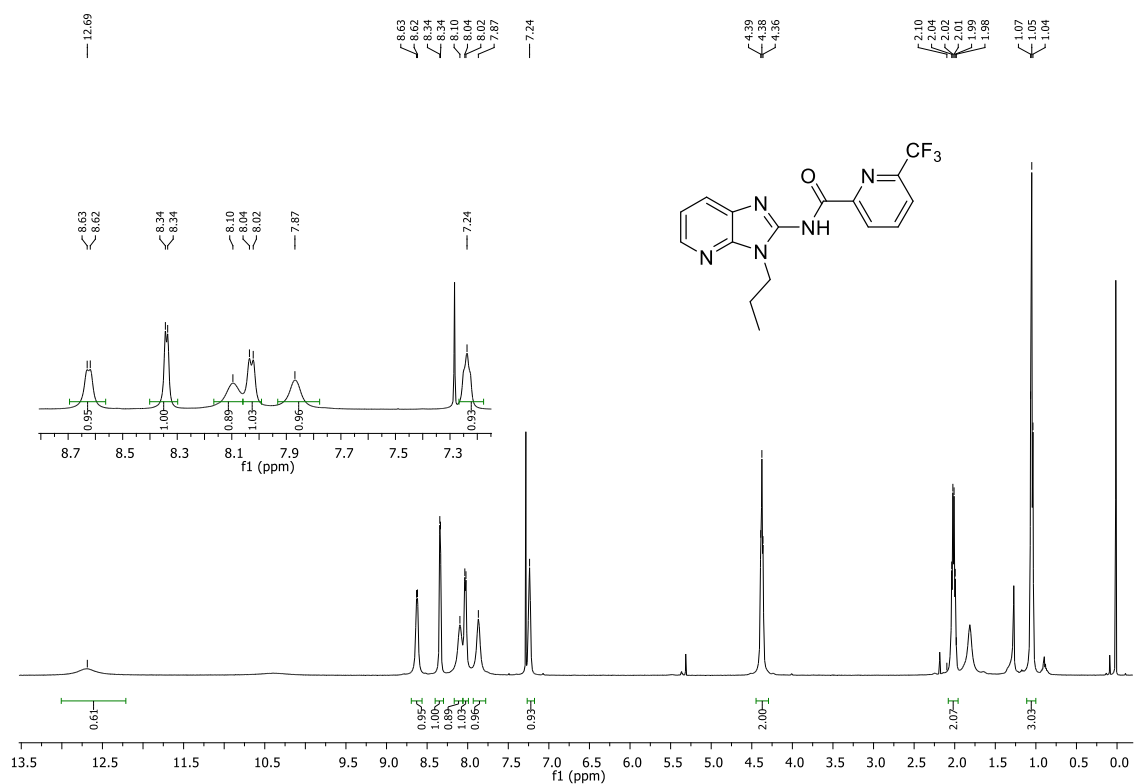
¹H NMR of 26 (400 MHz, CDCl₃)



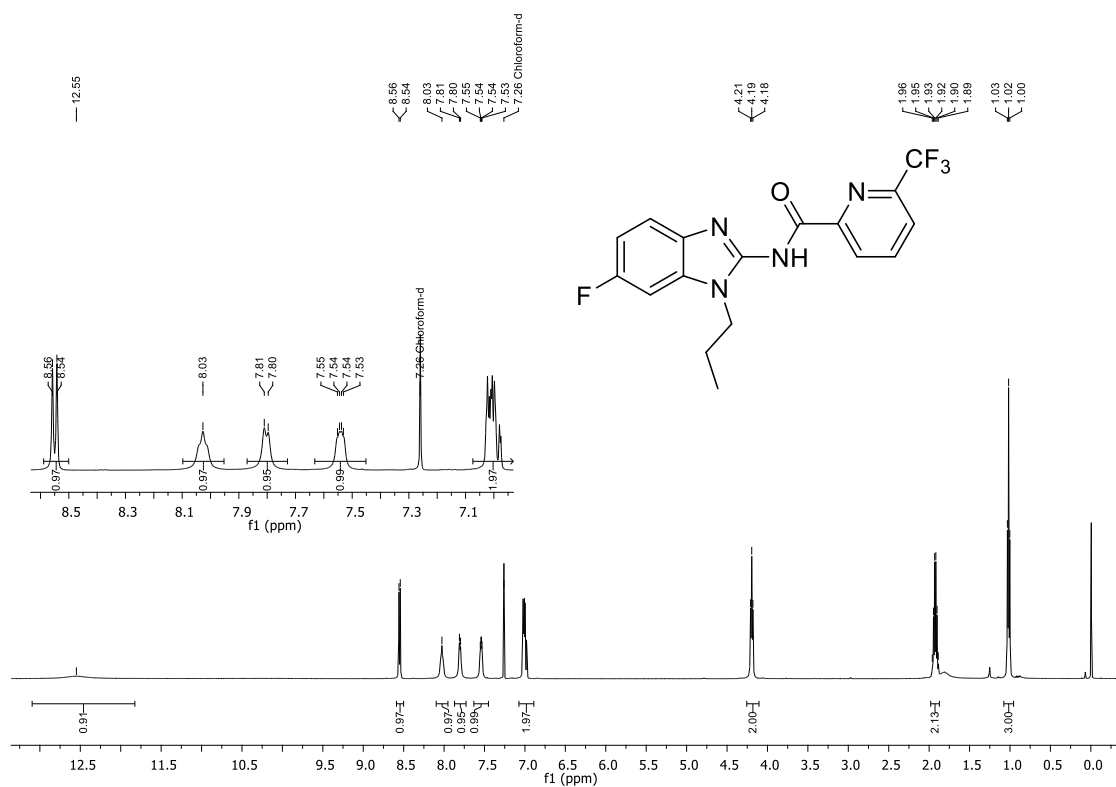
¹³C NMR of 26 (101 MHz, CDCl₃)



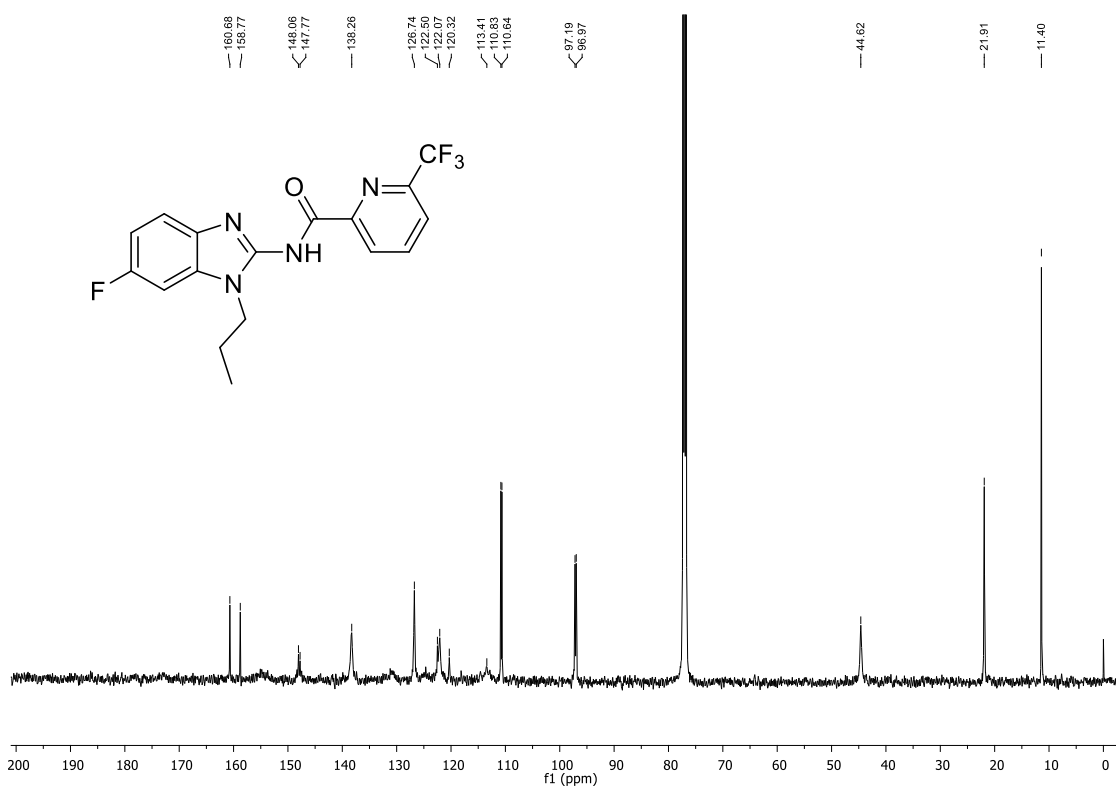
¹H NMR of 27 (500 MHz, CDCl₃)



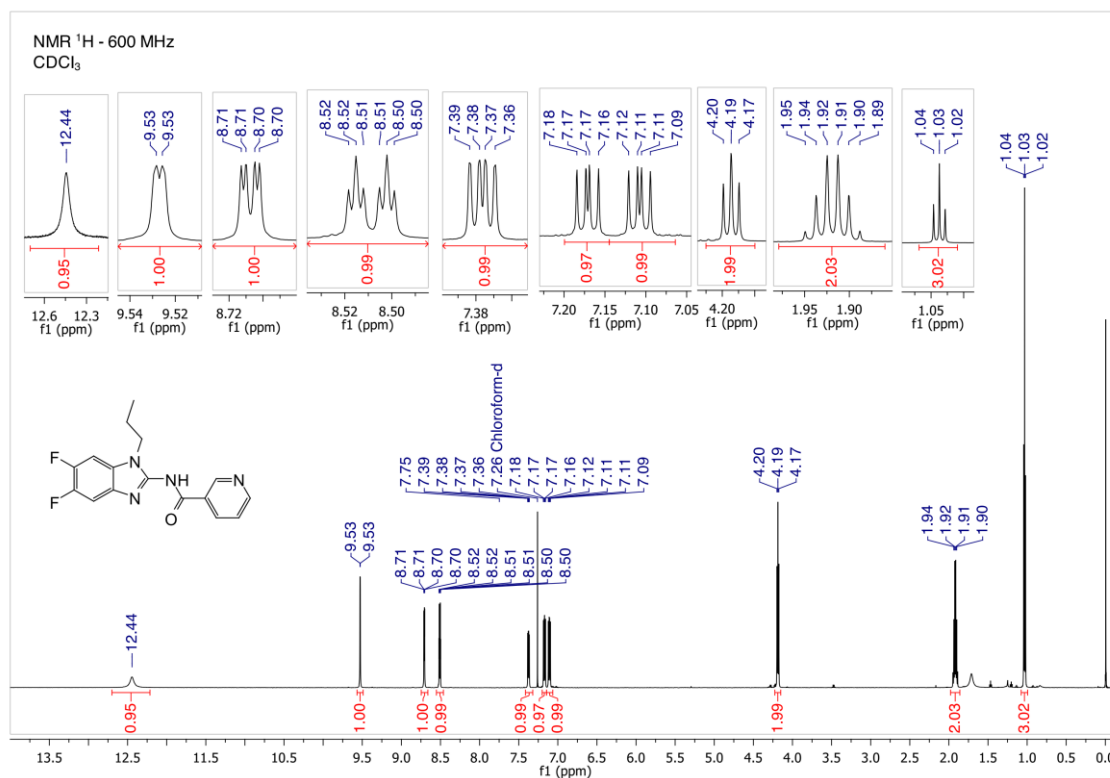
¹H NMR of 28 (500 MHz, CDCl₃)



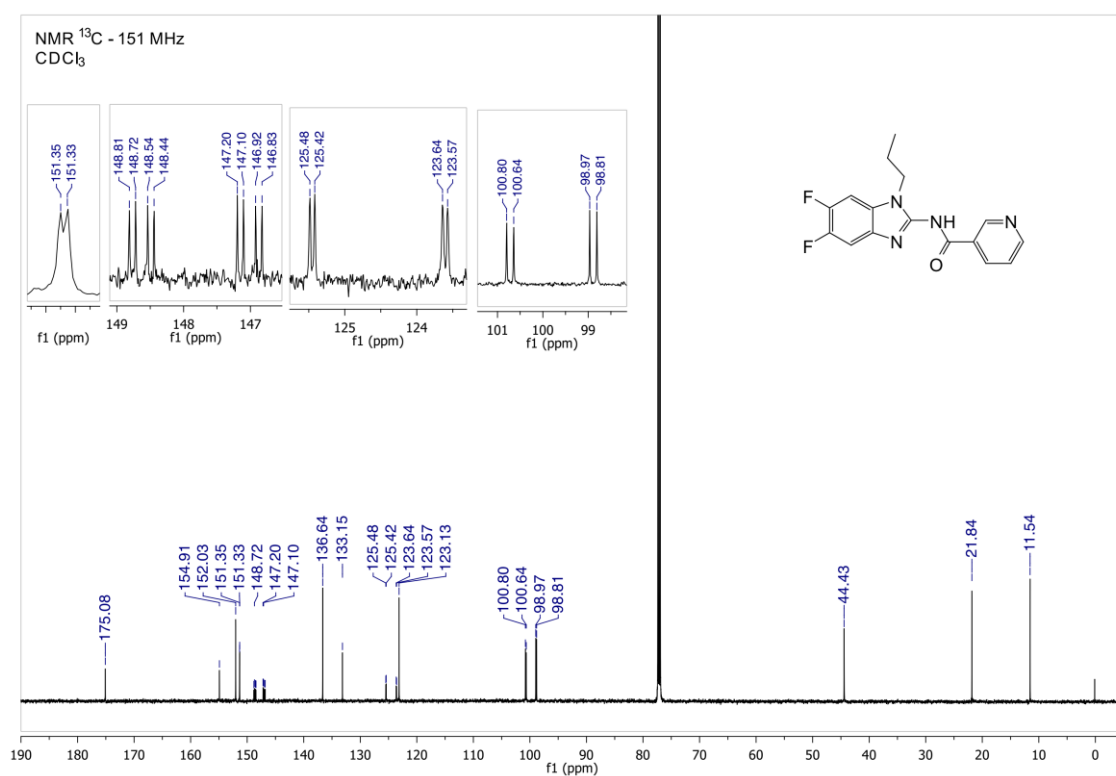
¹H NMR of 29 (500 MHz, CDCl₃)



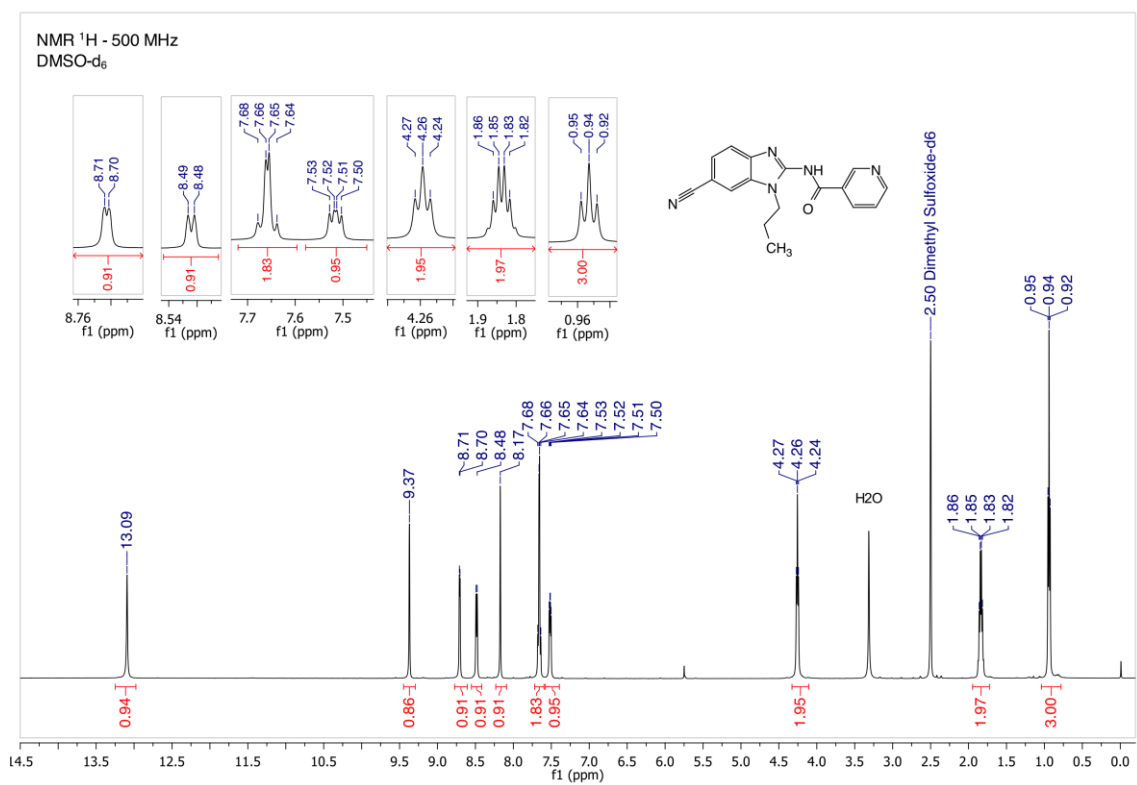
¹³C NMR of 29 (126 MHz, CDCl₃)



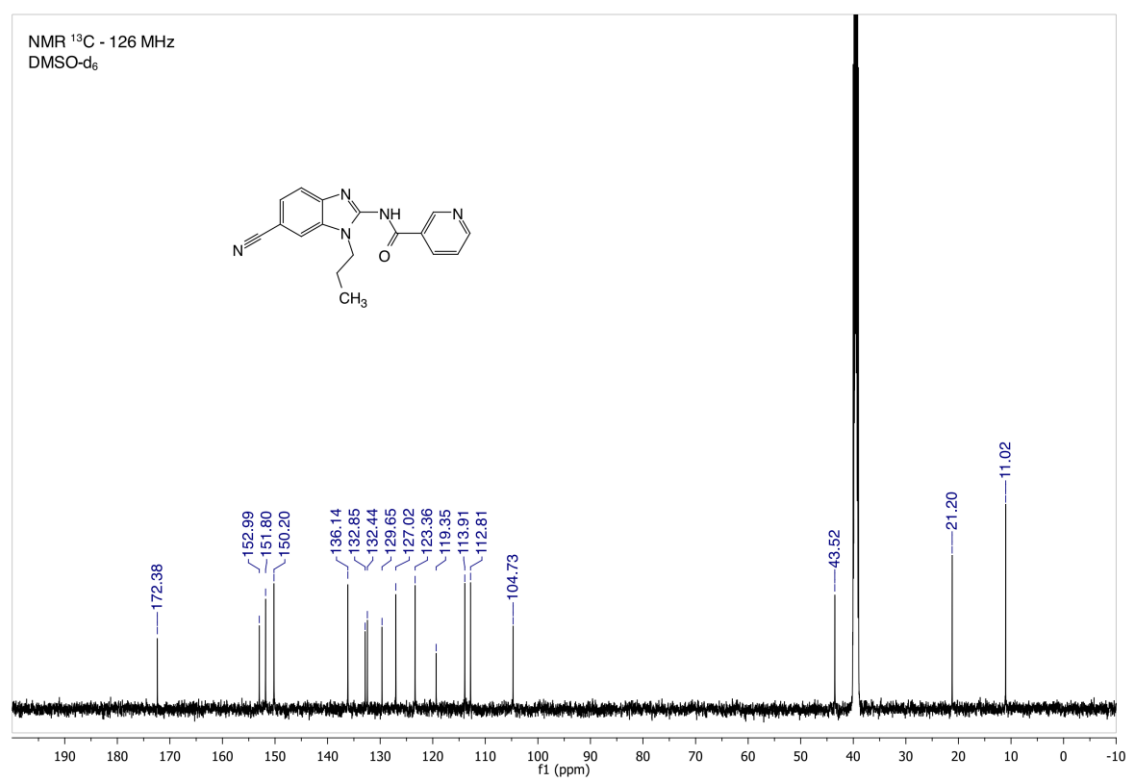
^1H NMR of 30 (600 MHz, CDCl₃)



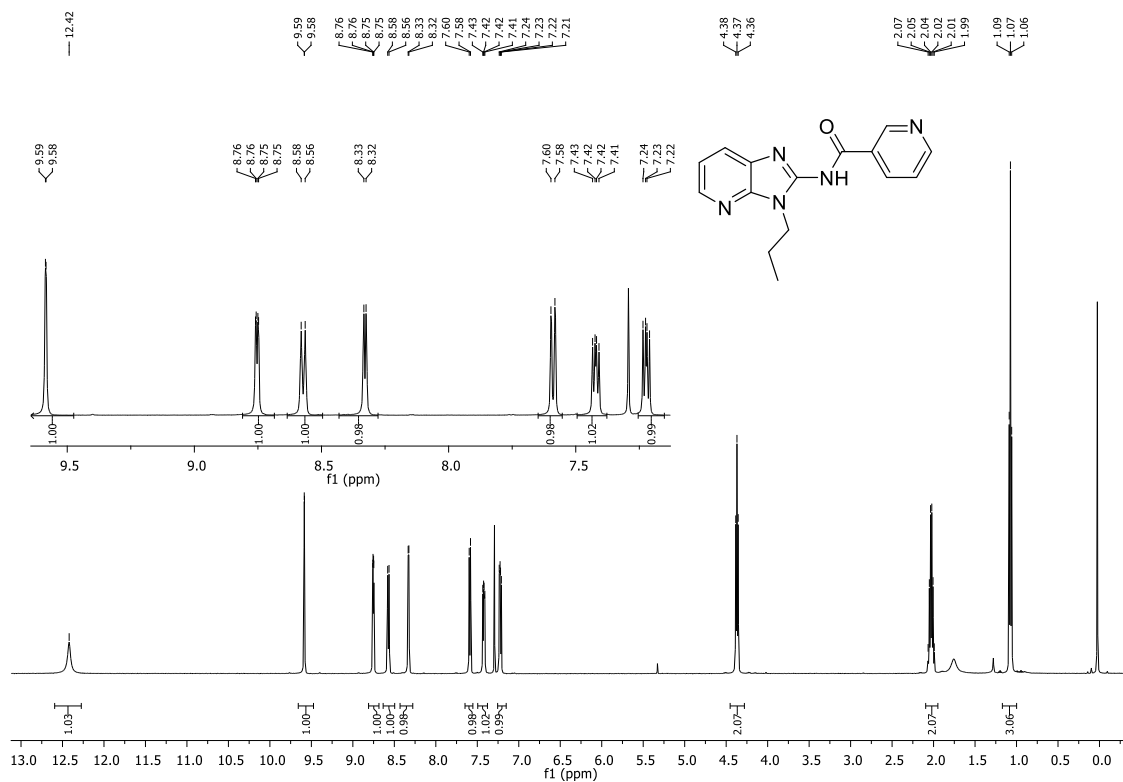
^{13}C NMR of 30 (151 MHz, CDCl₃)



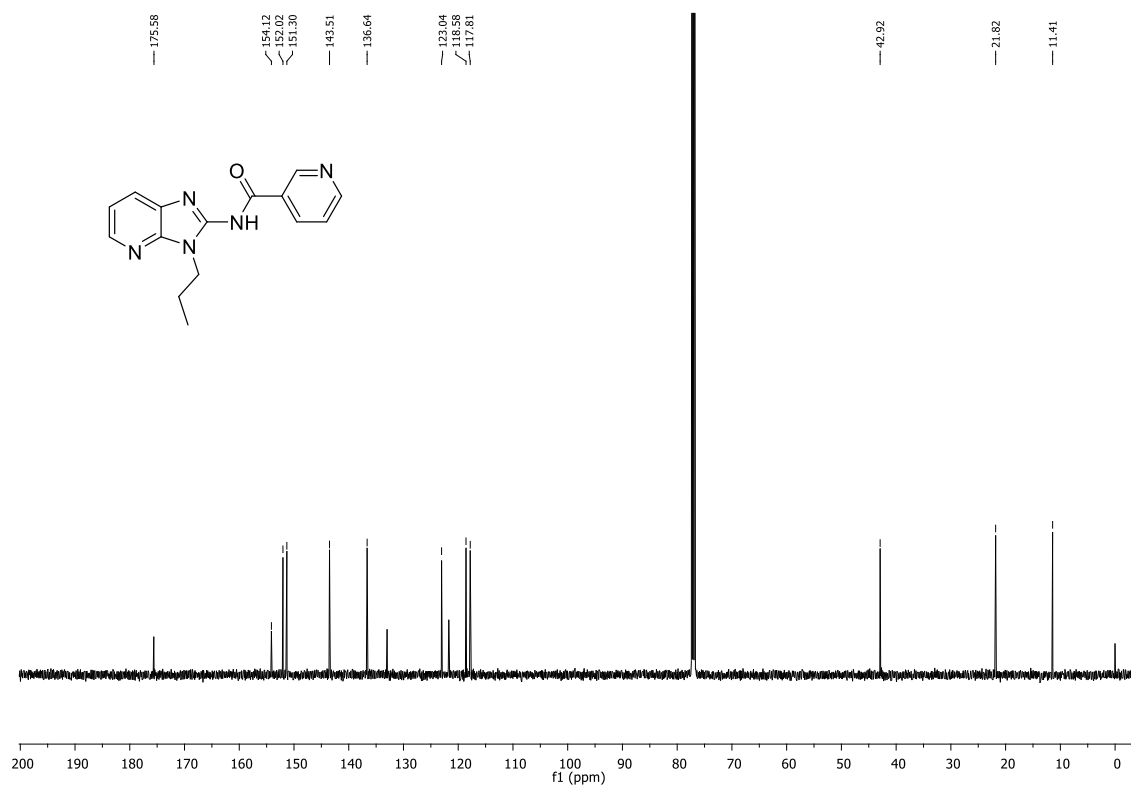
^1H NMR of 31 (500 MHz, DMSO)



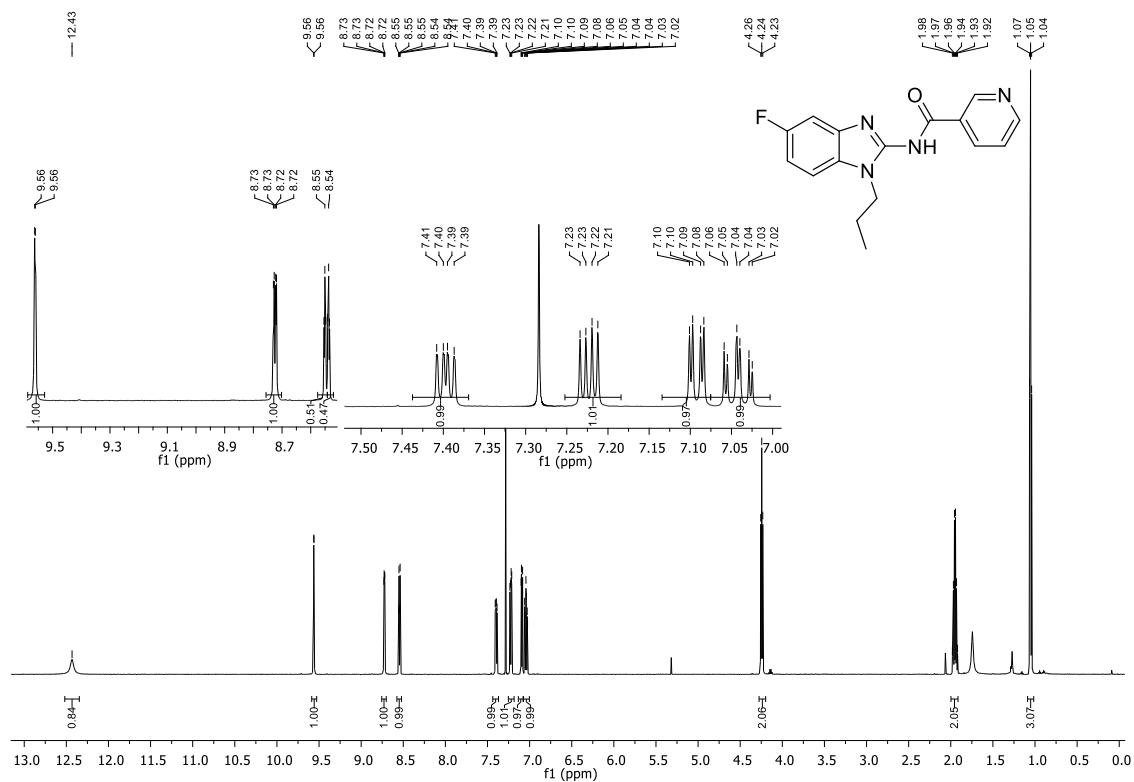
^{13}C NMR of 31 (126 MHz, DMSO)



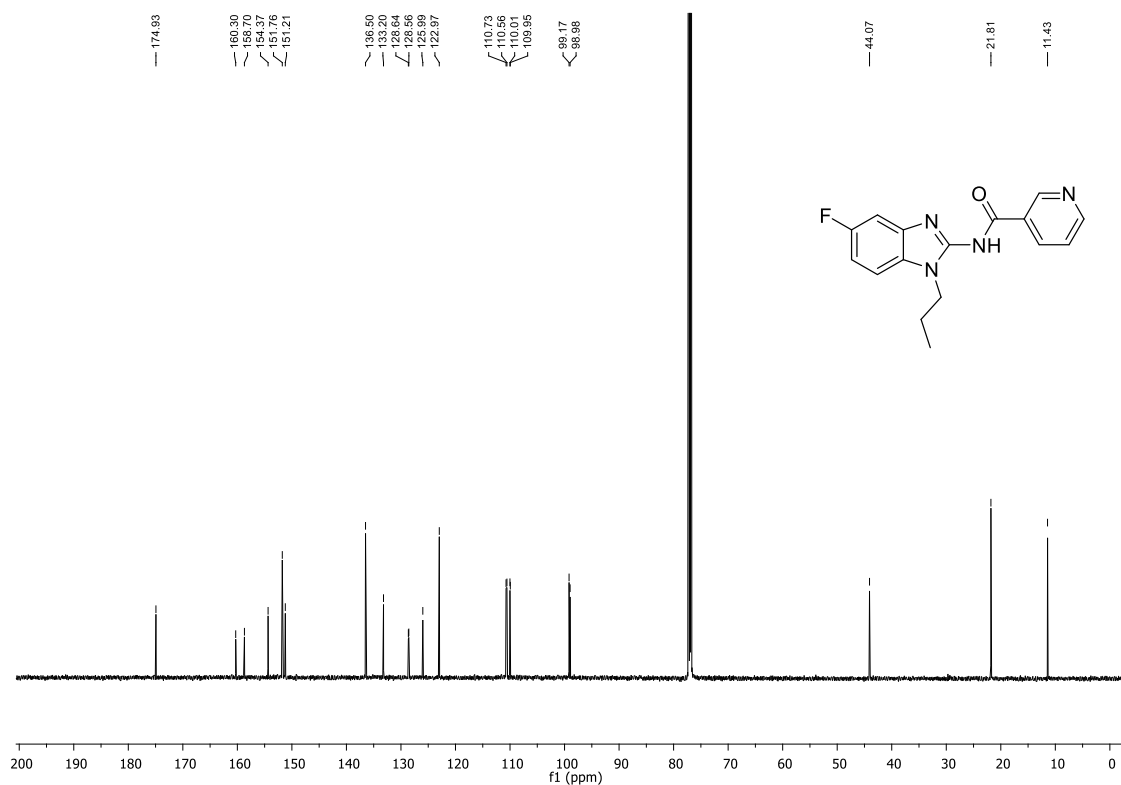
¹H NMR of 32 (500 MHz, CDCl₃)



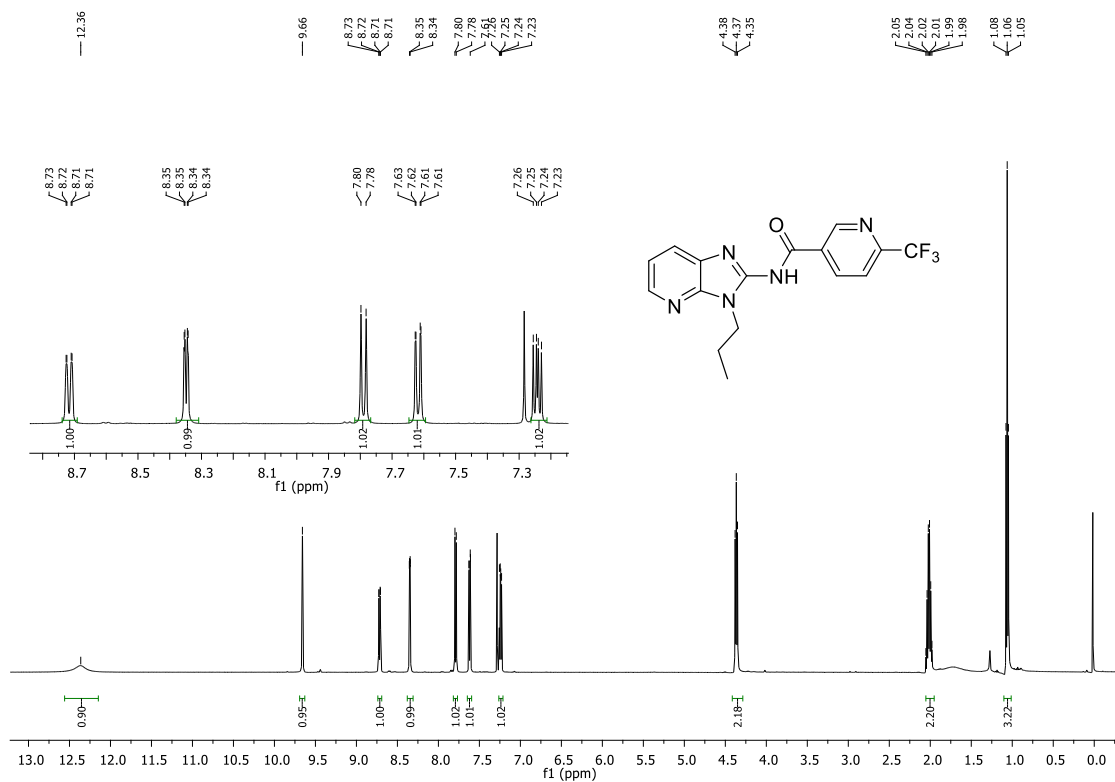
¹³C NMR of 32 (126 MHz, CDCl₃)



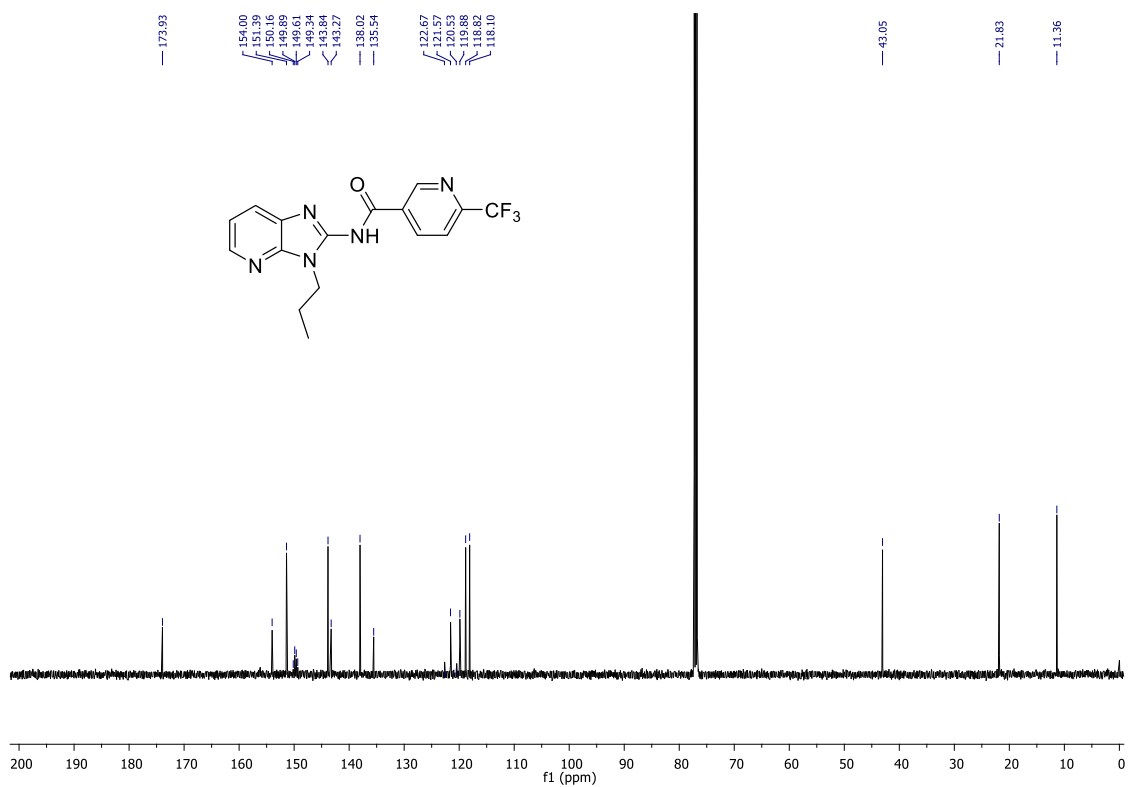
¹H NMR of 33 (600 MHz, CDCl₃)



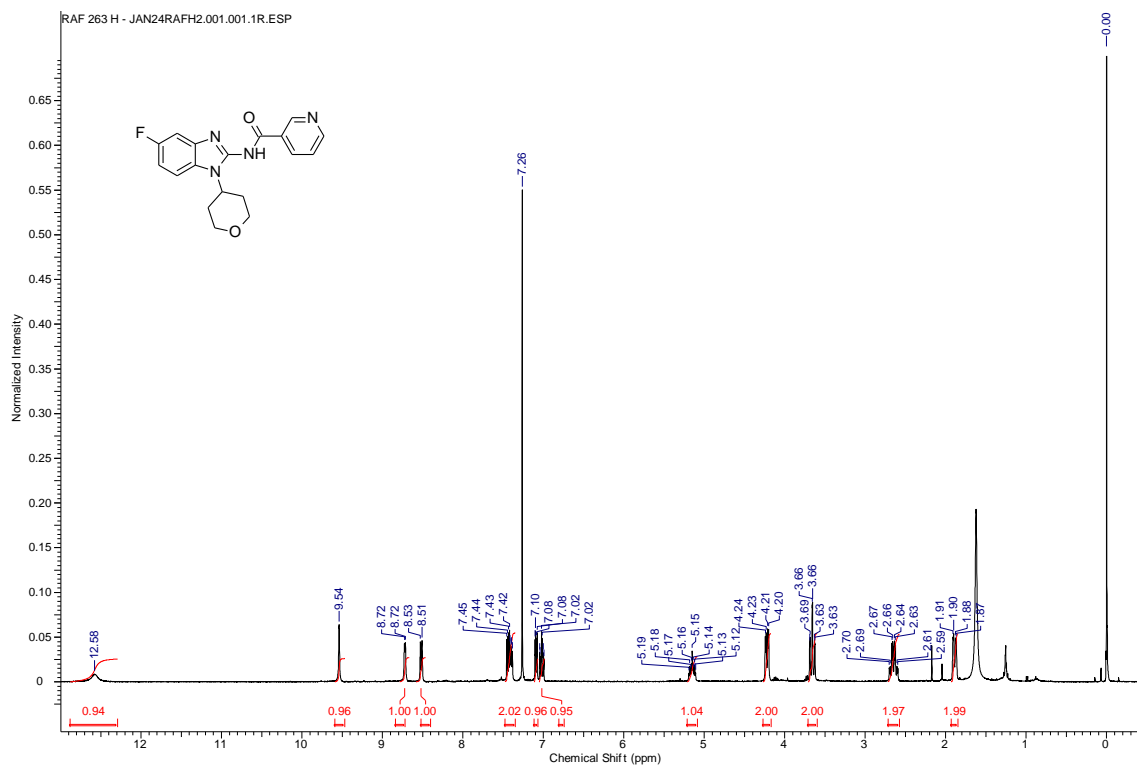
¹³C NMR of 33 (151 MHz, CDCl₃)



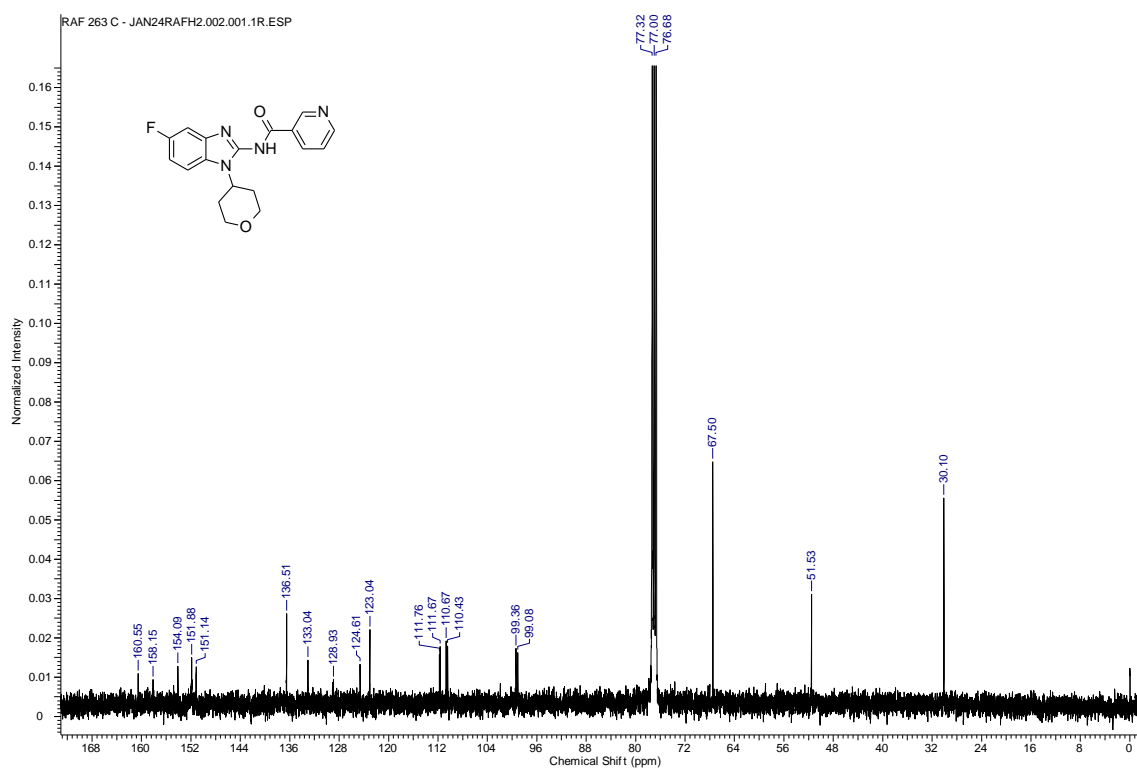
¹H NMR of 34 (500 MHz, CDCl₃)



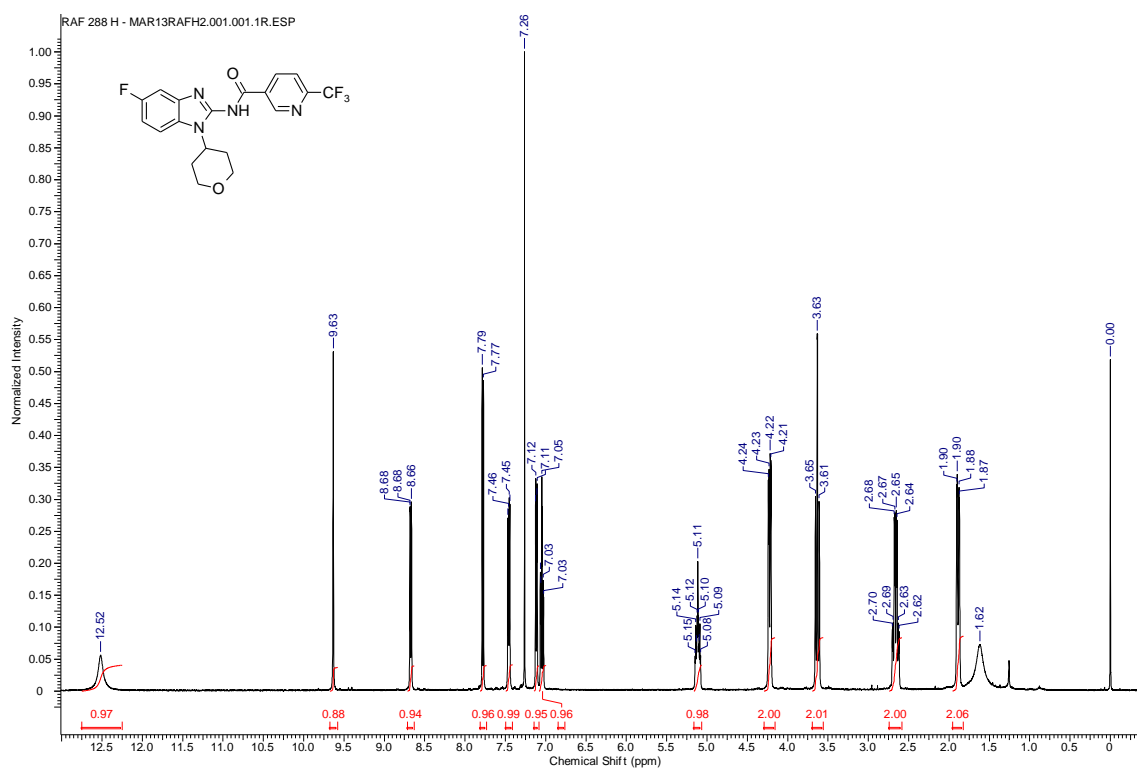
¹³C NMR of 34 (126 MHz, CDCl₃)



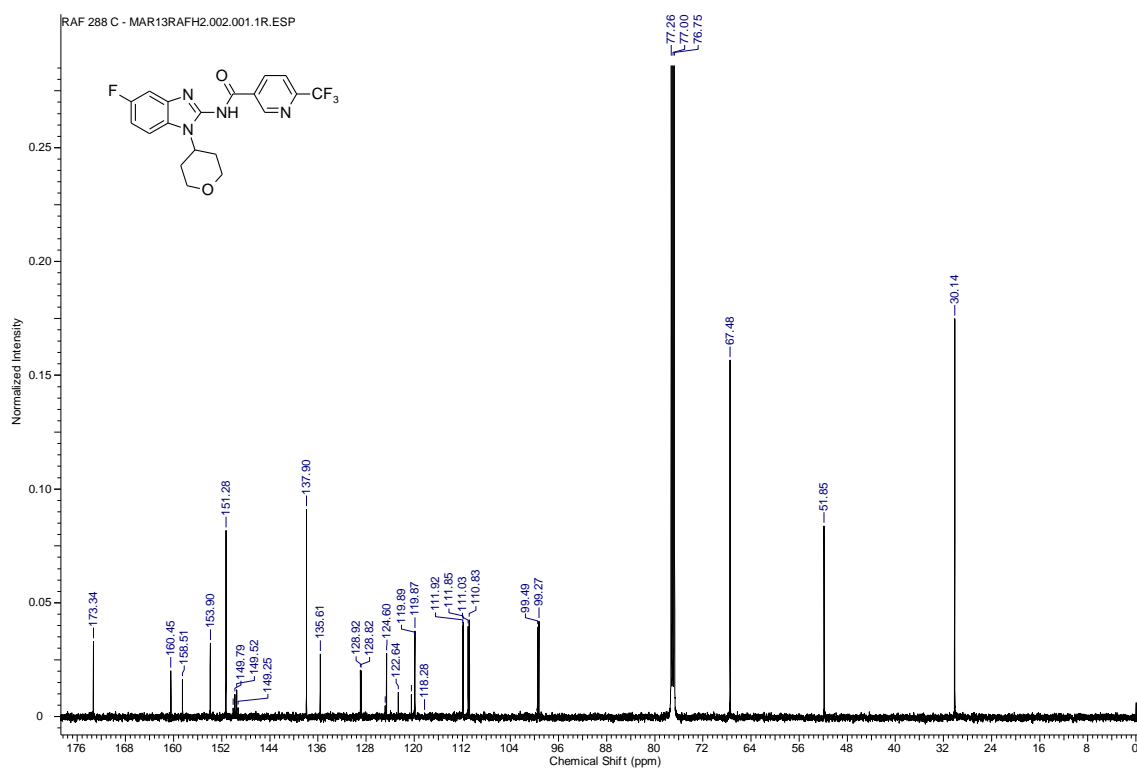
¹H NMR of 36 (400 MHz. CDCl₃)



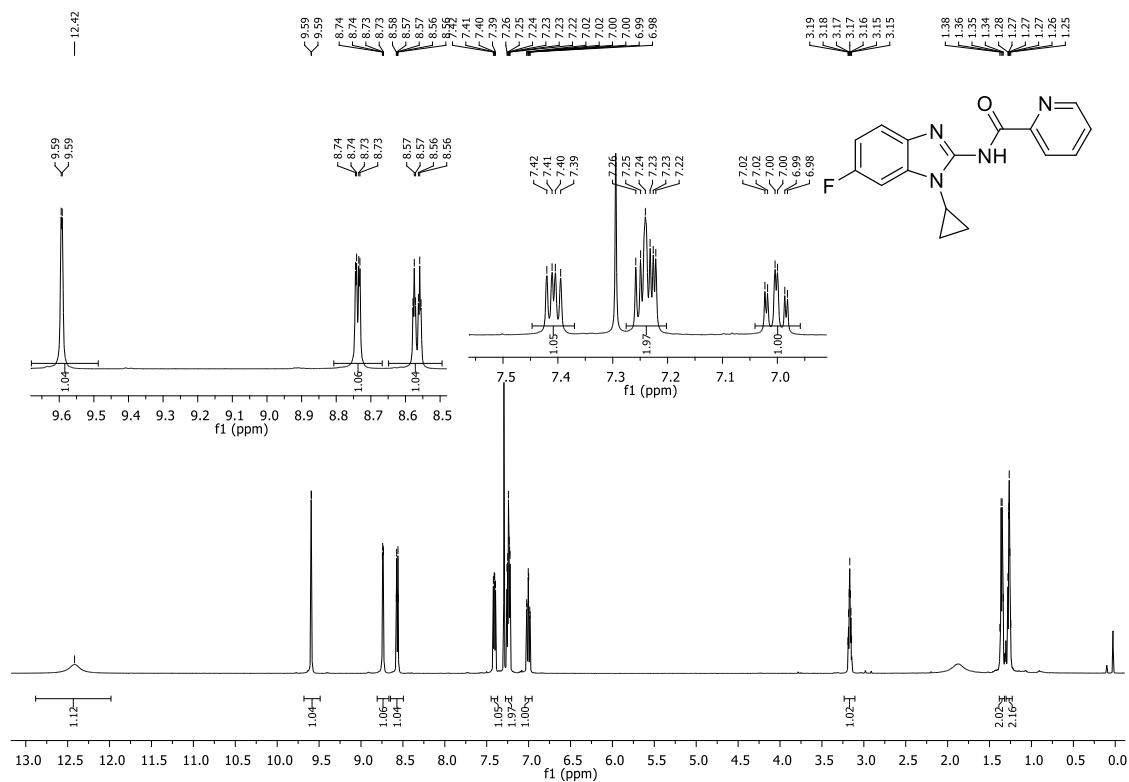
¹³C NMR of 36 (100 MHz. CDCl₃)



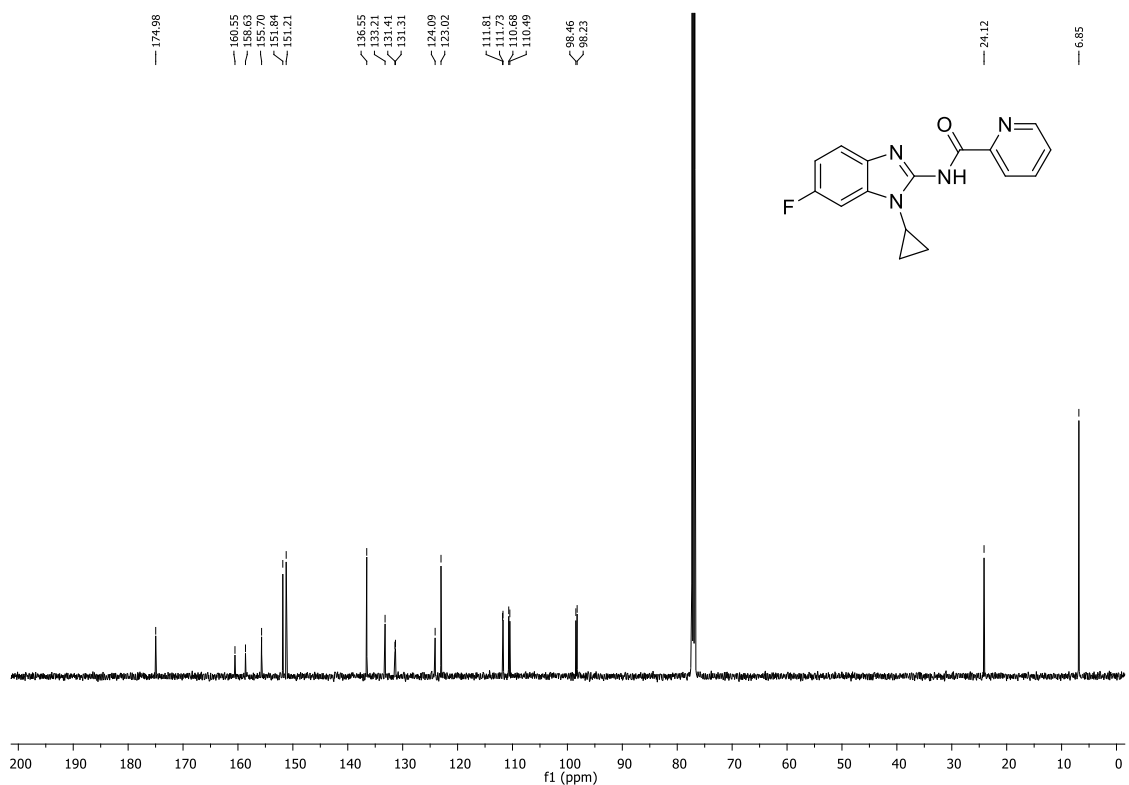
¹H NMR of 37 (500 MHz. CDCl₃)



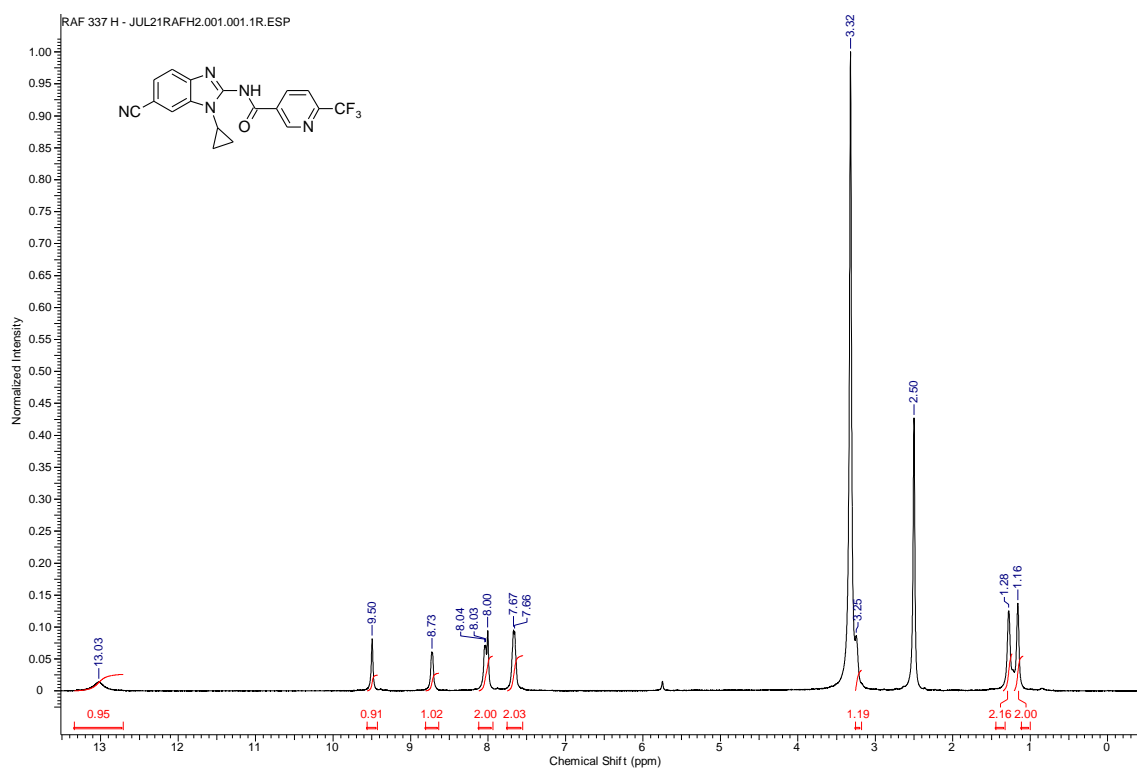
¹³C NMR of 37 (125 MHz. CDCl₃)



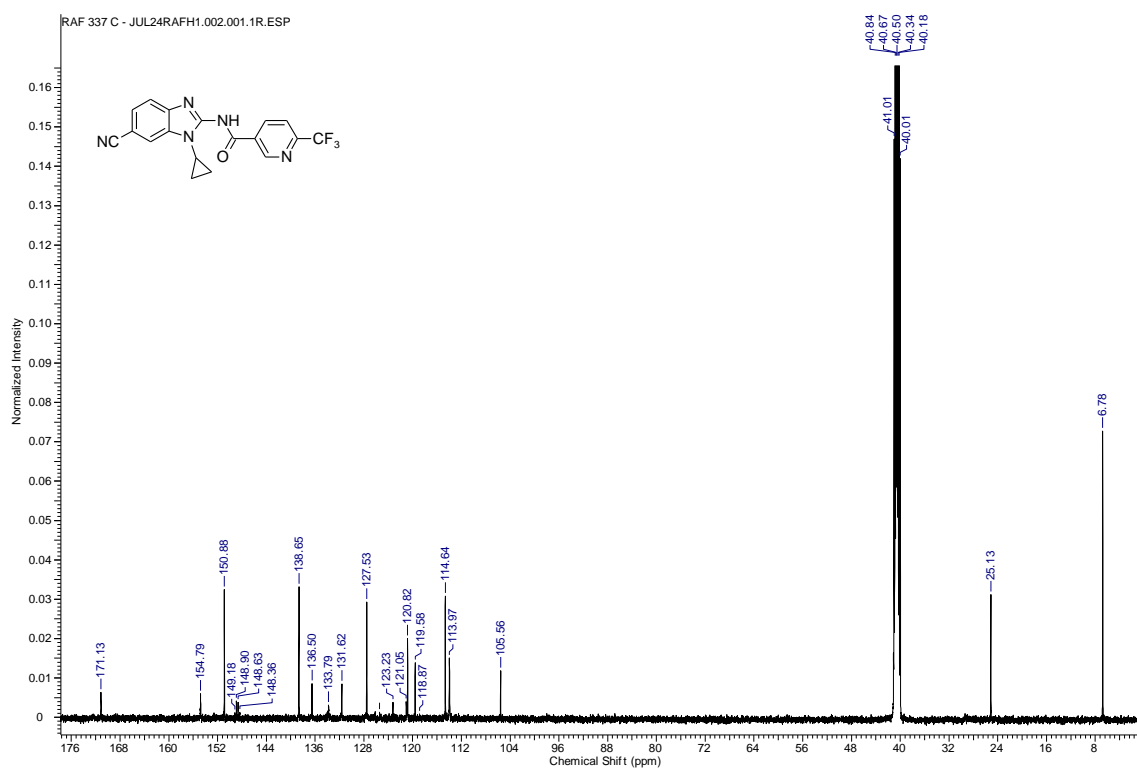
¹H NMR of 38 (500 MHz, CDCl₃)



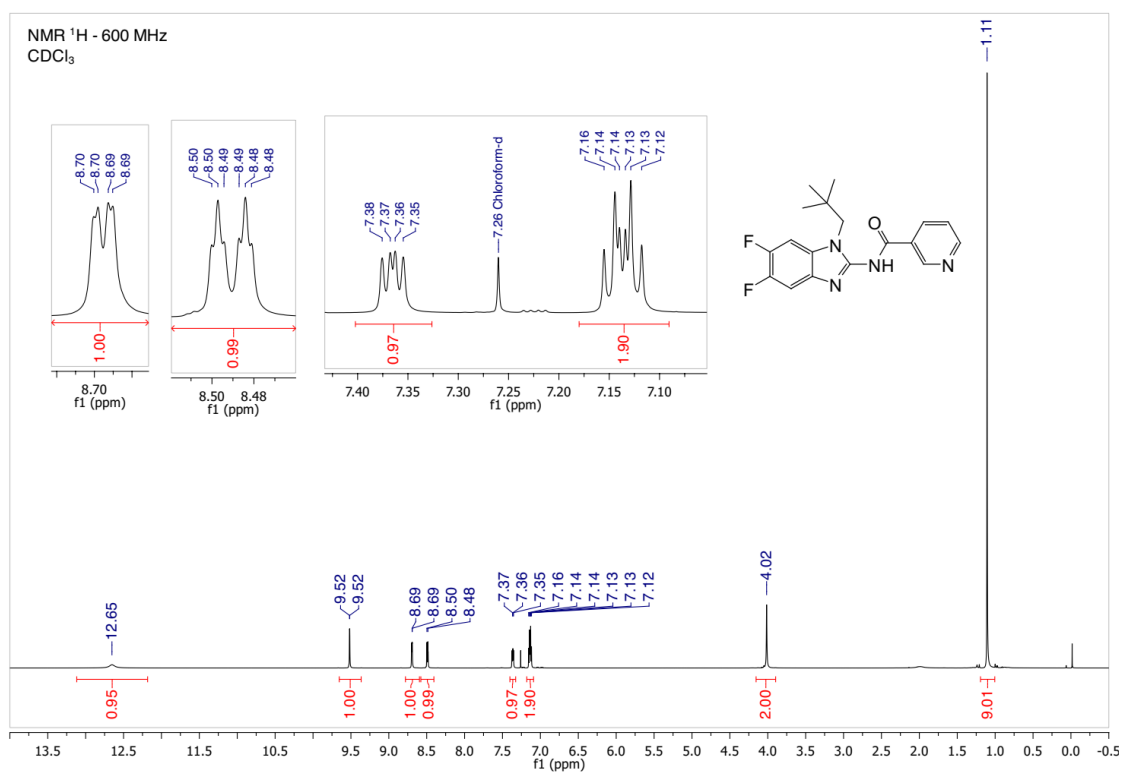
¹³C NMR of 38 (126 MHz, CDCl₃)



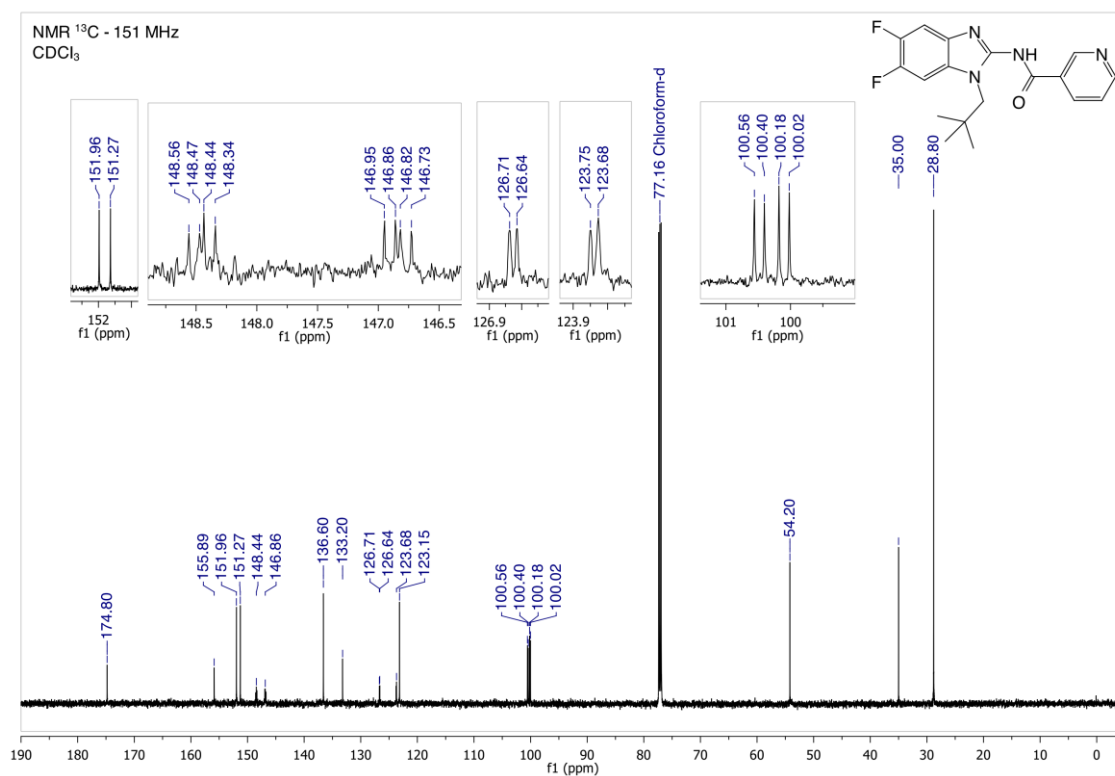
¹H NMR of 39 (500 MHz. DMSO)



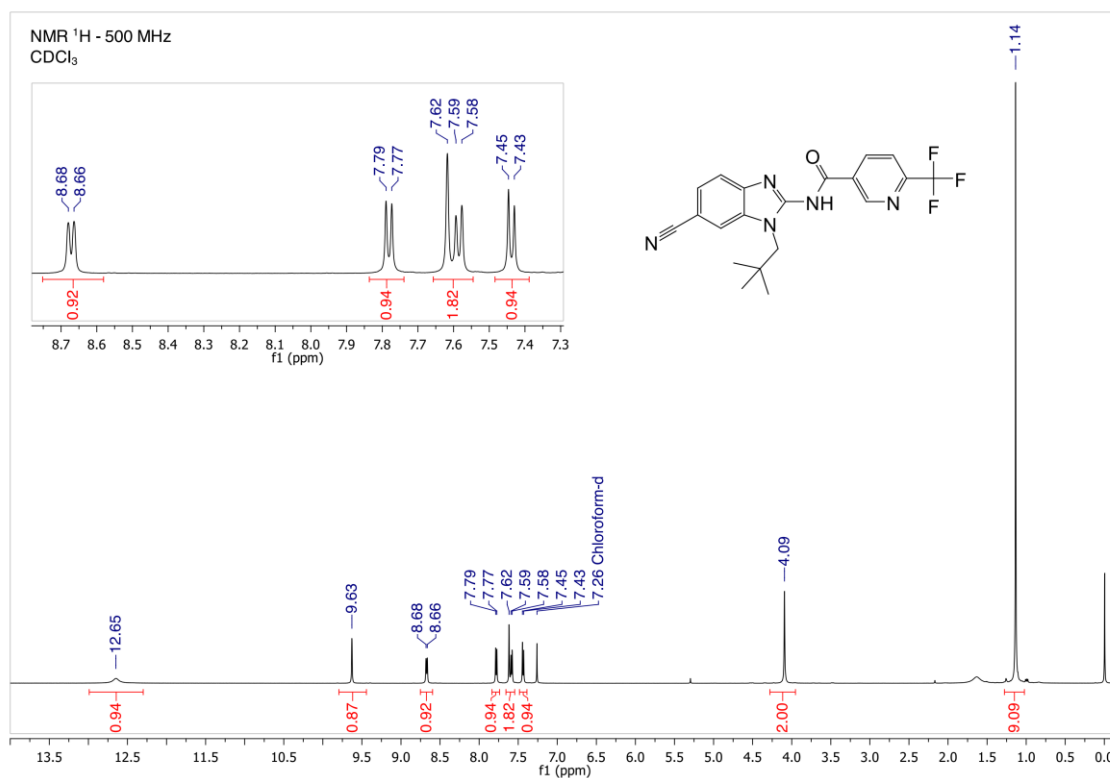
¹³C NMR of 39 (125 MHz. DMSO)



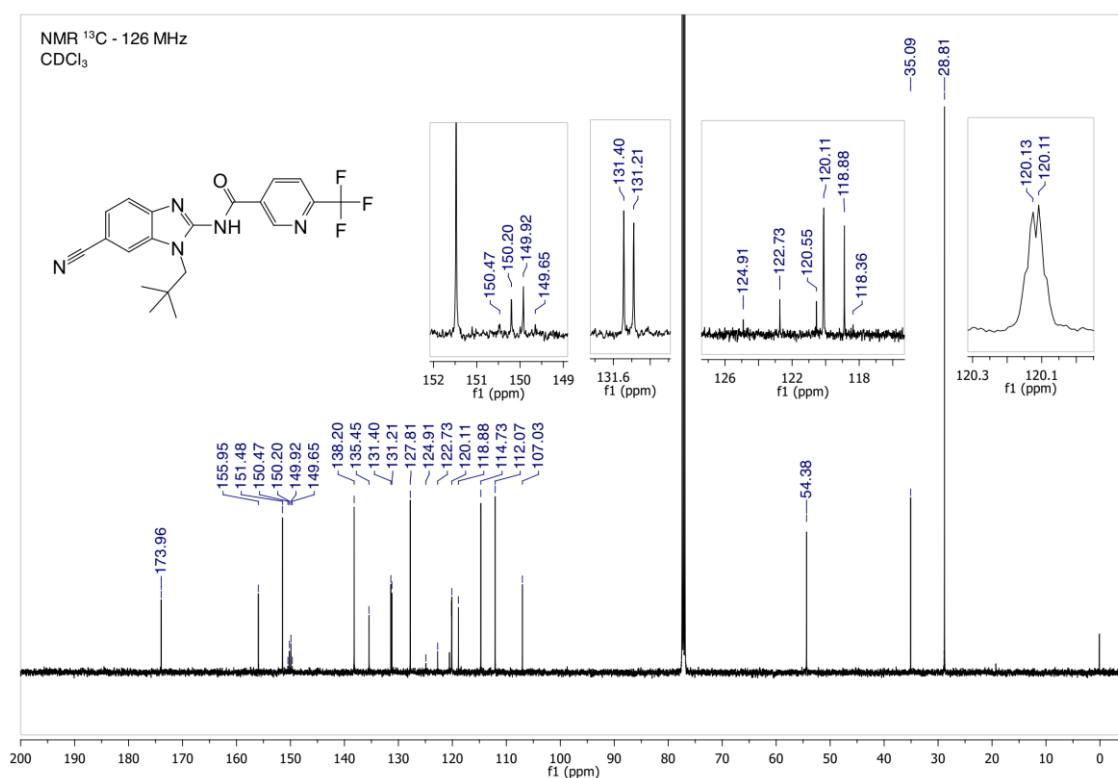
^1H NMR of 40 (600 MHz, CDCl_3)



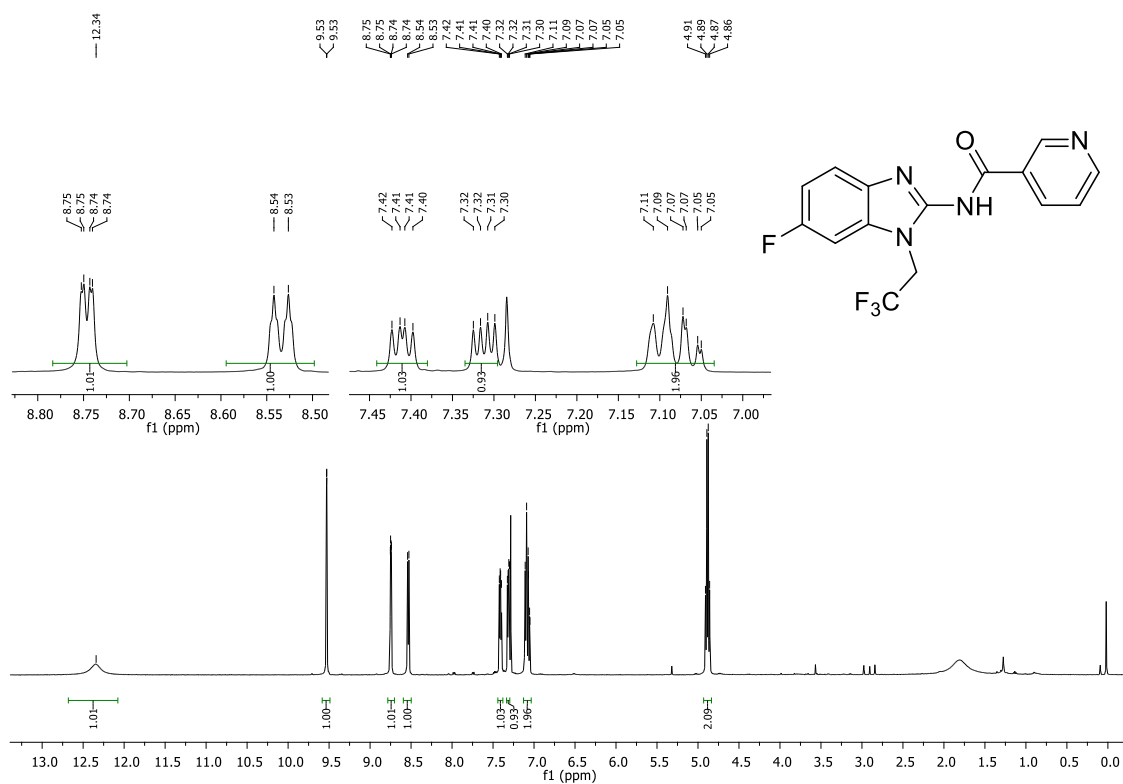
^{13}C NMR of 40 (151 MHz, CDCl_3)



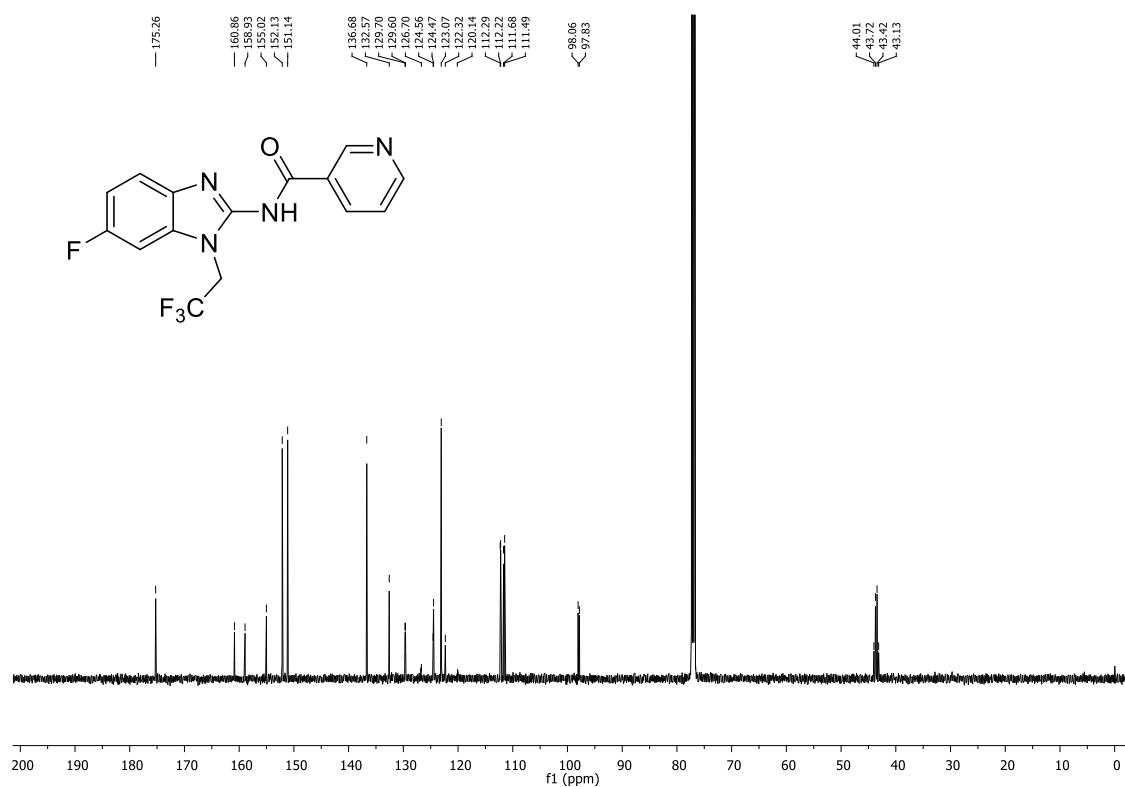
^1H NMR of 42 (500 MHz, CDCl_3)



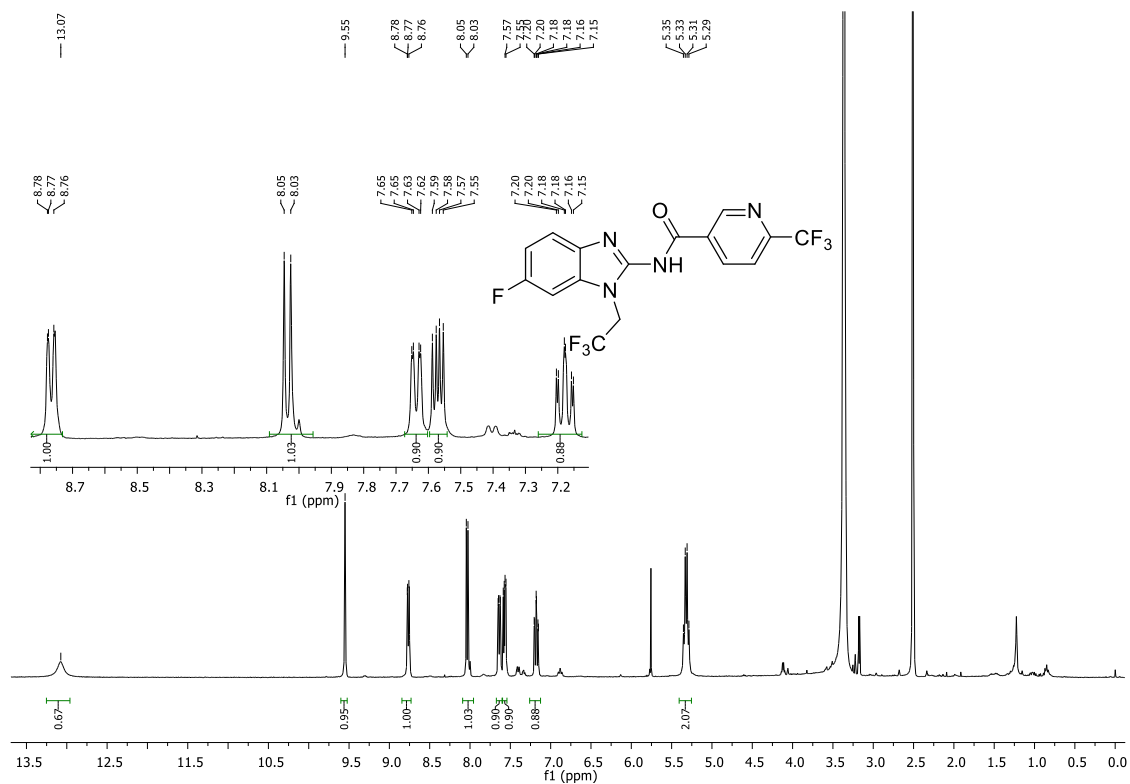
^{13}C NMR of 42 (126 MHz, CDCl_3)



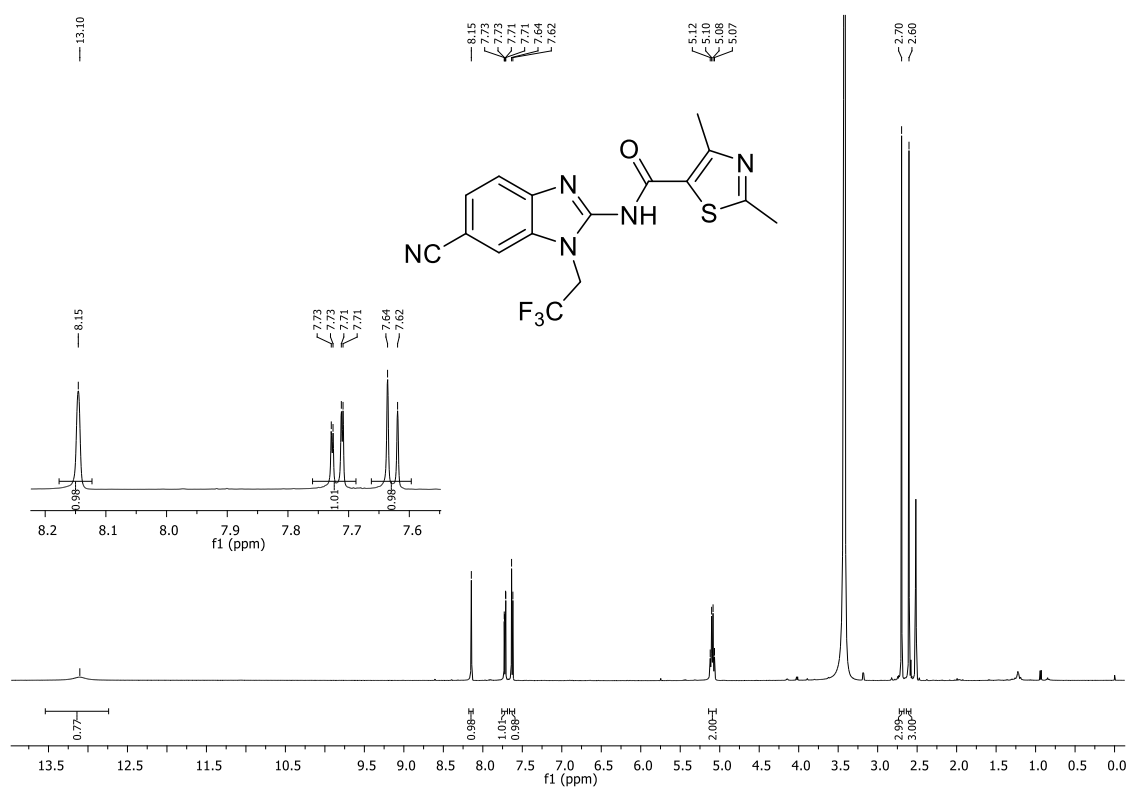
¹H NMR of 43 (500 MHz, CDCl₃)



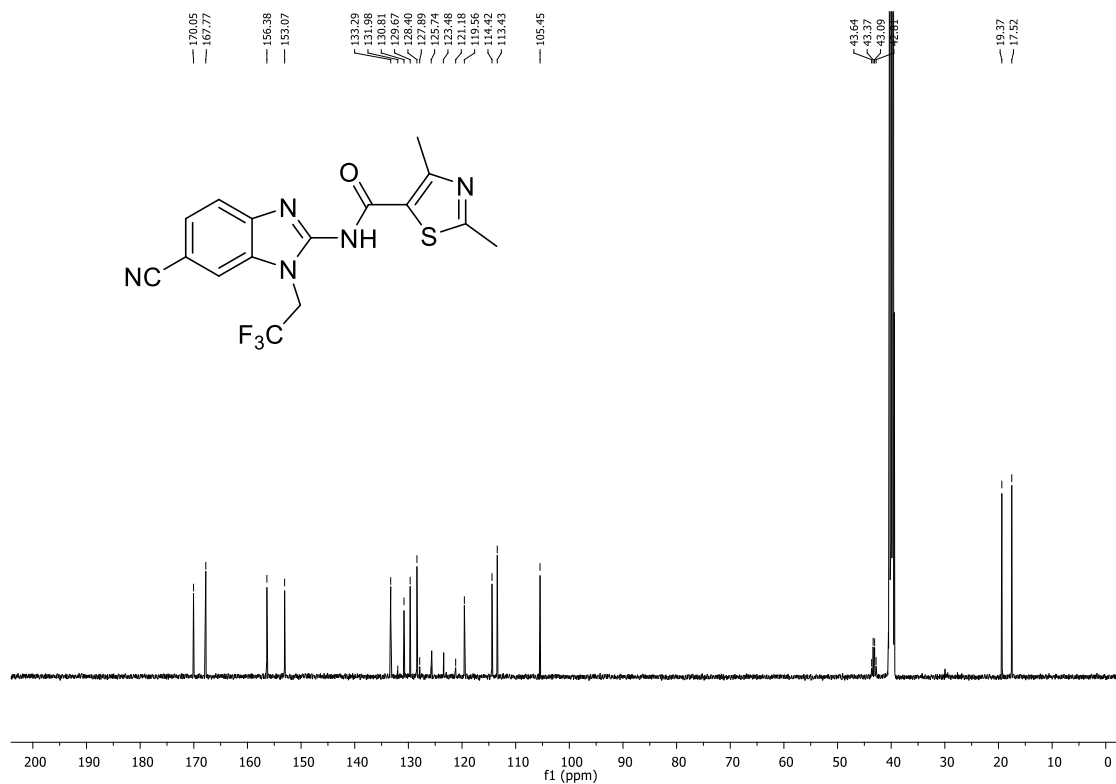
¹³C NMR of 43 (126 MHz, CDCl₃)



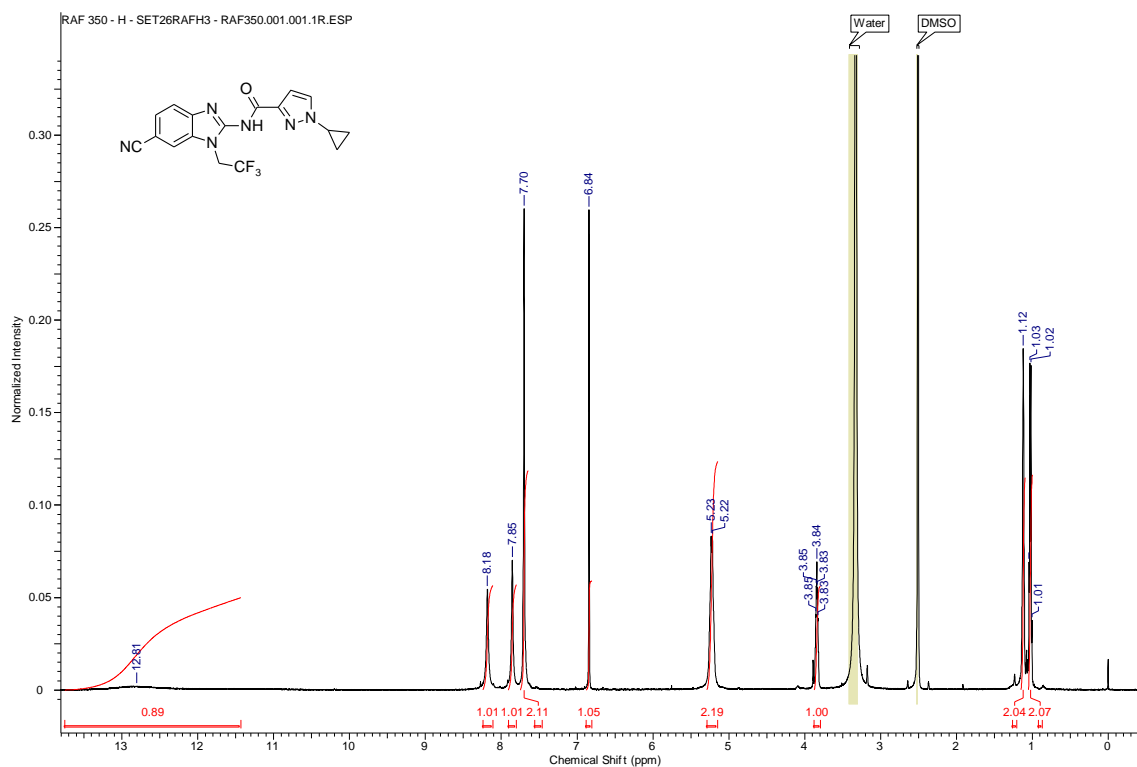
¹H NMR of 44 (400 MHz, DMSO)



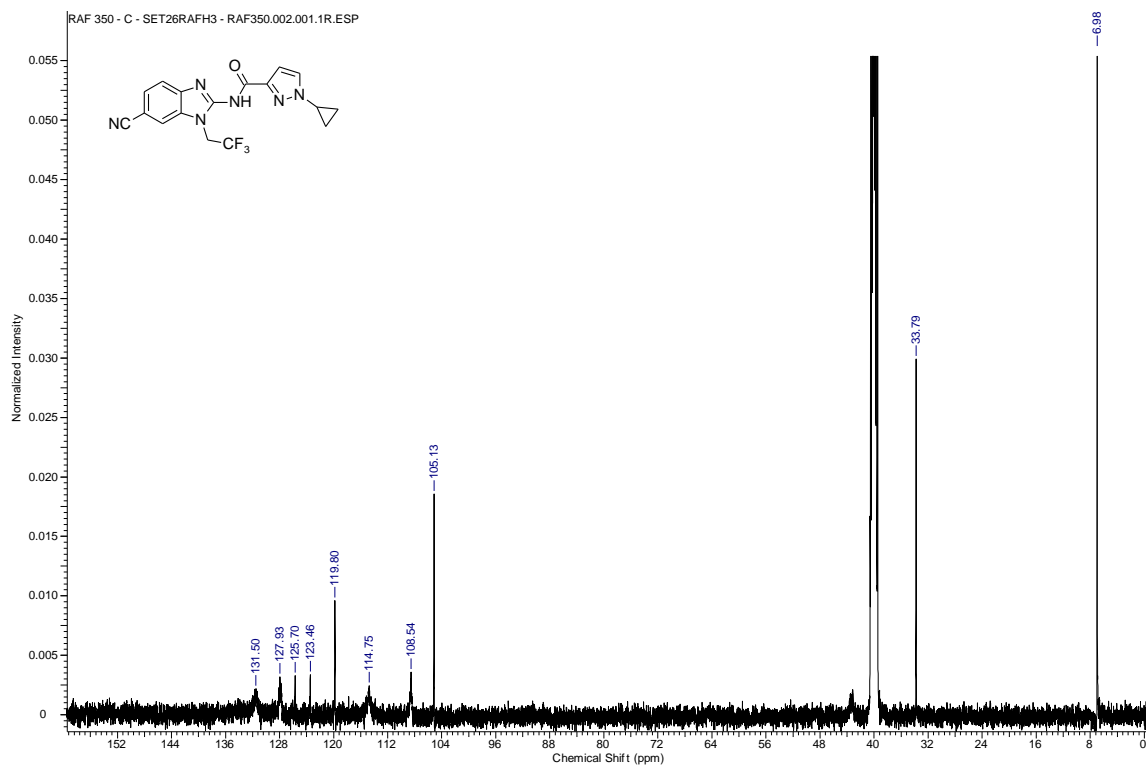
¹H NMR of 49 (500 MHz, DMSO)



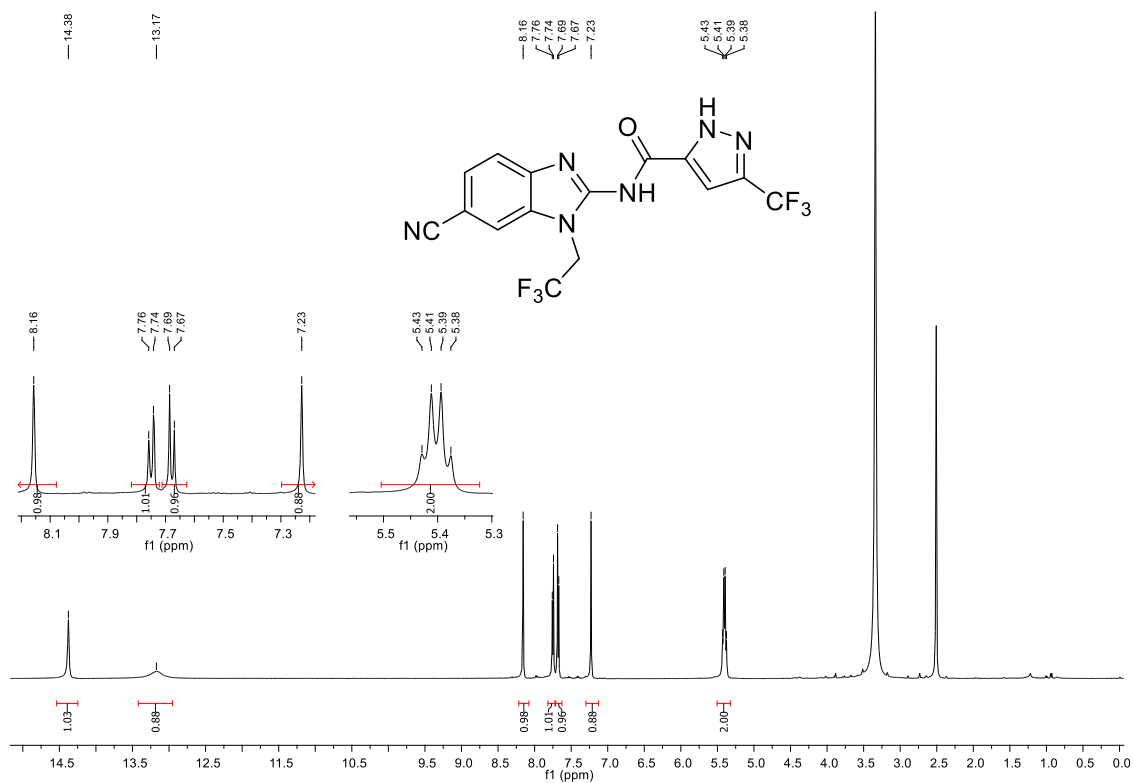
¹³C NMR of 49 (126 MHz, DMSO)



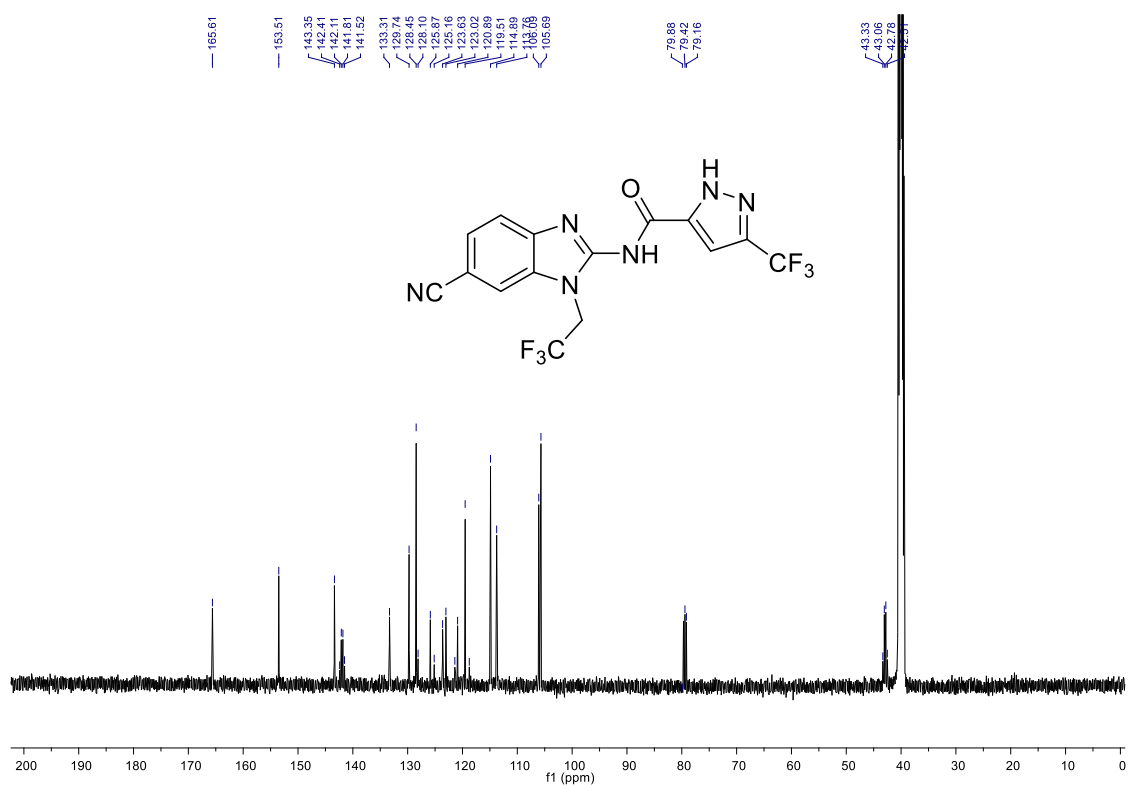
¹H NMR of 52 (500 MHz, DMSO)



¹³C NMR of 52 (125 MHz, DMSO)



¹H NMR of 54 (500 MHz, DMSO)



¹³C NMR of 54 (126 MHz, DMSO)

References

- 1- Ferreira RAA, J. C. M. P. K. P. S. B. F. L. e. a., 2021. 2-aminobenzimidazoles for leishmaniasis: From initial hit discovery to in vivo profiling.. *PLoS Neglected Tropical Diseases*, 15(2), p. e0009196.
- 2- Wengang Guo, J. W. Y. L. C. L., 2014. Construction of anti-1,2-diols bearing chiral tertiary alcohol moiety using free hydroxyacetone as aldol donor by imidazole. *Tetrahedron*, Volume 70, pp. 6561-6568.